Silyl Cation-promoted C–F Activation

Dissertation

zur

Erlangung der naturwissenschaftlichen Doktorwürde
(Dr. sc. nat.)

vorgelegt der

Mathematisch-naturwissenschaftlichen Fakultät

der

Universität Zürich

von

Oliver Allemann

von

Welschenrohr SO

Promotionskomitee

Prof. Dr. Jay S. Siegel (Vorsitz)
Prof. Dr. Kim K. Baldridge
Dr. Henning J. Jessen

Zürich, 2014

Acknowledgment

I would like to thank:

Prof. Jay S. Siegel
for allowing me to be part of his group to do my PhD, for his great guidance and for giving me the freedom to development my own thoughts, for sharing his creative ideas and distinct opinions.

Prof. Kim K. Baldridge
for her outstanding calculations and for being there for all of us.

Dr. Simon Duttwyler & Paola Romanato
for introducing me to the field of silyl cation chemistry and for sharing their knowledge, for their excellent work that made it easy for me to gain ground in this rather exotic area of research.

PD Laurent Bigler and Urs Stalder
for measuring all those mass spectra.

Prof. Anthony Linden
for taking time to measure and solve my crystal structures.

Simon Jurt
for helping out with tricky NMR measurements and spectrum interpretation.

Irene Lehmann
for elaborating a quantitative HPLC study.

Alessandra Wüthrich & Celine Imgrüth
for their work in the lab

Silvia Rocha, Derik Frantz, Becky Abramson, Roman Maag, Michael Felber, Sebastian Imstepf, Alexander Szentkuti, Jêrome Ungricht
for the great times we had at Uni.

Siegel/Finney/Stuparu/Jessen Group Members Past and Present
for a nice working atmosphere.

Salome Fässler & Sarah Ammann
for taking care of complicated administrative work.

CMSZH Graduate School
for financial support and connecting the PhD students from the different institutes

Manuela Brütsch
for her support during the final year of my PhD, including exam, defense, defense apero, and for brightening up the daily Uni routine.

My Family & Friends
for their constant support and for distracting me from research if necessary.

Abstract

Silyl Cation-promoted C–F Activation

by

Oliver Allemann

University of Zurich

Prof. Dr. Jay S. Siegel, Chair

Using a highly reactive silyl cation paired with a carborane anion, carbon-fluorine (Ar–F) bonds could be activated towards intramolecular aryl-aryl coupling. Exposure of a fluorophenyl substrate to one equivalent of triisopropylsilyl cation and a sterically hindered base, causes the generation of a short-lived phenyl cation that is intramolecularly attacked by an aromatic moiety, thereby forming a cyclized polyaromatic hydrocarbon. The general concept was extended to a catalytic reaction protocol, which takes advantage of the highly acidic proton liberated during the product formation by reforming silyl cations from dimethyldimesityl silane upon protodesilylation. To start the reaction, a catalytic amount of silyl cation or a very strong Brønsted acid (e.g. protonated mesitylene) can be employed. A further enhancement was achieved by application of microwave irradiation. The reaction time was decreased substantially and the necessary amount of initiator could be reduced. The methodology was implemented on various substrates, resulting in formation of five- and six-membered rings being part of small Polycyclic aromatic hydrocarbons. The scope could be expanded to substrates containing fluoropyridyl moieties, although at the cost of the necessity of an additional equivalent of silyl cation to saturate the Lewis basic lone pairs of the nitrogen atom contained in the molecule. Molecules bearing a TIPS-protected alcohol group could not only be transformed to cyclized product, but were also deprotected during the course of the reaction. Furthermore, these

transformations could be performed in a catalytic fashion, 5 mol-% of silyl cation was sufficient.

A different reactivity was observed for substrates that posses a methyl group close to the C–F bond within the same molecule. The abstraction of fluoride results in formation of a carbon-carbon bond between methyl and fluorophenyl to give cycclized product. Deuterium labeling studies provided further insight into the reaction mechanism and a 1,2-insertion reaction of phenyl cation into the C–H bond was suggested to explain this cyclization. Benzylic and non-benzylic methyl groups could be activated towards such a reactivity, therby forming five- or six-membered rings.

Carefully designed starting materials can then provide the base for the synthesis of novel compounds, using either method presented in this thesis, the intramolecular arylation or the CH–insertion reaction protocol.

Zusammenfassung

Silyl Cation-promoted C–F Activation
von
Oliver Allemann
Universität Zürich
Prof. Dr. Jay S. Siegel, Vorsitz

Mit Hilfe von Silylkationen konnten Kohlenstoff-Fluor-Bindungen (Ar–F) aktiviert werden, was zu intramolekularen Ringschlüssen durch Aryl-Aryl Verknüpfungen führte. Die Verwendung von einem Equivalent von Triisopropylsily Carboran Derivat und einem Equivalent einer sterisch gehinderten Base zur Umsetzung eines Fluorophenyl Substrats führt zur kurzzeitigen Entstehung eines Phenyl Kations, welches intramolekular von einer Arylgruppe angegriffen wird und somit zyklisiertes polyaromatisches Kohlenwasserstoff hervorbringt. Die Methode wurde weiterentwickelt, sodass eine katalytische Menge an Silylkation ausreicht für die Umsetzung von Startmaterial zu Produkt. Dies wurde erreicht durch den Einsatz von Dimethyldimesitylsilan, welches die beim Ringschluss entstehenden Protonen abfängt und somit Silylkationen durch Protodesilylierung regeneriert. Um die Reaktion zu starten kann entweder ein Silylkation oder eine sehr starke Brønsted-Säure (z.B. Mesitylen–H^+) benutzt werden. Durch Heizen der Reaktion mit Mkrowellenstrahlung kann die Reaktionsdauer und die Menge an eingesetztem Initiator deutlich reduziert werden. Die Methodik wurde auf eine Reihe verschiedener Substrate angewendet, was zur Entstehung von 5-und 6-gliedrigen Ringen führte. Der Anwendungsbereich der Reaktion konnte auf Substrate, welche ein Fluoropyridin beinhalten ausgeweitet werden. Dazu ist allerdings die Verwendung von einem zusätzlichen Equivalent Silylkation nötig. Moleküle welche eine TIPS-geschützte Alkoholfunktion besitzen können

ebenfalls umgesetzt werden, und man erhält nicht bloss zyklisiertes, sondern auch entschütztes Produkt.

In Substraten welche eine Methylgruppe in der Nähe der C–F Bindung aufweisen, konnte eine neuartige Reaktivität beobachtet werden. Durch Abstrahierung von Fluorid entsteht zwischen der Methylgruppe und dem Fluorophenyl ine neue Bindung und somit ein zusätzlicher Ring. Ein Experiment in dem eine Deuterium-markierte Methylgruppe verwendet wurde, gibt Hinweise auf den Mechanismus der Kopplung zwischen Fluoroaryl und Methyl. Die Deuteriumverteilung im Produkt legt eine 1,2-Insertion vom Phenylkation in die C–H Bindung der Methylgruppe nahe.

Durch die Synthese von passenden Ausgangsverbindungen können durch Verwendung der in dieser Arbeit beschriebenen Methoden (intramolekulare Arylierung und C–H Insertion) neuartige Substanzen hergestellt werden, welche ein konjugiertes Kohlenwasserstoff-Skelett aufweisen.

Table of Contents

List of Figures

List of Schemes

List of Tables

1 Introduction

1.1 Silyl Cations

1.1.1 General

The organic silicon species have always been overshadowed by the huge demand for elemental silicon, caused by its extensive use as semiconductor for the manufacturing of electronic devices. Among the diverse applications in organic synthesis, from protecting group chemistry to coupling reactions (e.g. Hiyama coupling), silyl cation chemistry currently only represents a minor fraction. A reason for that is certainly the fact that the synthesis and proper handling of silyl cations in condensed phase has only been learnt in the last two decades. But considering their reactivity, they bear a high potential for a variety of transformations and also for promoting reactions that have not even been considered possible.

Whereas the study of silyl cations in gas phase had been ongoing for a while, it was only in the 1990s when the first trialkylsilylium-like species isolated in solution were reported by Lambert and Reed.[1] But still, the search for a true silyl cation, possessing a planar coordination sphere, was ongoing. There are several features of the silicon atom that contribute to the difficulty of that task. Due to its direct proximity in the same group of the periodic table, silicon is often compared to carbon. But when doing so, it soon becomes evident that they behave quite differently. Whereas carbon readily forms strong multiple bonds, to carbon or other second row heteroatoms, silicon prefers single bonds and a high coordination number. These tendencies are of importance when it comes to the stabilization of the corresponding cations. Carbocations are easily stabilized by conjugated π-systems or heteroatoms. Because there is a beneficial overlap of empty p-orbital of the carbon atom and the neighboring, filled π-orbital or electron lone pair, the positive charge is distributed over a larger area, which reduces the reactivity of the carbocation. For a silyl cation this π-p overlap is not as effective. On one hand the Si–A bond is longer; on the other hand the empty p-orbital of the Si^+ is a 3p orbital and therefore, symmetrically, does

not match well with the substituent's filled 2p orbital (Figure 1.1). Such an overlap would contribute to a double bond character between positively charged atom and the substituent, and helps understand why this works well for carbon, but not for silicon. The same applies for alkyl substituted cations, where hyperconjugation of the C–H sigma bond with the empty p-orbital can stabilize the positive charge.

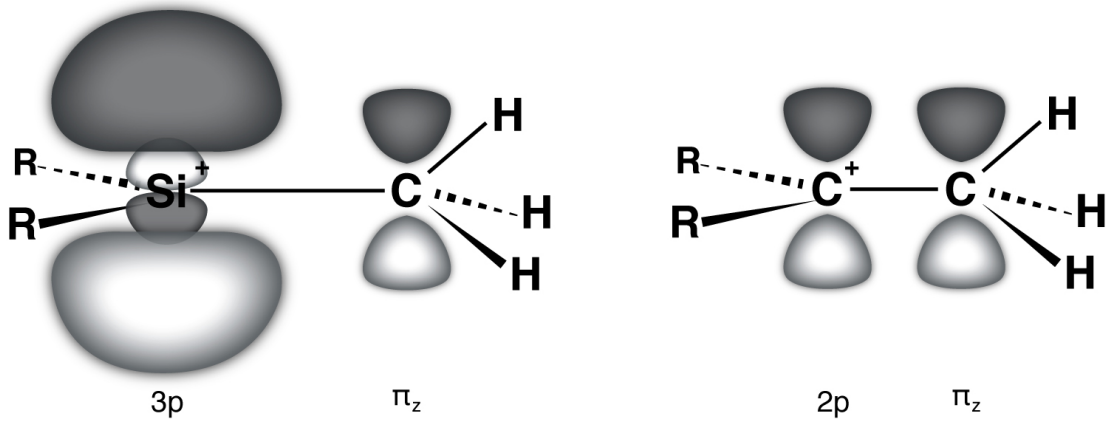

Figure 1.1. Comparison of hyperconjugation of a methyl substituent with both a silyl cation and a carbocation. 2p-2p overlap is more effective than 3p-2p overlap, due to the similar geometry and the shorter distance of C–C compared to Si–C.

There is an example of a silyl cation with three alkyl thiol substituents.[2] Indeed, in that case the 3p-3p overlap is more effective, and hence the double bond character of the Si–S bonds is more pronounced. But this again raises the question of the location of the positive charge, and whether one deals with a silyl cation or rather a sulfonium ion.

Another considerable difference between carbon and silicon is their affinity towards first-row atoms, i.e. their bond dissociation energies. Silicon forms exceptionally strong bonds with electronegative atoms like fluorine, oxygen and nitrogen (Table 1.1). But when it comes to carbon or hydrogen the Si–C or Si–H bonds become comparable to the stability of a C–C or C–H bond respectively. Although the table shows merely a tendency, and does not account for heterolytic bond cleavage, this occurrence is crucial for the synthesis of silyl cations as we will see later on. But first, it is important to clarify what criteria can be used to determine the cationic character of a silylium ion (Figure 1.2). Because as often, there is not just black and white or in this case cation or not-cation, but there is a broad area in between, and there are different tools to measure these scales of gray. An important instrument nowadays is x-ray crystallography. With a crystal structure in hand, there are two main parameters

that can be measured. First, one can look at the average R–Si–R angle; meaning the angle that is spread from the silicon center to two substituents. The closer this angle is to 120° the more it is considered a tricoordinate silyl cation. In a tetravalent structure it would be 109.5°. Secondly, there is the distance of the silicon atom to the plane that passes through three connecting atoms of the substituents (out-of-plane distance). The shorter the distance, the more planar the structure and hence a stronger cationic character can be considered.

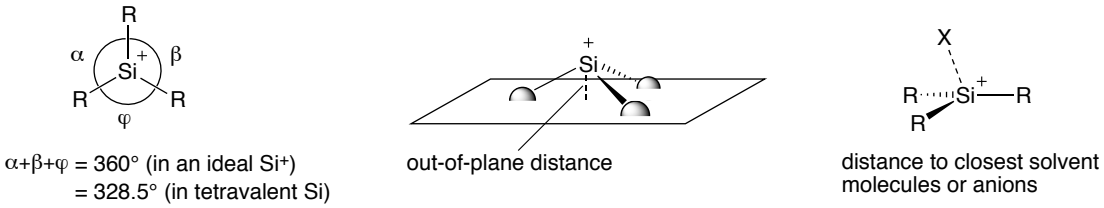

Figure 1.2. Important index numbers: Average R–Si–R angle, out-of-plane distance of the silicon atom, and distance to fourth ligand.

Additionally there are some interatomic distances that might be of relevance. The spacing between the silicon atom and a potential fourth substituent can be compared to their regular bond length. And also the intramolecular bond lengths of that fourth ligand can give an idea of how big its interaction with the silyl cation is, by comparing it to the free ligand.

Since it is not always an easy task to grow a crystal of the desired compound, there is another very useful method of assessing a silane's cationic character. Measuring the ^{29}Si NMR shift of the molecule of interest gives an indication of the electron density on the silicon atom. Whereas tetramethylsilane is standardized to be at 0 ppm, compounds with higher electron density on silicon result in negative values, lower e^- density results in positive values. For silicon the range is very wide. Silylium ion-like species isolated and reported so far are of course in the positive domain and reach up to 230 ppm. Some selected examples are given in Figure 1.4 in chapter 1.1.4.

1.1.2 Synthesis

A reasonable idea regarding the synthesis of a silyl cation would be to attach a good leaving group to the silicon. But as can be seen from Table 1.1, silicon forms very

strong bonds to common leaving groups (like halogens, O-tosylate or O-triflate). Therefore, the products formed during the synthesis of Si^+ have to be very weakly nucleophilic. And since silicon forms rather weak bonds to hydrogen and carbon, this is the way to tackle this challenge.

Table 1.1. Various bond dissociation energies (BDEs) of organic molecules, comparing C–X to Si–X bonds.

	–CH_3	**–SiH_3**	**–CMe_3**	**–$SiMe_3$**
H–	439	384	400	396
Me–	377	375	364	394
MeHN–	–	–	–	418
H_2N–	356	–	356	–
HO–	–	–	398	556
MeO–	–	–	353	515
F–	460	636	496	661
Cl–	350	456	352	490
Br–	294	377	293	427

The most used approaches currently rely on the mixing of a silane with a carbocation (Scheme 1.1). The formation of the silyl cation is then driven by thermodynamics; hydride transfer from silicon to carbon involves cleavage of a Si–H bond and formation of a stronger C–H bond. This usually only requires stirring in an adequate solvent at room temperature for a couple of hours.

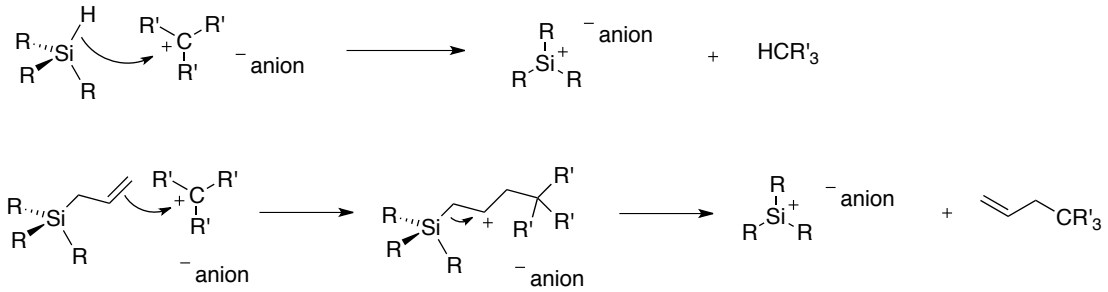

Scheme 1.1. Two common synthetic ways to prepare silyl cations; the hydride shift and the allyl approach.

The Si–C to C–C approach is implemented by using an allyl leaving group. Its doublebond is added to the carbocation, forming the carbon-carbon bond, followed by the release of Si^+. It is often applied for silanes bearing bulky substituents, to

facilitate the contact of the two reaction partners. What has not been mentioned so far, but plays an essential role, is the anion, which is first paired up with the carbocation and then ends up with the silyl cation. This topic is treated in the next subchapter.

1.1.3 Anions

Due to the immense electrophilicity of silyl cations, the choice of the anion is crucial. In order to form a true cation and not an ion pair or a covalent bond, it is necessary to use a very weakly coordinating anion (WCA).[3] And if it had not been for the accomplishments in that field, silyl cation research would not have advanced as it has. As the name already suggests, WCA have a widely distributed negative charge and are therefore only slightly nucleophilic. It also has to be considered that the definition of weak coordination has changed over time. Whereas earlier, I^-, ClO_4^-, or PF_6^- were considered WCAs, the discovery of new highly reactive cations demonstrated their limits. Two classes of anions have proven to be exceptionally reliable, especially in the field of silyl cations. These are the carboranes, which are based on icosahedral boron clusters, developed in the lab of C. A. Reed. And there are tetraaryl borates, of which the perfluorinated species are of special interest in the context of silyl cations. Some examples are displayed in Figure 1.3.

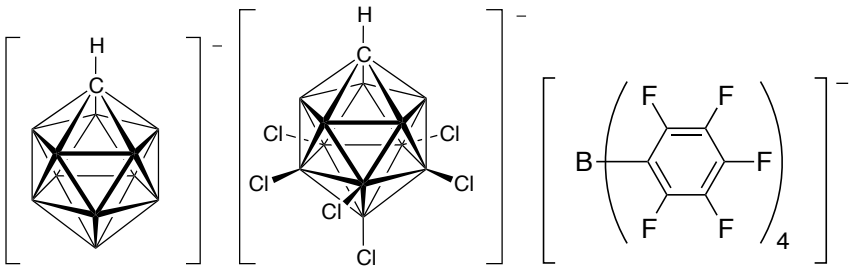

Figure 1.3. Three examples of very weekly coordinating anions; the boron clusters (carboranes), represented by $[CHB_{11}H_{11}]^-$, where each corner is equivalent to B–H and the hexachloro substituted analog. On the right, there is an example of fluorinated tetraaryl borate.

Carboranes have proven to be very stable towards thermal stress and robust in highly acidic environments.[4] Additionally, they often exhibit an increased tendency to form crystals. There is a large variety of derivatives that has been synthesized and characterized.[5] For example halogenation of positions 7–12 makes them less

coordinating and nucleophilic, and at the same time more inert (chemically and thermally). It is a bit counterintuitive that the larger and softer halogens result in more coordinating anions compared to the smaller ones. Halogenation of all boron atoms leads to even less coordinating anions. The carborane that is used in this work is the hexachloro-carborane (Cl_6).

$[B(C_6F_5)_4]^-$ (taken as an example for the tetraaryl borates) on the other hand is less resistant to such harsh conditions.[6] This is the reason why, after some preliminary experiments, it was not considered for usage for the methods discussed in the main chapters. Nevertheless it has its place in silyl cation chemistry and has the advantage of being synthesized rather cheap and easily.

Several methods exist that help to determine the nucleophilicity (or lack of coordination) of anions. For example the average carbonyl stretching frequency of $FeCp(CO)_2Y$ complexes can be examined as a function of the counterion (Y^-) that is used.[7] A higher frequency is equivalent to decreased π backbonding (donation of electron density from the metal to the π*(CO) orbital), which correlates to a stronger cationic character of the metal. This shows a weaker coordination of the anion under investigation. Another method for ranking WCAs that relies on transition metal complexes is the measuring of the out-of-plane displacement of the iron atom towards the anion in an iron(II)tetraphenylporphyrin anion complex (Fe(TPP)Y).[8] Of course a single crystal is needed in order to be able to make these observations. A solution-based method is the determination of the ^{29}Si chemical shift of silyl cations paired with the anion of interest. This approach will be explained shortly.[9] The rankings generated by these different srategies can show slight irregularities in their order. But that is not surprising due to the unique properties of the Lewis acids used.

Another of the anion's characteristics that can make a difference is the solvation energy. Comparing Br_6-carborane with TFPB as counterion of silyl cation; the parameter that has been observed was the tendency of dissociation in toluene (in exchange for a solvent molecule). ^{29}Si NMR shifts of solvent-free solid samples were compared to shifts of dissolved compound. Although being considered less nucleophilic towards Si^+ (from solid-state NMR), the carborane tends to dissociate less from the silicon (resulting in a lower ^{29}Si NMR shift difference of solid vs. dissolved), because, compared to TFPB, less energy is gained by solvation in aromatic solvents.[1b]

1.1.4 Examples

A selection of a couple of silyl cations that have been synthesized in solution, sorted by their ^{29}Si NMR shift, are shown in Figure 1.4. Some of the simplest silyl cations are triethyl (**1**) and triisopropyl (**2**) silylium ions.[10] Since **1** is sterically not very demanding, this kind of cation often experiences interaction with any nucleophile that is present, usually solvent molecules or anions. This is reflected by the ^{29}Si NMR shift and also by the other parameters determined by X-ray crystallography (C–Si–C bond angle and out-of-plane distance). Since there is a fourth ligand, the coordination sphere is not trigonal planar, but starts to adapt a tetragonal symmetry. The ^{29}Si NMR signal is shifted upfield due to electron donation stemming from the π-system of the solvent or free electron pairs of the anion. Cation **2** is better shielded, hence showing a higher ^{29}Si NMR shift.

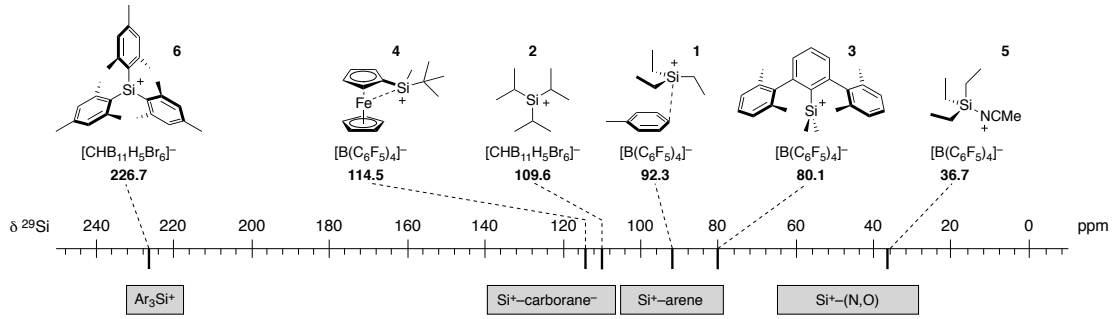

Figure 1.4. Overview of different silyl cations arranged by their ^{29}Si NMR shift.

The possibility of intramolecular donation of electron density to the silicon of course also exists. This has been demonstrated in several different systems. An example for that are the terphenyl compounds developed in our group.[11] In these molecules the silicon atom can coordinate to one of the flanking rings thereby decreasing the silicon atom's positive charge. For example cation **3**, shown in Figure 1.4 contains two xylyl groups attached to the central phenyl ring. Effects of different substituents on the flanking rings have been studied.[12] The group of Oestreich synthesized a ferrocenyl-stabilized silyl cation (**4**), which can be used in synthetic transformations.[13] The molecule is designed in a way that an interaction between between Si and Fe can occur. Coordination of heteroatoms, either intramolecularly or by Lewis basic solvent molecules, drastically move the chemical shift upfield. E.g. the adduct of Et_3Si^+ and

MeCN shown above (**5**) more resembles an ammonium ion than a silyl cation, due to a distribution of the positive charge from the silicon towards the nitrogen atom.

The quest for a free silylium ion ended in 2002, when Lambert and Reed reported a crystal structure of compound **6**, Lambert's trimesitylsilyl cation paired with Reed's $[CHB_{11}H_5Br_6]^-$ carborane anion.[14] The summation of the three C–Si–C angles was described to be 359.9° (±0.2°) and a ^{29}Si NMR shift of 227 ppm was observed in the solid state. This shift was compared to that of the cation in benzene and with $[B(C_6F_5)_4]^-$ as counterion (225.5 ppm) and to the calculated one in gas-phase (226-230 ppm). The only very little differences show that the silyl cation is exceptionally well shielded from the surrounding that it is barely influenced by changes in its immediate environment (like exchange of anion or presence of solvent molecules). The planarity of the silicon coordination sphere, the similarity of the shifts in solid, solution and gas-phase (calc.) suggest that there is no interaction of solvent molecules or anion with the silicon center. There is a close proximity of the *o*-methyl groups to the silicon, but the interaction is thought to be minor (due to only marginal perturbations of the mesitylene). And from these observations it was concluded that a free silylium ion is present. This example perfectly shows that the Si^+ has to be extremely well sterically shielded in order to maintain its cationic character.

As the NMR scale in Figure 1.3 indicates, there is still a lot of unexplored area to investigate.

1.1.5 Reactivity

The better the silyl cations are understood, the more researchers will use them for organic synthesis. There are two distinct properties, which are promising towards the development of a Si^+-based reagent, the extreme Lewis acidity and the exceptional fluorophilicity. Latter will be discussed in another chapter (CF activation).

Most examples for Lewis acid-promoted reactions using silyl cations are probably found in Diels–Alder chemistry. The simple toluene coordinated triethylsilylium ion[15] and the ferrocenyl-stabilized cation[13, 16] could be applied as catalysts for these kinds of transformations. Both silyl cations accelerate demanding Diels–Alder cycloadditions, allowing for low catalyst loading and low reaction temperature. Two selcted examples are shown in Scheme 1.2.

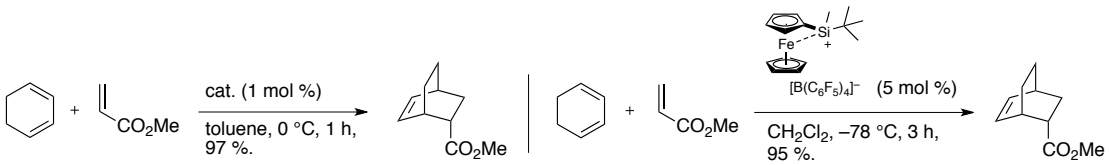

Scheme 1.2. Diels–Alder reactions catalized by silyl cations.

Sawamura *et al.* additionally tested the $[Et_3Si(toluene)]^+$ in Mukaiyama Aldol reactions, where the cation also showed a higher activity compared to conventional Lewis acids like Me_3SiOTf or $Me_3SiN(OTf)_2$ (Scheme 1.3).

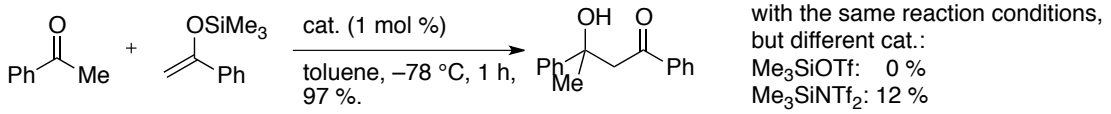

Scheme 1.3. Mukayiama Aldol reaction catalyzed by a silyl cation, showing much higher reactivity than other Lewis acids.

A less prominent example is the deoxygenation of ketones, which was performed by the group of Sakurai in 1992 and is shown in Figure 1.4.[17] *In situ* generation of a silyl cation from trialkyl silane, triphenylchloromethane, and sodium tetrakis(3,5-trifluormethylbenzene)borate (Y^-) can reduce benzophenone to diphenylmethane with a yield of 87 %. Two hydride transfers from trialkylsilane to the intermediate carbonium ions (first and third reaction intermediate in Scheme 1.4) lead to the deoxinated product.

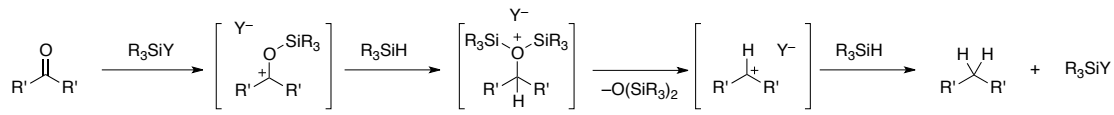

Scheme 1.4. Mechanism of the deoxygenation of ketones using silyl cations, generated in situ.

Oestreich *et al.* reported a similar reaction in 2011.[18] But instead of having a full reduction to the methylene, it stopped at the alcohol level, i.e. the silyl ether (Scheme 1.5). In this case it was taken advantage of the hydride donor strength of the ferrocenylsilane, which reduces the carbonyl-silylium complex to result in an active silylium ion and a silyl ether. This is contrary to the route of the deoxygenation, where the silane not only reduces the activated carbonyl, but additionally forms a silylcarboxonium ion again.

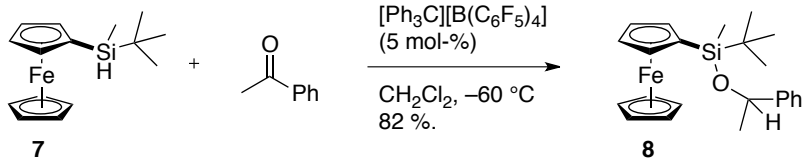

7 8

Scheme 1.5. Reductive hydrosilylation of a carbonyl group, performed in a catalytic fashion, using in situ generated silyl cation.

1.2 C–F Bond Activation

Carbon-Fluorine bonds have gained more and more attention in the last decades. An important reason for that is the discovery of fluorine as substituent in pharmaceuticals, where it affects various properties of an active compound (*e.g.* metabolism, distribution, polarity) and is essential in today's medicinal chemistry.[19] But also in the field of material science fluorine has gained significance, being essential in distinct polymers and liquid crystals. What emerged from the grown interest is a plethora of synthetic pathways for introducing fluorine in organic molecules. With this vast availability of fluoroorganic compounds, a synthetic chemist of course wants to explore the possibilities provided by these carbon-fluorine bonds with regard to chemical transformations. Apart from a small section about the incorporation of fluorine atoms, this subchapter deals with different methods of C–F bond activation and cleavage, and the chances that rise from them.

1.2.1 The Carbon-Fluorine Bond and Its Formation

Considering the chemical and thermal stability of polytetrafluoroethylene (PTFE) or the persistency of chlorofluorocarbons in nature, one already gets an intuitive idea about the carbon-fluorine bond. BDE of the examples shown in Table 1.2 confirm this suspicion - it is one of the strongest single bonds carbon does form. There are two main reasons that contribute to that. The carbon-fluorine bond has a large amount of shared electron density (high electron density at the bond critical point increases the

bond strength), but also a substantial difference in actual atomic charges (which enhances the Coulombic force between the two atoms). And because both atoms belong to the second period of the periodic table, the interatomic distance stays rather short.

Table 1.2. C–F bond dissociation energies of some organic molecules.

	Me–**F**		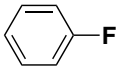	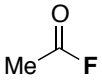
BDE of C–F bond ($kJmol^{-1}$)	480	463	532	511

The simplest reagent for introducing fluorine atoms would be elemental fluorine gas. But since it is so reactive and very difficult to handle, these procedures will be omitted here. First experiments conducted with fluorine gas in 1886 by Mossain and coworkers all ended up in sometimes violent explosions, no matter if the reaction was run at room temperature or cooled with liquid nitrogen.

The next simplest fluorine source is hydrofluoric acid. But also HF is very laborious to handle, due to its corrosive properties (also towards glassware) and its toxicity in combination with a local anesthetizing effect. It can be used as aqueous solution (50 %) or as "tamed hydrofluoric acid" (70 % HF in pyridine or Et_3N-3HF). The most common reactions performed with these reagents are hydrofluorinations or in general nucleophilic fluorinations. The fluoride anion in protic solvents is a poor nucleophile, because it is a good hydrogen bond acceptor and thereby stabilized by the solvent. In aprotic polar solvents however, it turns into a potent nucleophile (also its basicity is much higher).

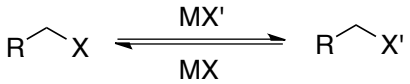

Scheme 1.6. The Finkelstein reaction; exchanging halides or pseudohalides with other halides.

A well-known name reaction for the synthesis of fluoroalkanes is the Finkelstein reaction (Scheme 1.6). By treating an alkyl halide (or pseudohalide) with an alkali metal halide (e.g. KF, KI), the original halide is replaced by an SN_2 reaction. The

equilibrium of the reaction depends mostly on the nucleophilicity of the halide and the quality of the leaving group. An additional factor can be the solubility of the alkali metal halide.

Lewis acid-promoted fluorination is already an old concept, originating in 1892. By the route shown in Scheme 1.7 various fluorine-containing compounds and intermediates can be synthesized.

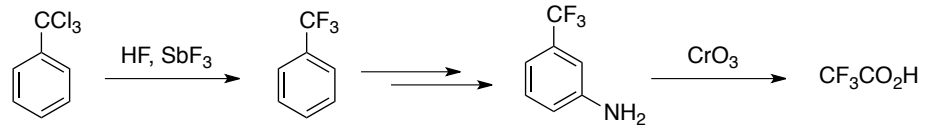

Scheme 1.7. Introduction of fluoride in benzylic position using HF and a Lewis Acid.

Hydrofluorination reactions are preferably carried out with coordinated hydrofluoric acid. Alternatively, an electrophilic halogenating reagent can be added to perform halofluorination (Scheme 1.8).

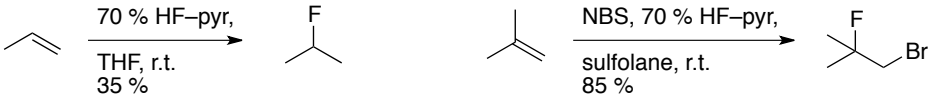

Scheme 1.8. Addition of fluorine to a double bond, optionally halofluorination by adding NBS.

Within time many different reagents working as fluoride source that are stable and more easily to handle than hydrofluoric acid have been developed (some are shown in Figure 1.5). Most of them function best as deoxofluorinating agents, but they are usually applicable in other nucleophilic reactions as well.

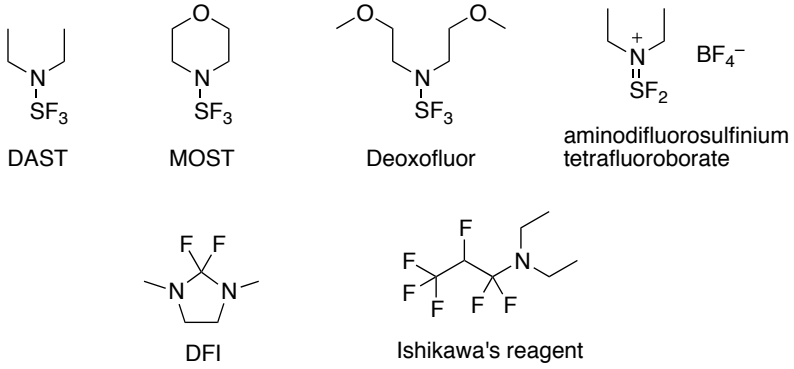

Figure 1.5. Selection of easy-to-handle nucleophilic fluorinating agents.

Fluoroaromatic compounds can be prepared by reductive aromatization of fluorinated alkanes, but introduction of fluorine to an aromatic compound is known too. A prominent example thereof is the Balz-Schiemann reaction (Scheme 1.9). Whereas the first procedure involved the risky isolation of a diazonium salt, newer variants use a more direct approach and are therefore easier to scale up.

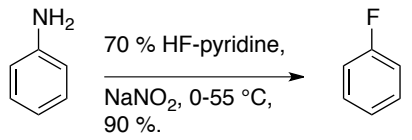

Scheme 1.9. Baltz-Schiemann reaction, transforming aniline into a fluorobenzene via diazonium intermediate.

A development that opened up many new opportunities in fluorine-related chemistry was the discovery of electrophilic fluorinating agents. Some of the most common reagents are shown in Figure 1.6. They allow for fluorination at relatively mild conditions, suitable for late-stage introduction of fluorine in a complex pharmaceutical compound for example. But also direct electrophilic aromatic substitution is possible.

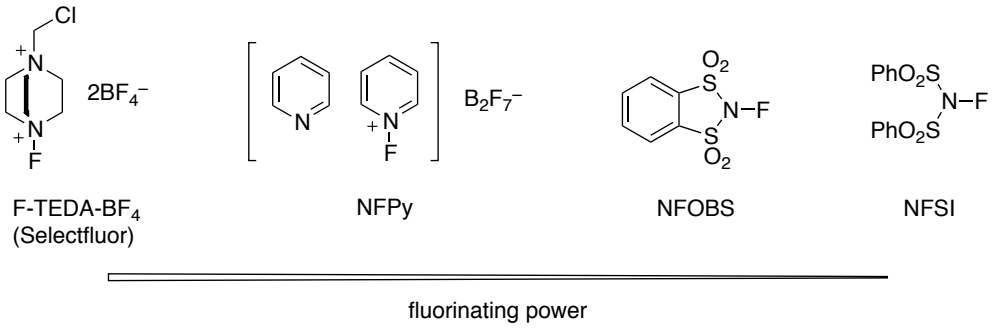

Figure 1.6. Selection of some commonly used electrophilic fluorinating agents, arranged in decreasing fluorinating power (left to right).

An example of electrophilc addition of fluorine to a complex molecule is given in Scheme 1.10, where Selectfluor is used to add F^+ to a vinyl ester in steroid **9**, affording the final product **10**. The addition is regioselective and high-yielding.[20]

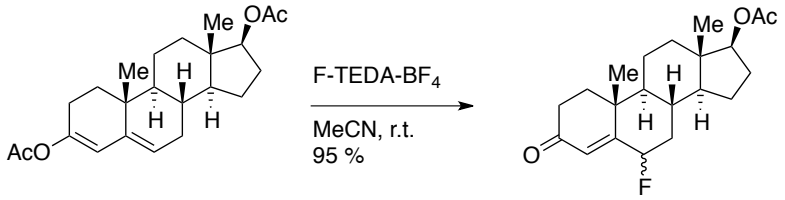

Scheme 1.10. Late-stage introduction of fluorine atom into a steroid derivative, using Selectfluor.

The electrophilc aromatic fluorination is only applied in a few cases of which one example is given in Scheme 1.11.[21] Using the N-fluoropyridinium salt, 1-naphthol was fluorinated in dichloromethane to result in 2-fluoro-1-naphthol, 4-fluoro-1-naphthol, and 2,2-difluoro-1-naphthalenone. It becomes apparent from the mixture of products that this methodology suffers from low selectivity. Furthermore the separation of these isomers renders a severe problem, because of the similar boiling points and polarities of the compounds. And with excellent alternatives like the Baltz-Schiemann reaction or halogen exchange chemistry electrophilic aromatic fluorination remains a field of minor interest.

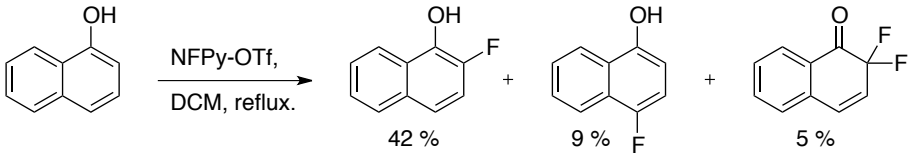

Scheme 1.11. Direct fluorination of 1-naphthol using NFPy, resulting in 2 regioisomers and one doubly fluorinated product.

1.2.2 Carbon–Fluorine Bond Activation

As mentioned before, due to the strong interaction between carbon and fluorine they build up a very inert bond. This bears the advantage that it is not affected by many different reaction conditions that are designed to transform other functional groups. But if activation of the C–F bond and its alteration are desirable, it represents a challenge to find ways to overcome this barrier by either kinetically or thermodynamically favorable reactions. As we will see, the prior is mainly achieved with metals or strong nucleophiles, the later by formation of even stronger bonds.

1.2.2.1 Using Transition Metals

A common way to break carbon-halogen bonds is by oxidative addition to a metal. But while this works very well for iodine, bromine, and even chlorine, it is very slow or not happening at all for fluorine. Therefore the usual reaction conditions for classic coupling reactions leave the fluoroarene unchanged. The first example of catalytic C-C bond formation by cleaving an C(sp^2)-F bond was reported in 1973 by Tamao and Kumada. Catalyzed by a Nickel phosphine complex, fluoroarene was coupled with an isopropyl Grignard reagent to yield isopropylbenzene in 63 %.[22] Since the oxidative addition to Nickel seemed to be successful, Mahan and Fahey looked at this reaction more closely and found the addition to be quite slow. Some examples they reported showed a reaction time of weeks for a yield of only 50 %.[23] It could later be demonstrated that fluoropyridiyl substrates react much faster, which can be rationalized by a chelate-assisted oxidative addition.[24] It was possible to transfer this methodology to many other metals too. These involve Platinum and Palladium[25], Iridium,[26] Rhodium, Tungsten[27], Titanium[28], Zirconium[29], or Ruthenium.

Aizenberg and Milstein introduced a novel strategy for the oxidative addition of hexafluorobenzne in 1994, using a Rhodium complex coordinated by a silyl ligand (**11**).[30] Dimethylphenylsilane facilitates the addition by electron donation to the metal center; but also the formation of a fluorosilane represents a further driving force. Like this, catalytic hydrodefluorination of hexa- and pentafluorobenzene was achieved by forming an intermediate Rhodium-fluoroarene complex (**12**). This stable complex can also be used in further transformations. An example is given in Scheme 1.12 that shows regioselective replacement of fluorine by hydrogen. In this case, silyl ether served as source of hydrogen.

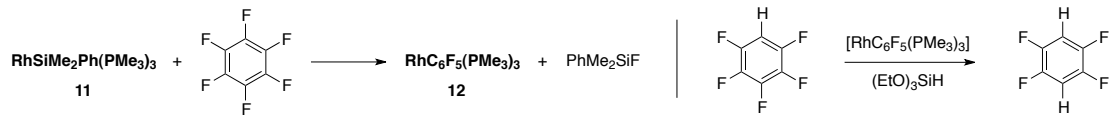

Scheme 1.12. Oxidative addition of perfluorobenzene to a rhodium complex, facilitated by a silane ligand. This complex could then be applied in catalytic hydrodefluorination of pentafluorbenzene.

Only long time after the first reports of the Kumada-Tamao-Corriu reaction, the aryl-aryl coupling could be achieved. Ni-catalyzed cross coupling of fluoroarenes with aryl grignards was performed with N-heterocyclic carbenes[31] and pincer-type ligands.[32]

An example is provided in Scheme 1.13, showing results from Herrmann *et al*. published in 2001. Various mono-substituted fluorobenzenes were coupled with aryl Grignards to result in the corresponding biphenyl derivatives in usually very good yield. Bidentate phosphine ligands were applied in the synthesis of N-heterocyclic biaryls.[33]

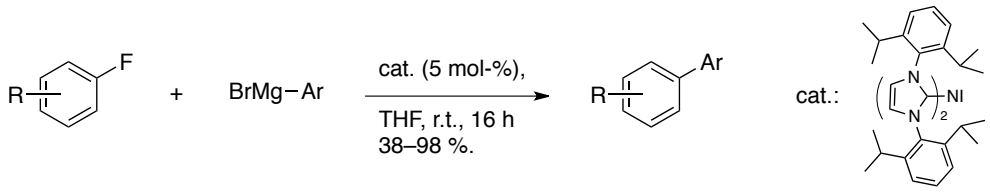

Scheme 1.13. Cross-coupling procedure reacting fluoroarenes with aryl Grignards, catalyzed by a complex of nickel and N-heterocyclic carbene ligands.

Whereas bromo- and iodo arenes undergo rapid Lithium-halogen exchange when exposed to BuLi, fluoroarenes react in a different way. In this case, ortho-deprotonation is much faster and can then lead to elimination of LiF and formation of benzyne. Chlorine analogs undergo aryne formation even faster. The possibility of nucleophilic aromatic substitution by BuLi will be discussed later on.

In contrast to the aromatic system, in fluoroalkanes Li-F exchange can occur. Reaction of primary aliphatic fluorine with excess Lithium yields alkyl lithium, which can be functionalized using an electrophile. Alternatively, Zirconium complexes have been used to reductively defluorinate primary and secondary alkanes.[34]

1.2.2.2 Using Lewis Acids

Several experiments towards C–F activation promoted by Lewis acids were reported by Olah *et al*. They performed studies on the isomerization of halobenzenes under Friedel–Crafts conditions.[35] While no isomerization to difluorobenzene could be observed, it was shown that fluorobenzene can undergo halogen exchange with $AlCl_3$ or $AlBr_3$ at 150-240 °C, resulting in chlorobenzene and bromobenzene. Additionally small amounts of fluorobiphenyls were observed, caused by an electrophilic arylation of a Lewis acid-activated complex. Only ortho- and para-monofluorobiphenyls were observed, supporting the assumption of an electrophilic arylation of fluorobenzene. This stands in contrast to the other halobenzenes. Bromobenzene easily undergoes

isomerization to dibromobenzene, but exchange with $AlCl_3$ is slow and arlyation products could not be observed. An overview of these experiments is given in Scheme 1.14.

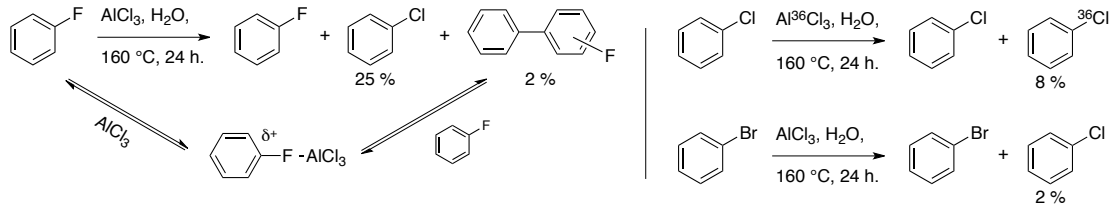

Scheme 1.14. Fluorobenzene can undergo halogen exchange and arylation reactions under Friedel–Crafts conditions at high temperatures. Chloro- and bromobenzene on the other hand do not.

Other reports presented studies on halogen exchange in fluoroalkanes using BBr_3 or $AlCl_3$, or electrophilic substitution of sp^3 hybridized C–F bonds with organoaluminum reagents.[36] Because fluoride in fluoroalkanes can coordinate to Lewis acids more strongly than the other halogens, the carbon-fluorine bond gets activated more easily. It is therefore also possible to selectively activate a C–F bond over a C–Cl bond in a Friedel–Crafts alkylation reaction for example, and one ends up with chloroalkylated arene. This was demonstrated by Olah in 1964.[37]
Activations using the very Lewis acidic silyl cations are treated in a separate chapter.

1.2.2.3 Other Methods

Unlike in S_N2-type reactions, where the elimination is part of the rate determining step (rds), and therefore causing a reactivity profile depending on leaving group qualities (I>Br>Cl>F)[1], aromatic nucleophilic substitution (S_NAr) shows a different picture. Since the rds involves the disruption of the ring's aromaticity during the addition of the nucleophile, the reactivity is reversed due to the high electronegativity of fluorine and the resulting partial positive charge on the carbon atom. If 4-bromo-1-fluorobenzene is reacted with sodium methoxide in MeOH/NMP, the only product observed is 4-bromoanisole. Addition of a metal catalyst (CuBr) and omitting the polar aprotic solvent (NMP) results in formation of 4-fluoroanisole.[38] CuBr is needed

[1] But under acidic conditions, fluoride can be replaced by other halogens, treating the fluoroalkane with HX, probably facilitated by hydrogen bond formation ($RF^{\cdots}HX$), which loosens the fluorocarbon bond.

for the catalytic replacement of bromine and the aprotic solvent is necessary for the S_NAr to occur. This inversion of reactivity is shown in Scheme 1.15. Usually, a strong nucleophile for the reaction with fluoroarene is necessary, i.e. a deprotonated amine, alcohol or thiol. In the case of perfluorinated arenes however S_NAr already occurs without base catalyst.[39]

Scheme 1.15. Reversed regioselectivity of the nucleophilic attack of sodium methoxide with or without CuBr and NMP respectively.

It has been shown that also the hardness of the nucleophile affects the reactivity. While hard nucleophiles react in the order discussed above, for soft ones (e.g. thiolates) the reactivity is inverted again (I>Br>Cl>F).[40]

A quite recent advance in the activation of fluoroarenes was made by Amsharov *et al.*, using activated aluminum(III)oxide (Al_2O_3) as a reagent to promote intramolecular C–C bond formation.[41] Al_2O_3 was activated by annealing at 500 °C and 10^{-3} mbar for 15 min. A large excess thereof was then used to perform ring closing reactions - two examples are pictured in Scheme 1.16. One example shows the transformation of fluorophenylnaphthalene **14** to fluoranthene (**15**), the other one the generation of PAH **16** from substrate **17**. The products are obtained from Soxhlet extraction with toluene, depending on the solubility of the product for up to 3 days. Reaction time and yield vary quite a lot. The reaction takes from 10 minutes up to several days; the yields lie between 30 % and 100 %. There seems to be a relation between the proximity of the C–H and the C–F carbons, i.e. the strain that is introduced in the newly formed cycle. Also an example with an electron deficient ring bearing the C–F bond resulted in a very long reaction time. No explanations were given in the publication.

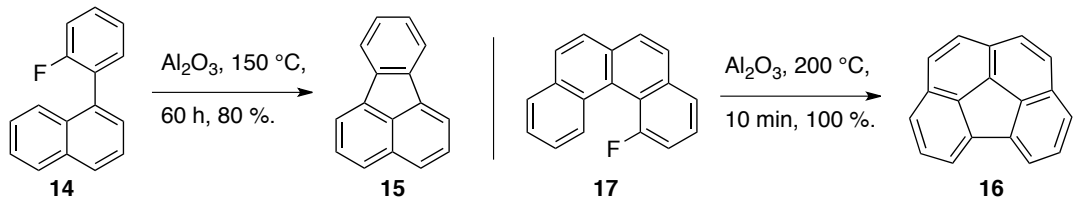

14 **15** **17** **16**

Scheme 1.16. Aluminum oxide-mediated C–F activation followed by intramolecular cyclization.

Several reports on the activation of fluoroalkenes were published as well.[42] They mostly react via an associative mechanism (addition-elimination), because the sp^2 carbon is highly activated towards nucleophilic attack. A method that has greater significance in the context of this work was developed by Ichikawa and coworkers.[43] Several polycyclic aromatic hydrocarbons containing a [4]helicene moiety could successfully be synthesized by activating a *gem*-difluoroalkene with acid, inducing ring formation and subsequent aromatization. The mechanism that was proposed is a domino Friedel–Crafts-type cyclization in which the double bond gets protonated and the resulting difluorocarbocation adds to the arene. A simple example is given in Scheme 1.17 and by attaching naphthyl moieties instead of phenyl in substrate **13**, synthesis of [5]- and [6]helicene can be achieved.

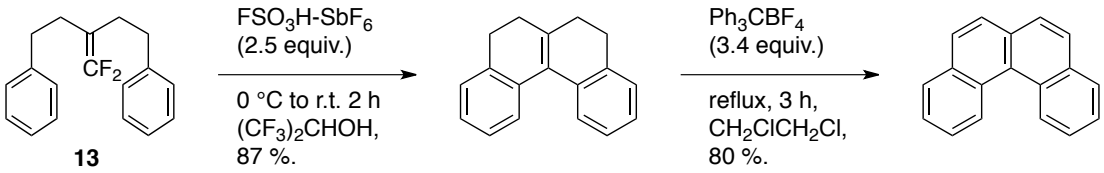

Scheme 1.17. Synthesis of [4]helicene by a Friedel–Crafts-type cyclization of a gem-difluoroalkene

1.2.2.4 Using Silyl Cations

Recently, many efforts in the field of siliyl cation chemistry are directed towards C–F bond cleavage. This tendency arises from the fact that silicon and fluorine form exceptionally strong bonds, of which can be taken advantage. The first successful attempt of catalytic hydrodefluorination of aliphatic and benzylic C–F bonds at room temperature was achieved by Ozerov *et al.* in 2005.[44] The method is based on the *in situ* generation of silyl cations, using trityl cation **18** and an excess of triethylsilane. This excess not only forms the initial silyl cation by reacting with the catalytic amount of **18**, it also transfers hydrides to the carbocations that are formed by fluoride abstraction. Like this, the silyl cation is regeneratedThe method was further improved with regard to robustness by using a carborane counter ion (instead of BArF) and a different silane. When the reaction was performed in benzene, the Friedel-Crafts product could be observed, namely the alkyl benzene. The reaction conditions had no effect on aromatic C–F bonds.[45] Later on, also alkyl chlorides and bromides were

hydrodehalogenated successfully.[46] Some selected examples are shown in Scheme 1.18.

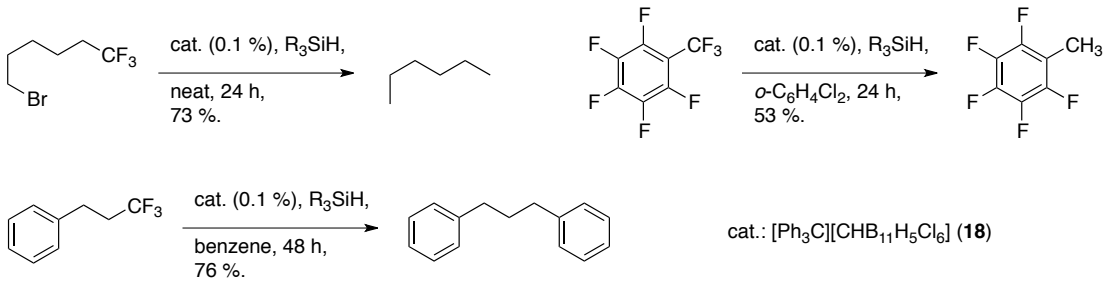

Scheme 1.18. Different hydrodehalogenations performed at room temperature, relying on the in situ generation of silyl cations by Si–H to C^+ hydride transfer.

Similar reactivity in hydrodefluorination reactions was found for the positively charged, hydrogen-bridged disilane **19** developed in the laboratory of Th. Müller (see Scheme 1.19).[47] Using fluoroalkanes and the disilyl cation, this catalytic system was extended towards a Friedel–Crafts-type protocol to alkylate benzene,[48] similar to the reaction reported by Ozerov. Fluorodekane, fluorocyclohexane, and fluoroadamantante in presence of benzene and catalyst resulted in multiple alkylation of benzene. Also the usage of TMSPh instead of benzene could not prevent overalkylation, since formation of the first addition, resulted in further activation of the product towards Friedel–Crafts alkylation, making the alkylbenzene more competitive against the phenylsilane.

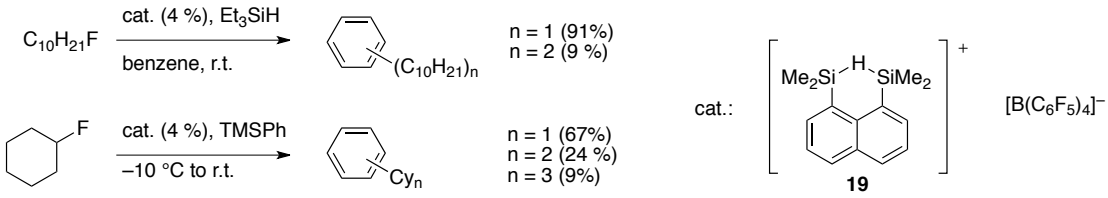

Scheme 1.19. Friedel–Crafts alkylation protocol using the fluorophile disilyl cation, leading to multiply alkylated benzenes.

In our group, first experiments toward carbon-fluorine bond activation were conducted with silyl cation **3**, which is based on an *o*-terphenyl carbon scaffold.[49] When **3** was stirred in fluorobenzene at room temperature for 12 hours, abstraction of fluorine could be observed. Evidence therefor was found in the isolation of fluorosilane **20**. But also the fluorophenyl adduct **21** could be detected, in which the phenyl ring was connected with one of the flanking xylyl groups (Scheme 1.20). This

showed the incipient formation of a phenyl cation, caused by abstraction of fluoride by the silyl cation. It was suggested that the reaction did not proceed via nucleophilic addition and elimination (regular S_NAr), but rather by a concerted mechanism involving the proximity of at least two molecules in the transition state. These experiments paved the way for the method discussed in the main chapters.

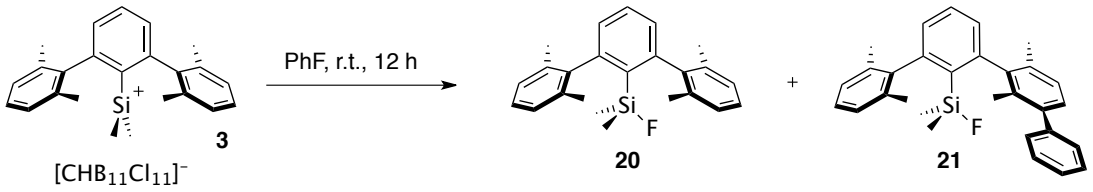

Scheme 1.20. Activation of fluorobenzene, achieved by terphenyl-based silyl cation at room temperature.

1.3 PAHs

1.3.1 Syntheses

The domain of polycyclic aromatic hydrocarbons reaches from naphthalene (the smallest members of the family) to fullerenes, carbon nanotubes and large sheets of graphene monolayer. Some small and planar PAHs are shown in Figure 1.6 (naphthalene (**22**), triphenylene (**23**), and hexabenzocoronene (**24**)). Examples of bent and larger PAH are displayed in Figures 1.8–1.10. The synthesis of PAHs mostly depends on the size of the desired compound. Whereas small PAHs require a bottom-up synthesis, very large aromatic systems are obtained by top-down approaches more conveniently.

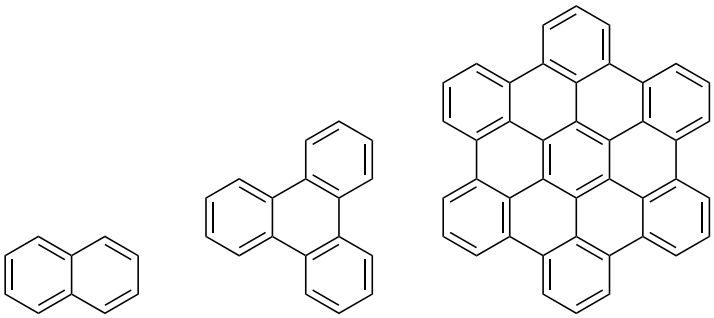

22 **23** **24**

Figure 1.7. Selection of three PAHs; naphthalene, triphenylene, and hexabenzocoronene.

1.3.1.1 Top-Down

Using laser vaporization on a graphite substrate in 1984 afforded a wide variety of carbon clusters.[50] Also contained in this mixture was the C_{60} Buckminsterfullerene (Figure 1.8). Later on, with the same technique, and under distinct reaction conditions, generation of exclusively C_{60} could be obtained, although still in low yield.[51] This changed five years later when the evaporation of a graphite electrode under vacuum resulted in much larger quantities of C_{60}.[52] An arc between two graphite electrodes is ignited, leading to evaporation of carbon. This new procedure led to a high availability of the compound, thus boosting the research on this unique material.

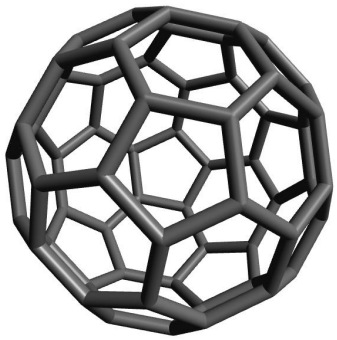

Figure 1.8. Depiction of a C_{60} Fullerene.

Both, laser ablation and arc vaporization can also lead to carbon nanotubes (CNTs). This observation was made in 1991 shortly after the development of the arc technique.[53] It was improved by addition of metal catalyst, which promoted the formation of single-walled CNTs.[54] Also laser ablation afforded swCNT with added

catalyst.[55] Again, this method is not very high yielding, but produces nanotubes with controlled diameter and diameter distribution. CNTs are basically rolled-up sheets of graphene, forming tubes. An example is shown in Figure 1.8.

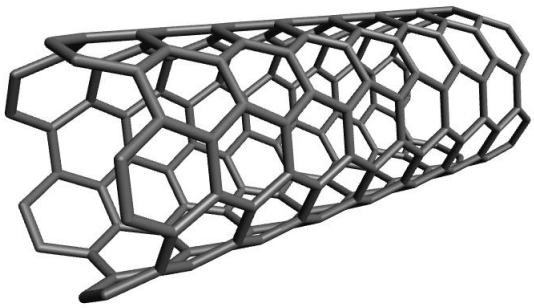

Figure 1.9. Depiction of a carbon nanotube (CNT), showing a zic-zac edge structure.

Chemical vapor deposition (CVD) provides a potent alternative for the synthesis of CNTs. In a very reliable procedure, catalyst particles are formed *in situ* by thermal decomposition in a heated carbon monoxide stream at 1-10 atm and 800-1200 °C.[56] Upon deposition of carbon at the catalyst particle, swCNTs are formed, whose diameter and yield can be controlled by changing certain reaction parameters.

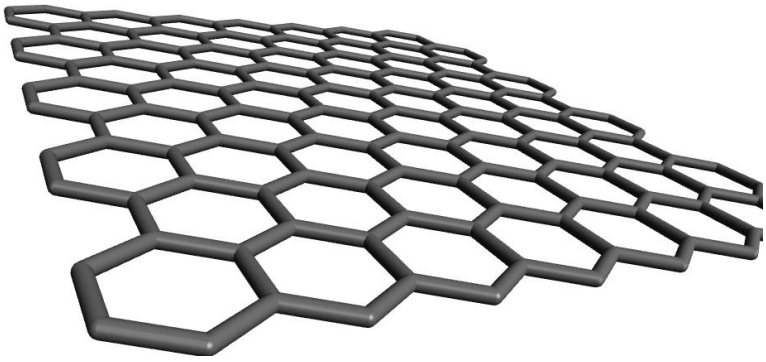

Figure 1.10. Depiction of single-layer graphene, usually referred to as graphite.

Few-layer graphene (including single-layer graphene) was prepared for the first time by mechanical exfoliation.[57] It was obtained by repeated peeling of highly-oriented

pyrolytic graphite using scotch tape. With this convenient approach large PAH in form of single-layer graphene can be isolated. The possibility of creating tailored, well-defined sheets is missing though.

1.3.1.2 Bottom-Up

Bulidung up PAH from small aromatic molecules is usually associated with a multi-step synthesis, depending on the size of the desired product. Most of the methods rely on intramolecular cyclization as the crucial step, which requires the coupling partners to be placed accordingly in the molecule. Even though this pathway turns out to be more costly, many researchers dedicated their career to finding elaborate syntheses of small to large PAH. This is easily rationalized by the fact that with a bottom-up approach, well-defined structures can be tailored.

One of the most popular methods depends on the Scholl Reaction, an oxidative cyclodehydrogenation that is promoted by a Lewis acid. There are two possibilities, intramolecular and intermolecular annulation. The requisite for the first is a predefined network of arenes that has a conformation that allows the formation of 5- or 6-membered rings. There are many reports on the successful usage thereof, also with highly extended systems.[58] However, in cases where different annulations are possible within one molecule, the lack of any directing or leaving group makes the method prone to selectivity issues.[59] An example is given in Scheme 1.21, which shows the formation of the large PAH **25** from the polyphenyl **26**, synthesized in the group of K. Müllen, is shown in Scheme 1.21.

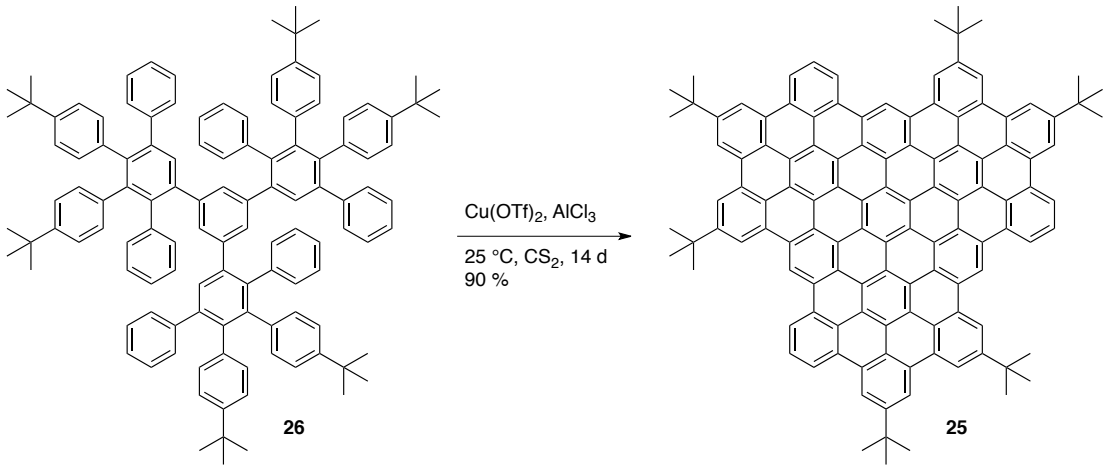

Scheme 1.21. Synthesis of a very large PAH using $AlCl_3$. The starting material was obtained by Diels–Alder reaction of alkyne with cyclopentenaone derivatives.[60]

A method, which is popular for the synthesis of geodesmic PAH (bowl-shaped PAH), is the flash vacuum pyrolysis (FVP).[61] It is based on exposure of the substrate to very high temperature during a short time in gas phase. In an FVP apparatus the starting material is evaporated and, using a nitrogen flow, transported to the hot zone where it is transformed to product, and eventually collected in a cooling trap.[62] To prevent bimolecular reactions, the rate with which the substrate is transported to the reaction zone, is rather slow. The consequence is a dependency of the reaction time on the scale of the reaction. Placing a halogen atom in the right positions can result in higher yields and selectivities because it facilitates radical formation.[63] The yields are usually below 40 % and one also has to consider the stability of the starting material or product since temperatures of over 1000 °C are quite harsh conditions. FVP was applied by L. Scott *et al.* to synthesize dibenzocorannulene (Scheme 1.22).

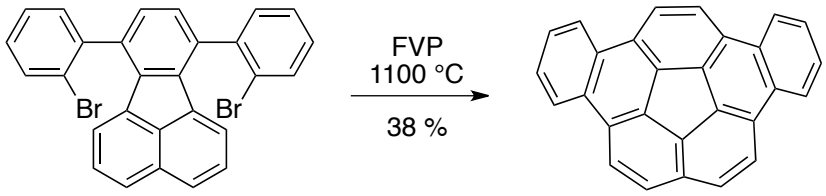

Scheme 1.22. Synthesis of dibenzo[a,g]corannulene using flash vacuum pyrolysis.[61a]

An alternative method thereto involves the intramolecular coupling of an aryl bromide or triflate with an unactivated arene, catalized by Palladium. The reaction conditions comprise high temperatures and a Pd(II) species to result in good to high yields, depending on the strain that comes along with the formation of the cycle(s). Scheme 1.23 shows an example by J. Rice.[64]

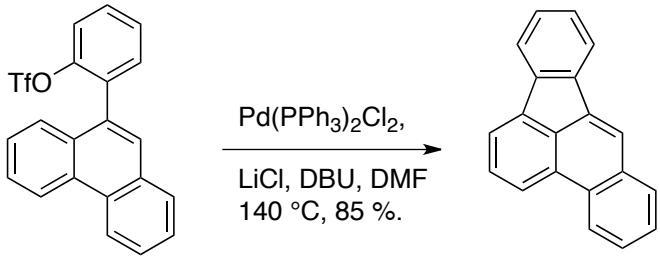

Scheme 1.23. Example of a Palladium-catalized cyclization leading to benzo[b]fluoranthene.[64b]

There are various other procedures described for the synthesis of specific PAH. Their strategies for the cyclization include strong base,[65] a low-valent Ti-based reductive

system,[66] ring closing metathesis[67], or photochemical cyclization,[68] just to name some.

What is important towards applications of PAH is derivatization or functionalization. Since the methods presented are all not very tolerant towards functional groups, the general strategy is to introduce heteroatoms after the synthesis of the PAH.

1.3.2 Applications

The low HOMO-LUMO gap that is characteristic for the extended π-system of the PAH makes them promising components for devises in the field of optoelectronis. Also the unique electronic properties of the planar structures can be interesting toward the development of nanoelectronics. This subchapter gives a brief overview of where PAH or functionalized PAH are applied in material research. Presented are only some prominent examples and a rudimentary description of the way they work. In research their is a much broader scope of applied PAHs, like microbial fuel cells, receptors, photopolic materials, or photochromism, just to mention a few.

1.3.2.1 Semiconductors

As the name already indicates, the conductivity of semiconductors lies between that of insulators and conductors. The different properties stem from the band gap of the valence band to the conduction band, which in metals is zero and for insulators becomes very large. In order for a material to be able to conduct electrons, the energy of the band gap has to be small enough to be overcome by electrons. Therefore, semiconductors have an enhanced conductivity at high temperatures (when the electron's energy is large), and basically none at very low temperatures. Another way to improve the conductivity is achieved by doping the semiconductor with well-defined impurities that create free electrons or holes in the material, and thereby providing mobile charges.

While common semiconductors are made of silicon, germanium, or gallium-arsenide, they can also be built up from organic molecules (low molecular weight single molecules or polymers - a couple of examples are shown in Figure 1.11). The

fundamental difference lies in the intermolecular bonding, which in organic molecules is only based on van der Waals and dipole interactions (compared to covalently bonded Si for example). On one hand this results in different mechanical properties like reduced hardness, making them highly adaptable. On the other hand there is a much weaker delocalization of electrons, which leads to a lower charge carrier mobility and thereby decreasing the performance (with regard to electronic devices).

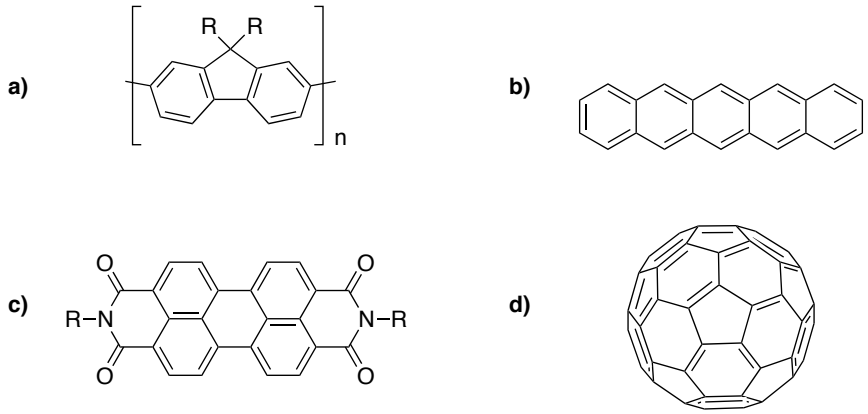

Figure 1.11. Selected examples of some organic semiconductors. a) polyfluorene (PFO), b) pentacene, c) perylene-3,4,9,10-tetracarboxylic-3,4,9,10-diimide (PTCDI), d) C_{60} Fullerene.

One main advantage of organic semiconductors lies in the production. Whereas traditional Si-based devices require high-temperature and high-vacuum deposition processes as well as sophisticated photolitographic patterning methods, organic materials can be deposited from the gas phase at low temperatures. Available methods for polymers are spin-coating or printing. As a consequence, these materials can be transferred onto flexible plastic, which gives the opportunity of creating bendable (or foldable) and lighter devices. And the low costs of these procedures allow for a cheap production of organic semiconductor-based materials.

1.3.2.2 Organic Field-Effect Transistors (OFETs)

A transistor is an electronic device that can function as an amplifier or as a switch, i.e. it enhances the power of a signal or transforms voltage into an on-/off-signal respectively.

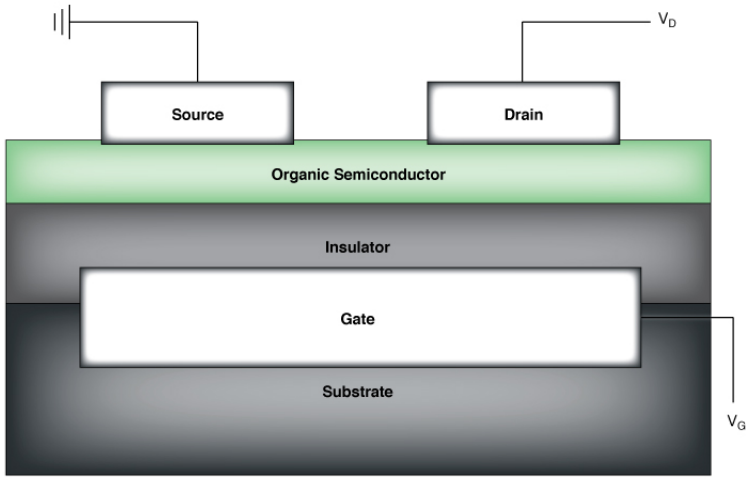

Figure 1.12. General build-up of an organic Field Effect Transistor (OFET). By Applying voltage at the gate, current (transportation of holes or electrons, depending on the organic semiconductor) can start to flow between source and drain.

A common build-up of an organic transistor is depicted in Fig. 1.12 and is an equivalent of its inorganic Si-based counterpart. It consists of three terminals of which the gate controls the current-flow between source and drain. The electric field generated by an applied voltage between gate and source induces enhanced charged carriers at the semiconductor-dielectric interface. Depending on the applied voltage (positive or negative) of the gate, either electrons (n-channel) or holes (p-channel) are accumulated and transported between the electrodes and thereby allow current flow. Unlike in classic Si-semiconductor-based devices, where the mode of conduction depends on the minority carriers (electrons for p-doped material and holes for n-doped semiconductor). But there are also preferred compounds in OFETs for each mode in order to increase the OFET's performance. Important measures therefore are the mobility (μ [$cm^2V^{-1}s^{-1}$]) and the on/off ratio of the transistor. The prior has a direct influence on the switching speed of the device and has in the meanwhile surpassed the charge mobility of a polycrystalline (amorphous) Si-device (0.1-1 $cm^2V^{-1}s^{-1}$), the latter gives information on how effective the device can shut down (I_{on}/I_{off}).

1.3.2.3 Organic Light-Emitting Diodes (OLEDs)

Another possibility of making use of PAHs are organic light-emitting diodes (OLEDs). In a simple set-up two layers of organic semiconductor are placed between two

electrodes (Figure 1.13). One of the semiconductor layers is predestined for transporting holes; the other one should favor carrying electrons. If voltage is applied in a way that the anode is connected to the hole-transport layer, it can inject holes into the organic material, which then travel towards the cathode. At the same time, the cathode injects electrons into the electron-transport layer. The electrons are transferred into the direction of the anode and near the junction of the two materials, in the luminescent ETL, holes and electrons can recombine and the organic molecules emit light in a specific wavelength. There are some important factors that have to be considered when choosing materials and designing an OLED. A high internal electroluminescence quantum efficiency (close to 1) is required. This means that most of the excited electrons should relax by emitting light.

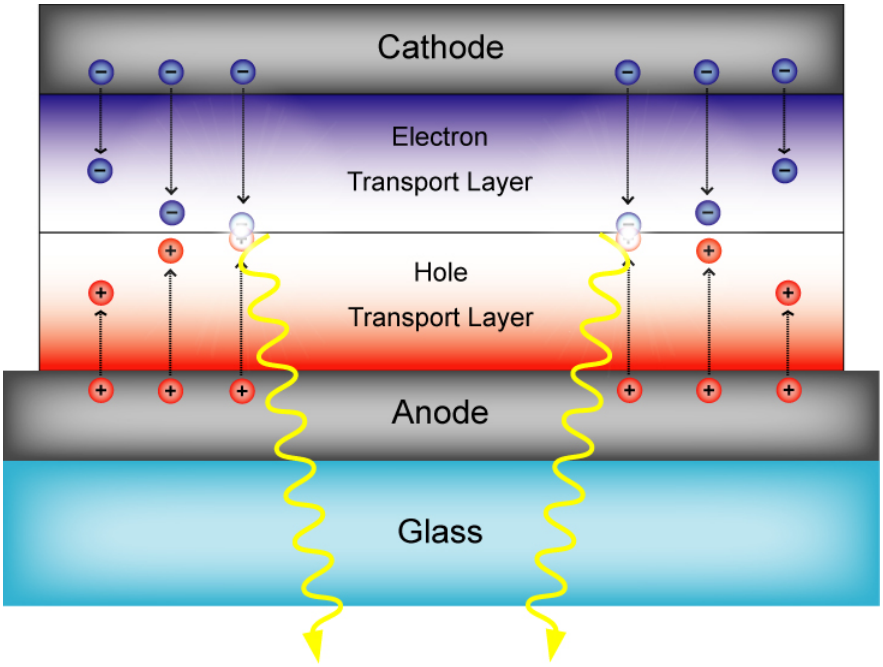

Figure 1.13. General set-up of an OLED device; application of a potential leads to recombination of holes and electrons at the junction of the two organic layers, which leads to emission of light.

A high fraction of the created photons must reach the surface, which describes the so-called outcoupling efficiency, and the energy loss during the conversion of excited electron to photon emission should be as small as possible. Like this the device can be operated at a low voltage.

1.3.2.4 Organic solar cells

Whereas in OLEDs one creates light from energy, in photovoltaic cells (or solar cells) one can gain electric power from absorbing light. Therefore the design and the operating mode of a solar cell are very similar to those of an OLED (shown in Figure 1.14). They exhibit the same sandwich geometry consisting of two electrodes, one conventional (e.g Aluminum) and one transparent, and an active layer in between. The operating principle is then just reversed, compared to an OLED: light is absorbed by the active layer and a photon is transformed into an exciton (bound excited electron-hole pair), which is then transferred to a region where the charges are separated (exciton dissociation).

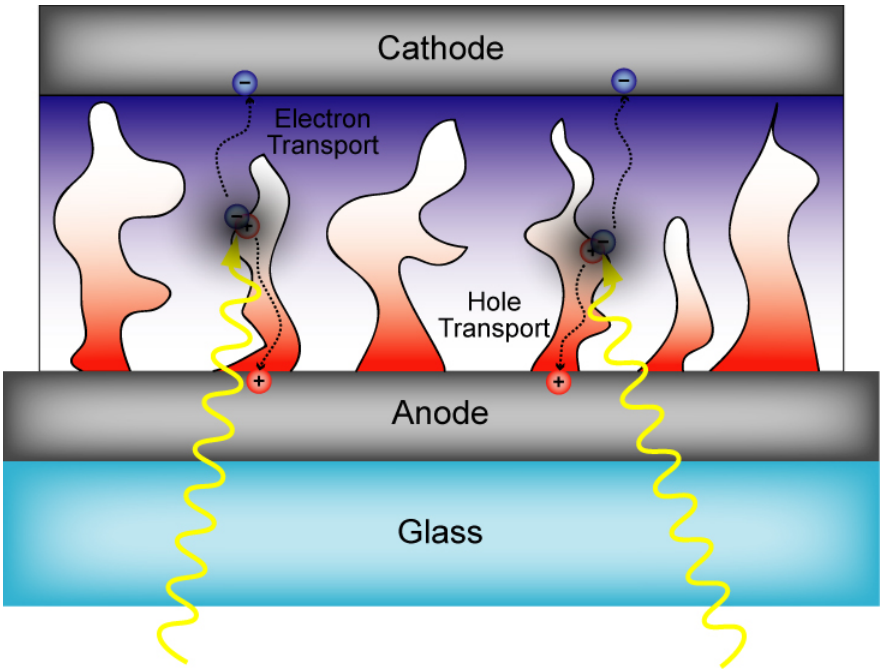

Figure 1.14. Composition of an organic photovoltaic cell using bulk heterojunctions to reduce distances between exciton creation and charge separation.

This can happen at the donor-acceptor interface, where the excited electron of the chromophor is transferred to the lower lying LUMO of the acceptor material. The hole and the electron then move towards opposite electrodes and thereby creating current flow. This whole process requires certain characteristics of design and materials. It is desirable for the organic compound (polymer or single molecule) to have a low band gap in order to be able to absorb a wide spectrum of the sun light. The band gap of a compound can be altered by derivatization or extention of the π-system. Also the processability is an important factor, because this is again a main advantage of

organic solar cells over Si-based solar cells. For small molecules vacuum evaporation/sublimation is a clean and convenient method for making thin films. Semiconductive conjugated polymers are usually processed by solution-based methods (like spin-coating or inkjet printing). The distance an exciton has to cover until its charges are separated has a direct influence on a sollar cell's efficiency. The shorter the distance between exciton creation and charge separation, the higher the probability of the exciton to be able to dissociate. The same applies for the thereby generated charges. The electron and holes should reach their corresponding electrode within their lifetime. This is why not only simple bilayers are considerd, but also so-called bulk heterojunction devices, which consist of blends of donor and acceptor components to keep distances to donor-acceptor interfaces below exciton diffusion length.

1.3.3 PAHs as Environmental Toxins[69]

PAHs were initially mostly known as ecotoxicological hazards. Since they make for 13 – 20 % of the composition of crude oil, most of the PAH enter the environment by incomplete combustion processes, like exhaust fumes or burning wood or coal. Also wash out of asphalt or tar enhances their concentration in nature. The most intense exposure to humans comes from smoking cigaretts, where PAH are contained in the tar. Because these compounds usually are nonvolatile and are not degraded by microbes (although photlytically oxidizable), they are very persistent pollutants and are accumulated in sediments. Besides the persistency, PAH show a strong lipophilic character (high K_{OW}).

$$K_{OW} = \frac{c_X \text{ in 1-octanol}}{c_X \text{ in water}}$$

Equation 1.1. The K_{OW} is determined by distribution of the compound of interest in a 1:1 1-octanol/water mixture, and is a very common benchmark for the lipophilicity of a chemical.

This usually means that they have the tendency to penetrate the lipid bilayer of a cell membrane much more easily and therefore accumulate faster in an organism (Figure

1.15). This property also depends on the distinct molecular features (e.g. size) though.

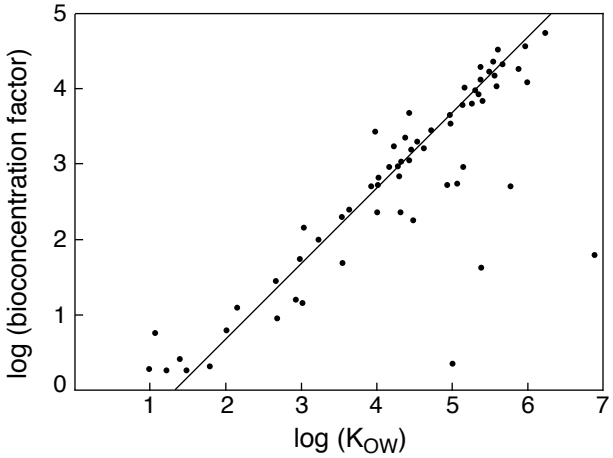

Figure 1.15. This graph shows the linear correlation of the partition coefficient K_{OW} and the bioconcentration factor - the higher K_{OW} of compound X, the higher the concentration in the cell.[70]

Most PAH are considered mutagenic or carcinogenic, especially due to very reactive metabolites. A factor that leads to their potency is the so called bay region occurring in certain non-linear PAH (e.g. benzo[a]pyrene).[71] PAH that contain such a region usually have a strong affinity towards the Cytochrome P450 system which can oxidize these compounds to alcohols or epoxides. These metabolites can then form bioconjugates, which leads to excretion and therefore detoxification. But certain metabolites in the pathway are very toxic, because they can bind RNA, DNA or peptides and this can be a cause for cancer. An example of detoxification and bioactivation is given for benzo[a]pyrene (BP) in Scheme 1.24. During this process the mutagenic metabolite **27** is produced, whereas the other pathways lead to degradation of the initial PAH.

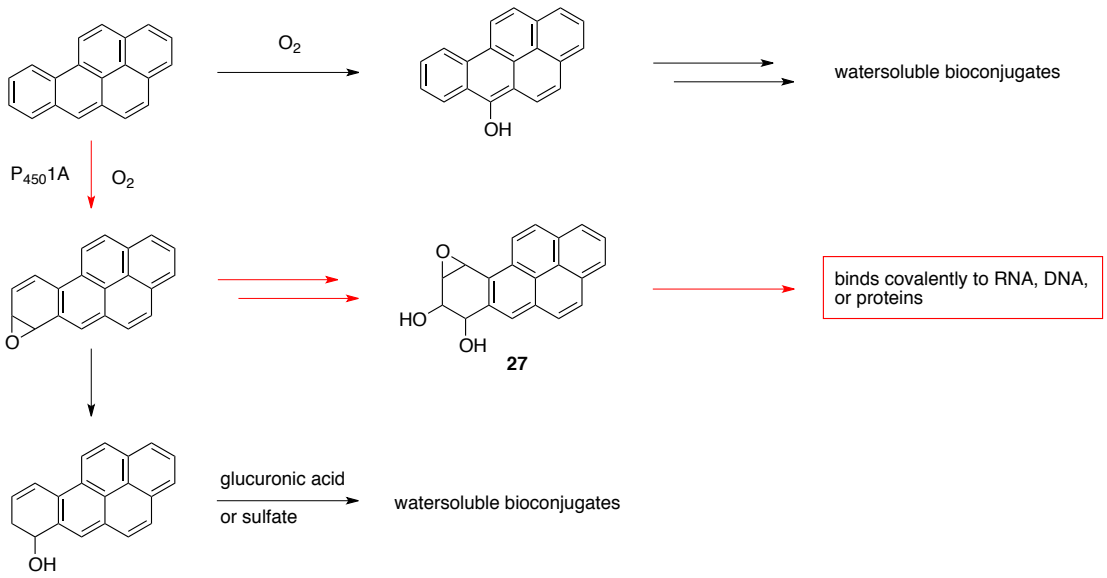

Scheme 1.24. The bioactivation pathway (red arrows) which leads to a mutagenic metabolite **27**, and the detoxification pathway (black arrows) which leads to bioconjugation and finally excretion.[69]

2 Friedel–Crafts-type Arylation by C–F Bond Activation

2.1 Intramolecular Arylation

2.1.1 Summary

A new strategy for the intramolecular coupling of fluoroarenes with arenes was developed. The activation of the C–F bond is achieved by applying a very strong Lewis acid, a silyl cation, thus taking advantage of the strong affinity of silicon towards fluorine. During the abstraction of fluoride by the silyl cation, the incipient phenyl cation is attacked intramolecularly by an adjacent aryl moiety. The proton liberated after the cyclization that forms the product can be captured by a sterically hindered base, like 2,6-tert-butylpyridine (**28**). With this approach, an equimolar amount of silyl cation is required. Alternatively, the base can be replaced by dimethyldimesitylsilane (DMDMS), which upon protodesilylation regenerates Si^+, thereby making the reaction catalytic with regard to the initiator (silyl cation or very strong acid). A proposed mechanism is depicted in Scheme 2.5. The catalytic reaction protocol could be improved by heating with microwave irradiation - reaction time and catalyst loading could be reduced significantly. The lack of a transition metal and sole use of a Lewis acid to activate a carbon-halogen bond to form a C–C bond to a non-activated arene, makes this procedure an extension of the Friedel–Crafts methodology to arylations.

2.1.2 Non-Catalytic Method

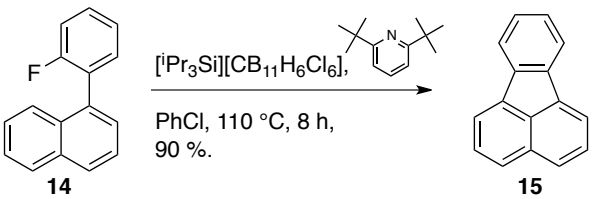

14 **15**

Scheme 2.1. C–F activation using 1 equiv. of triisopropylsilyl cation and 2,6-di-tert-butylpyridine as base.

The observation that led to the development of the intramolecular Friedel–Crafts-type arylation was already described in section 1.2.2.4 (Scheme 1.20). The fact that the silyl cation was able to abstract fluoride from fluoroarene was unprecedented and research efforts into this direction were intensified. It was assumed that an intermediate phenyl cation had formed, which was either captured by one of the flanking rings of the terphenyl silyl cation system or a nearby anion. Therefore, the development of an intramolecular reaction protocol appeared to be the next practical step. With the coupling partners already in place one does not need to worry about bringing them together.* As a model substrate, 1-(2-fluorophenyl)naphthalene was synthesized. Activation of the C–F bond by a silyl cation and subsequent nucleophilic attack by the naphthyl moiety would result in the loss of fluorosilane and in the formation of a five-membered ring to generate protonated fluoranthene (Scheme 2.2). The exact order of the substitution (addition-elimination, elimination-addition, or concerted) should not be of any concern right now. In order to remain controlled reaction conditions and to prevent acid-catalized polymerization, the proton must be captured by a base. But because silyl cations are such strong Lewis acids, the base has to be highly sterically demanding. Otherwise it might form a Lewis acid-base pair with the silyl cation, which would be deactivated towards C–F activation. First attempts were carried out with tri(*o*-tolyl)phosphine as a base – [$^{i}Pr_3Si$][$CHB_{11}H_5Cl_6$] was the silyl cation of choice. The triisopropyl silyl cation was expected to be reactive enough and it is a solid that can be stored easily in the glovebox, without decomposing. The carborane counterion was selected due to its robustness. Stirring the substrate and reagents in chlorobenzene at 110 °C for 12 h afforded fluoranthene in 80 % yield.

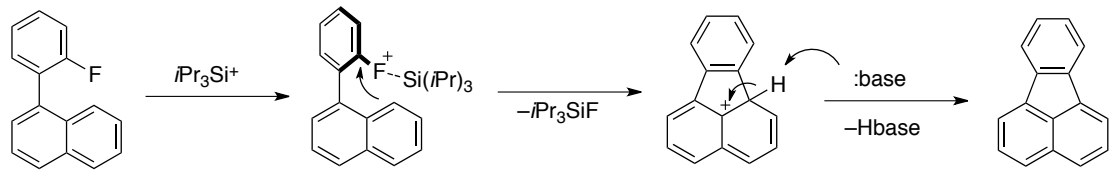

Scheme 2.2. Nucleophilic aromatic substitution promoted by a silyl cation and a base.

* Results of investigations towards an intermolecular procedure are discussed in a later chapter.

But problems with the purification of the product, caused by $[HP(o\text{-tol})_3]^+$ that was hard to separate from the product, led to the search of another base. 2,6-di-*tert*-butylpyridine was a viable replacement. There was no interaction with the silyl cation that would slow down the reaction, and also, the product could be separated easily by flash column chromatography. Reaction time of 8 h led to product formation with a yield of 90 % (Scheme 2.1). The carborane, of which an equimolar amount is needed, can be recovered during the work up, adding CsCl followed by precipitation of $Cs[CHB_{11}H_5Cl_6]$. But since this is the most expensive component, also a catalytic method was developed.

2.1.3 Catalytic Method

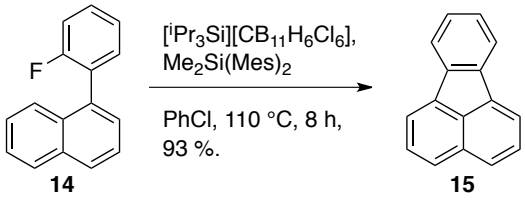

Scheme 2.3. Catalytic intramolecular cyclization using 10 mol-% of silyl cation and $Me_2Si(Mes)_2$ (DMDMS) as base and Si^+-source.

Looking at the reaction mechanism, it seems inevitable that an equimolar amount of silane is needed. But this does not mean, that one equivalent of silyl cation is necessary. Apart from the fluorosilane that is formed, there is also one equivalent of proton that is generated. The plan was to use this highly acidic proton to regenerate silyl cation. A possibility to do so is to make use of the concept of protodesilylation.[72] The protonation of a double bond or an aromatic moiety in alpha or beta position to a silicon atom, results in elimination of a formal positively charged SiR_3. Usually, this is accompanied by simultaneous attack of a halogen nucleophile at the silicon, to yield $XSiR_3$ and the alkene or arene. But under our non-nucleophilic reaction conditions it is possible to generate a silyl cation again, which of course could also be coordinated to the fluorine of the substrate, to solvent or the carborane anion.

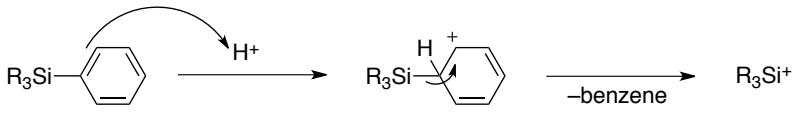

Scheme 2.4. Protodesilylation in very non-nucleophilic media can lead to the formation of silyl cation.

If the defluorination and the protodesilylation are combined, every product formation leads to the creation of a silyl cation, as long as there is enough silane available. Like this, the reaction protocol becomes catalytic with respect to the usage of carborane, and in return, the much cheaper silane is used in equimolar quantities. The proposed catalytic cycle is pictured in Scheme 2.5. Dimethyldimesitylsilane (DMDMS) proofed to be a suitable source for silylium ions. Under similar conditions as the non-catalytic method, the product was obtained in 93 % yield requiring only 10 mol-% of silyl cation (Scheme 2.3). Since the silyl cation is generated with an acidic proton, the reaction can be initiated with a strong Brønsted acid, too. A prerequisite is the release of carborane as conjugate base, to serve as counterion for the silyl cation. This way of initiation was successfully demonstrated by the use of protonated mesitylene paired with $[CHB_{11}H_5Cl_6]^-$.

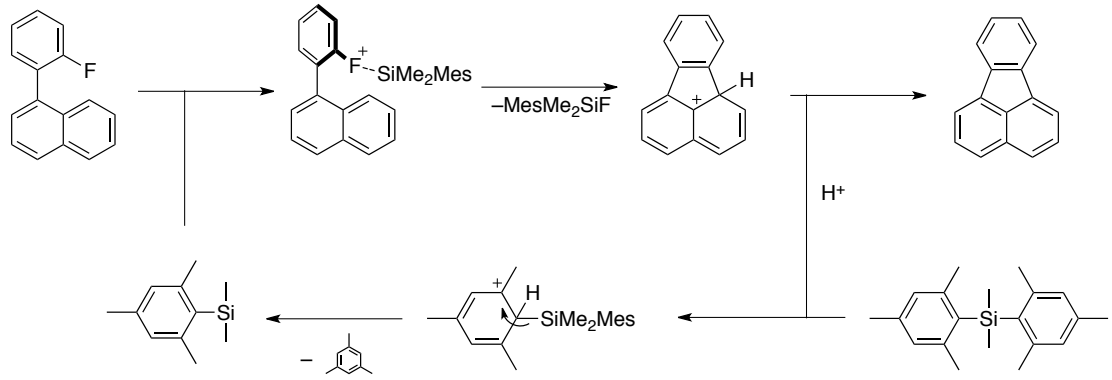

Scheme 2.5. Proposed catalytic cycle with product formation (top, left to right) and silyl cation regeneration (bottom, right to left).

2.1.4 Microwave Reaction

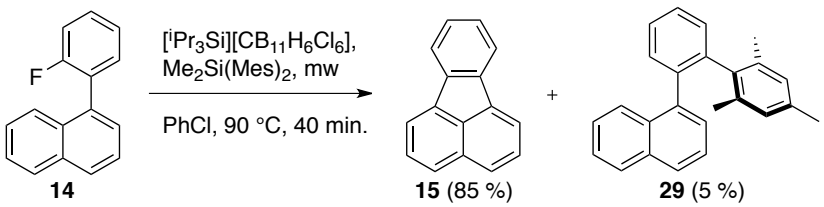

14 **15** (85 %) **29** (5 %)

Scheme 2.6. Intramolecular cyclization, applying microwave irradiation and 5 mol-% of silyl cation.

The catalytic method, which allows for a usage of only 10 mol-% of $[^iPr_3Si][CHB_{11}H_5Cl_6]$ as initiator, was further improved by heating the reaction in a

microwave reactor. The reaction time could be shortened from 8 h to 40 min (in case of the model substrate) and the catalyst loading could be reduced to only 5 mol-%. The yield is slightly lower due to a side reaction (Scheme 2.6) that is somehow facilitated by this method. The observation of the mesitylated phenylnaphthalene **29** suggests an intermolecular coupling between the starting material and mesitylene, either from solution or directly from DMDMS.

2.1.5 Mechanism

Table 2.1. Bond dissociation energies (BDE in kJ/mol), bond lengths (in Å), and the added up van der Waals radii (in Å) of the involved atoms.

bonds broken				**bonds formed**			
	BDE	bond length	combined vdW radii		BDE	bond length	combined vdW radii
Ph–F	532	1.36	3.17	Si–F	661	1.59	3.57
Ph–H	472	1.08	2.80	Ph–H	472	1.08	2.80
Ph–SiR_3	400	1.87	3.80	Ph–Ph	494	1.49	3.40

From looking at the bond dissociation energies (BDEs) of the bonds that are formed and the ones that are broken, it becomes evident that the overall reaction releases energy, i.e. it is thermodynamically favorable. The indicated BDEs in Table 2.1 are based on homolytic bond cleavage. And although our reaction does not proceed via radical pathway, the BDEs can adequately represent the driving force in this transformation. By making a statement about the thermodynamics of the reaction, it is not of any concern how the starting molecules are transformed to product. Potential energies in the beginning and in the end are compared. Also the products obtained consist of covalent bonds and do not result in ions (C–F does not become C^+ and F^-, but C–C and Si–F). This might not be very accurate, and therefore any quantitative statement will be avoided. Concerning the kinetics of the reaction, a calculation of the transition state revealed the abstraction of the fluorine as rate determining step (Figure 2.1). The transition state shows a highly stretched Ar–F bond (2.55 Å). Although it is still within the van der Waals radii of the two atoms (1.70 Å + 1.47 Å = 3.17 Å), it is far from a regular C(Ar)–F bond distance (1.36 Å).[73] This indicates a dissociation of fluorine, which is confirmed by the Si–F distance that is already very similar to the one in the product (1.60 Å).[74] The C–C bond to be formed has a length of 2.86 Å in the transition state. This is as well a huge difference to the

final C(Ar)–C(Ar) distance (1.47 Å). A dissociative mechanism seems to be predominant; the abstraction of the fluoride is more advanced compared to the addition of the naphthyl moiety. But one also has to mention that the lengths of the formed and broken bond at the transition state are still within the van der Waals radii of the involved atoms.

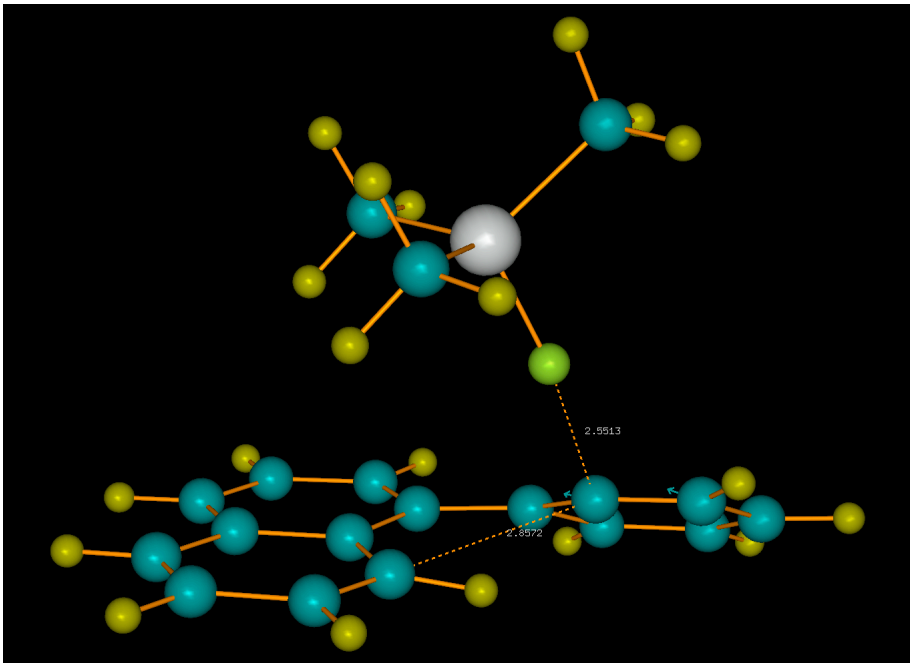

Figure 2.1. Calculated transition state of the intramolecular cyclization of 1(2-fluorophenyl)naphthalene to fluoranthene using a silyl cation for C–F bond activation (E_a=82.8 kJ/mol).

Figure 2.2 shows a scale of the lengths of the three bonds that are crucial in the transition state of the transformation of starting material to product: Formation of the Si–F bond, breaking of the Ar–F bond, and formation of the Ar–Ar bond. The green area represents the regular length of the corresponding bond, the yellow line is the distance, which was calculated for the transition state, and the red area implies the range of interaction between the two atoms, derived from their added van der Waals radii. One has to consider that the attractive force between two atoms does not decrease linearly with distance, but rather exponentially. What can be seen is that the abstraction of fluoride is almost completed, due to the short distance between silicon and fluorine and the almost non-existing interaction between arene and fluoride (close to distance of added van der Waals radii). Also the separation between the two arenes is very far from a typical bond length.

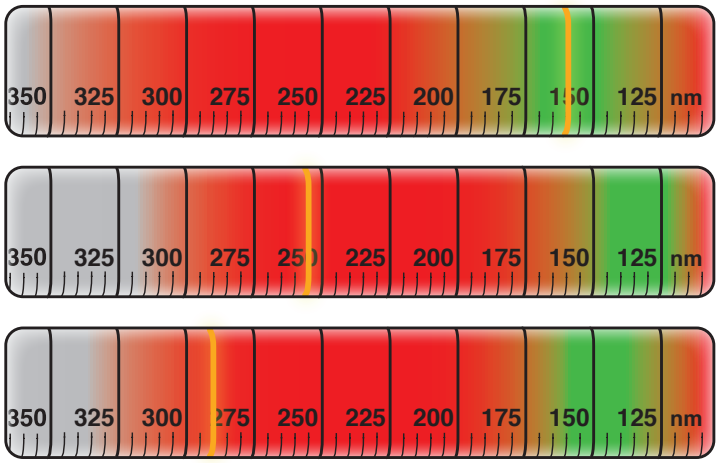

bond	distance in transition state
Si–F	160
Ar–F	255
Ar–Ar	286

Figure 2.2. Distances between atoms involved in the reaction during the transition state. Colored area is distance within van der Waals radii, green area is the regular bond length, the orange mark is the distance calculated for the transition state.

2.1.5.1 Influence of Electron Density of the Involved Aryl Rings

A series of terphenyl substrates containing methyl groups on either the fluoroarene, or the ring undergoing the nucleophilic attack (Structures **30**–**34**) was examined with regard to their reaction rate. The four substrates were subjected to a competition experiment, where each one was exposed to the reaction conditions in the presence of another terphenyl. The amount of reagents was chosen in a way that the reaction could not run to completion. The resulting ratios of the two different starting materials and the two corresponding products were analyzed by GC–MS.[2] The results are shown in Figure 2.3 and can be summarized by stating that the higher the electron density (induced by a methyl substituent), the faster the reaction occurs. There are a couple of considerations regarding this experiment. From the calculated transition state, one would expect a higher effect of a methyl group on the fluoroarene than on the other ring. The reason for that is the positive charge that is created on the fluoroarene by the abstraction of fluoride. The positive charge could be stabilized by electron-donating groups attached to the fluoroarene. Increased electron density on the attacking ring would make it more nucleophilic, but since the abstraction of fluoride is the rate determining step, the rate of the nucleophilic attack should not have a big influence on the overall rate. The experimental results, gained by the

[2] The relevant compounds were calibrated beforehand.

methyl-substituted terphenyl substrates, cannot really confirm this hypothesis. But it is also important to know that the differences in reaction rate are very small, indicating a diminishing effect of the methyl group. Bromine-substituted substrates gave much clearer results.

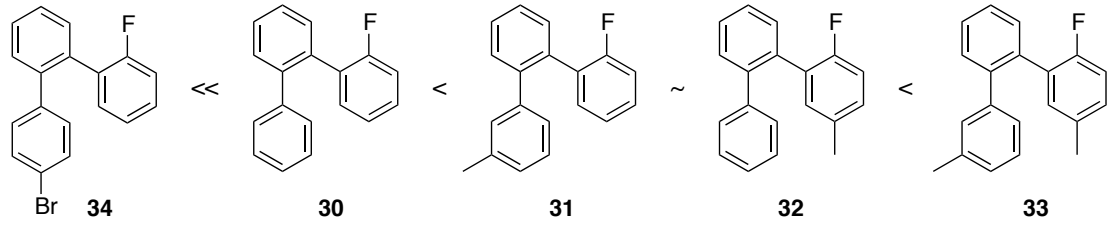

34 **30** **31** **32** **33**

Figure 2.3. Relative reactivities of substituted terphenyl substrates shows a dependency of the reaction time on the electron density on the involved rings.

The placement of a bromine atom on the ring that acts as nucleophile significantly slows down the reaction. For full conversion, 16 h of stirring at 110 °C (regular heating) were necessary. And in this case, the choice of the ring, which is substituted, has an immense effect. While compound **34** afforded product in high yield, though longer reaction time, application of reaction conditions on substrate **35**, with a 5-bromo-2-fluorophenyl moiety did not result in any product formation at all. This suggests that the fluorophenyl ring is more sensitive towards change in electron density after all.

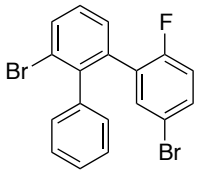

35

2.1.6 Elaboration of the Reaction Conditions

2.1.6.1 Solvent

Chlorobenzene turned out to be a very applicable solvent; it dissolved substrates as well as the silyl cation, and most of all, it did not interfere strongly with the cation. More electron rich or nucleophilic solvents might make the silyl cation less active with respect to C–F activation. This was observed in the case of toluene; using similar

reaction conditions, the conversion was only very low. One has to mention that the reaction was run at lower temperature (80 °C compared to 110 °C), but also microwave-assisted heating of the reaction mixture did not result in higher conversion. On the other hand, a cheaper and less toxic solvent would be desirable though.

2.1.6.2 Initiator

As mentioned before, there are two possibilities to initiate the reaction. One of them is the addition of a very strong acid, strong enough to protonate DMDMS. The conjugate base on the other hand must be very weak, so it does not inhibit the silyl cation regeneration. Additionally it mustn't be nucleophilic in order to prevent deactivation of the silyl cation. Super acids that fulfill these requirements are protonated carboranes,[4, 75] or protonated arenes with a carborane counterion.[5b] The latter, represented by protonated mesitylenium hexachlorocarborane $[C_9H_{13}][CHB_{11}H_5Cl_6]$, was successfully applied with the intramolecular arylation protocol. Usage of the same reaction conditions as shown in Scheme 2.3 resulted in product formation with a yield of 92 %. This therefore represents a viable alternative to the initiation by silyl cations.

The silyl cation used to start the reaction does not necessarily have to be synthesized beforehand; it can also be generated *in situ*. Therefor $[Ph_3C][CHB_{11}H_5Cl_6]$ and triisopropylsilane are added to the reaction mixture, forming the silyl cation by hydride transfer. This strategy was successfully applied on the model substrate as well, affording a yield of 89 %.

2.1.6.3 Silane

The choice of silane is essential for an efficient proceeding of the reaction. It not only has to easily accept protons released during product formation, it also has to generate a stable, yet reactive silyl cation to continue the catalytic cycle. Up until now, DMDMS has shown the best results in terms of reaction speed and reliability. There are some drawbacks and considerations that should be mentioned here. It was shown in our group that the silyl cation, which is thought to be formed upon protodesilylation of DMDMS, the dimethylmesitylsilylium ion, is not stable, but rearranges to trimesitylsilyl cation.[76] A very similar observation was made by Müller *et al*.[77] They report the rearrangement of dimesitylmethylsilylium ion to the

trimesitylsilyl cation. This does not necessarily mean that dimethyldimesitylsilyl cation does not exist under our reaction conditions; it might be stabilized by the fluoroarene or react before rearranging. Another hint on the reactive species is given by a GC-MS analysis of the reaction mixture after full conversion. Not only one fluorosilane is observed, but many different ones (Figure 2.4).

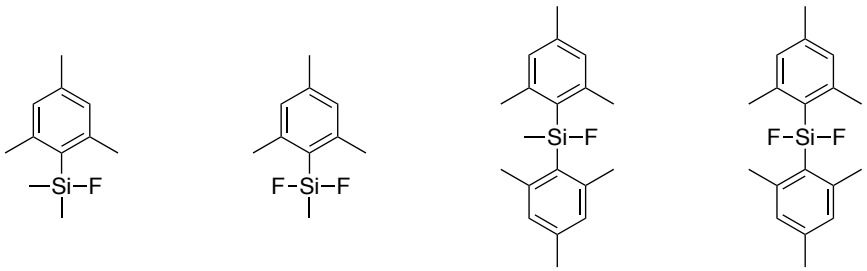

Figure 2.4. Different fluorosilanes that were observed by GC-MS, analyzing the reaction mixture.

One way of their generation was just mentioned; the dimethylmesitylsilyl cation could rearrange and then abstract fluoride. But what is also probable is a rearrangement of the fluorosilane formed during the reaction. It was suggested already by Ozerov *at al*. that fluorosilanes, under very Lewis acidic conditions, can exchange fluorine or alky groups.[45] What can be stated for sure is that the silane itself does not rearrange, because heating of the reaction mixture without starting material yields nothing but DMDMS.

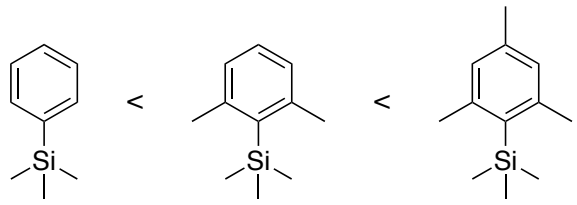

Figure 2.5. Relative reactivity observed for the three different TMS compounds.

Several different silanes were synthesized, but none of which could compete with DMDMS with respect to conversion and reaction time. An experiment with a series of trimethylsilanes showed that also the generation of the silyl cation, i.e. the protonation and protodesilylation, has an effect on the rate. The silane bearing the most electron rich substituent reacted fastest. What could also be observed in this experiment was that the silanes were consumed more rapidly than DMDMS, with respect to conversion of starting material. Whereas 1.1-1.2 equivalent DMDMS are

used during the transformation of 1 equivalent of fluoroarene, 1.2 equivalents of trimethylsilane derivative is already completely consumed at much lower conversion.

2.1.6.4 Microwave Settings

The microwave-assisted transformation of the model substrate requires the application of 200 W of power with turned-on cooling during 40 minutes. The temperature usually reaches around 90 °C towards the end of the reaction time. Because only one parameter can be held constant, the conditions vary from experiment to experiment. They are also influenced by the amount of solvent used or the concentration of the reaction mixture. But the intensity of irradiation seems to have the biggest influence, and because this stays at an equal level when cooling is turned on, the procedure is still reproducible. Attempts to reduce or avoid the formation of byproduct by lowering the power and hence the temperature, failed.

2.1.7 Overview of Applied Reaction Conditions

Table 2.2 shows an overview of reaction conditions applied to the model substrate **14**. Entries 1–3 represent the experiments using an equimolar amount of silyl cation as initiator. It shows that toluene is not an adequate solvent and 2,6-ditert-butylpyridine (**28**) is more suitable as a base than P(*o*-tol)$_3$, due to easier purification and the enhanced yield. An attempt of using tetrakis(pentafluorophenyl)borate as the anion resulted in significantly lower conversion, despite the longer reaction time (Entry 5). Although these conditions are not as effective as the corresponding approach using hexachlorocarborane as counterion (Entry 9), they can represent a feasible alternative, because the anion is synthesized faster and cheaper.

Entries 6 and 7 show the effect of catalyst loading; reducing the amount of initiator by 50 %, effected doubling of the reaction time. In the case of microwave-assisted heating, a catalyst loading of only 5 mol-% was sufficient to achieve a conversion of 100 % in only 40 min (Entry 8).

In situ generation of the silyl cation does not seem to have a big effect on the outcome of the reaction (Entry 9). Conversion and yield are very similar to reactions performed with addition of preformed $^{i}Pr_3Si^+$ (Entry 6).

Initiation of the reaction could also be achieved by the addition of a very strong acid (10 mol-% of protonated mesitylene, Entry 12). This supports the catalytic cycle proposed in Scheme 2.3. But since the protonated mesitylene was synthesized from a silyl cation itself, this explicit example is not of great practical use.

Entries 10 and 11 on one hand show that elevated temperature is indeed necessary to cause C(ar)–F activation (in contrary to C(sp^3)–F activation), and that also the proposed reaction intermediate $MesMe_2Si^+$ can initiate the reaction.

Table 2.2. Summary of the different reaction conditions applied on the model substrate **14**.

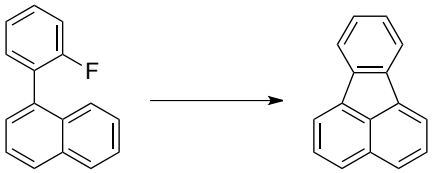

14 **15**

#	Cation	Anion	Base [a]	Solv.	T (°C)	Time (h)	Conv. (%) [b]	Yield (%) [c]
1	iPr_3Si^+	$[CB_{11}H_6Cl_6]^-$	P(*o*-tol)$_3$	PhMe	80	18	<10	–
2	iPr_3Si^+	$[CB_{11}H_6Cl_6]^-$	P(*o*-tol)$_3$	PhCl	110	15	100	80
3	iPr_3Si^+	$[CB_{11}H_6Cl_6]^-$	**28**	PhCl	110	8	100	90
4	iPr_3Si^+ [e]	$[CB_{11}H_6Cl_6]^-$	DMDMS	PhCl	65*	0.8	<10	–
5	Ph_3C^+/iPr_3SiH	$[B(C_6F_5)_4]^-$	DMDMS	PhCl	110	16	60	–
6	iPr_3Si^+ [d]	$[CB_{11}H_6Cl_6]^-$	DMDMS	PhCl	110	8	100	93
7	iPr_3Si^+ [e]	$[CB_{11}H_6Cl_6]^-$	DMDMS	PhCl	110	17	100	90
8	iPr_3Si^+ [e]	$[CB_{11}H_6Cl_6]^-$	DMDMS	PhCl	90*	0.67	100	85
9	Ph_3C^+/iPr_3SiH [d]	$[CB_{11}H_6Cl_6]^-$	DMDMS	PhCl	110	8	100	86
10	$Ph_3C^+/Me_2(Mes)SiH$ [d]	$[CB_{11}H_6Cl_6]^-$	DMDMS	PhCl	25	15	<10	–
11	$Ph_3C^+/Me_2(Mes)SiH$ [d]	$[CB_{11}H_6Cl_6]^-$	DMDMS	PhCl	110	8	100	89
12	Mesitylene–H^+ [d]	$[CB_{11}H_6Cl_6]^-$	DMDMS	PhCl	110	8	100	92

2.1.8 Conclusion & Outlook

The methodology presented here shows the possibility of activating the exceptionally strong C(Ar)–F bond. Transformations can be very rapid, applying heating by microwave irradiation. Further improvements should be targeted towards the reduction of side product formation. The availability of an alternative nucleophile, which is provided by DMDMS should be avoided. The search for another silane to replace DMDMS is not trivial though. Its performance relating to shortness of reaction time and conversion have yet to be met.

2.2 Scope

2.2.1 Summary

The method presented in the previous chapter could be applied to a variety of substrates to produce PAHs. Cyclizations leading to 5- and 6-membered rings could be achieved. Among the 5-membered rings, also strained molecules like indenocorannulene could be formed. Bromine substitution on the nucleophilic arene led to slower transformation, but nevertheless, a high yield resulted for the formation of bromo-triphenylene. By this methodology, small brominated PAHs can be synthesized, which can be further derivatized easily. The scope could also be extended to substrates containing other heteroatoms. The transformation of a fluoropyridyl substrate requires an additional equivalent of silyl cation to coordinate to the nitrogen lone pair and thereby enabling the C–F activation by the excess of Si^+. Alcohols are tolerated by the reaction conditions if protected by triisopropylsilane (TIPS). Applying the reaction protocol on a TIPS protected alcohol results in cyclization and deprotection.

2.2.2 General Considerations Towards the Scope of the Reaction

The success of the intramolecular Friedel–Crafts-type arylation protocol depends mainly on three factors:

- Strain that is introduced by the formation of the product (i.e. ring strain energy)
- Electron density of the involved aromatic rings
- Presence of heteroatoms and functional groups

Those points all represent variables that influence the height of the energy barrier that has to be overcome in order for product to form. In case of a high strain that is induced, fluoride can still be abstracted, but instead of the intramolecular ring closure nucleophilic attack of a solvent molecule or mesitylene might happen quicker (although still slow). With a low electron density on the fluorarene, the transition state gets destabilized, due to its positive charge. Low electron density on the attacking ring reduces the probability of bond formation, once the rings come close, since its nucleophilicity is decreased. Because of their Lewis basicity, heteroatoms or functional groups within the substrate or reaction mixture, can coordinate to the silyl cation. If this is the case the additional energy barrier consists of the silyl cation breaking free from the heteroatom lone pair. This attractive force can even result in a covalent bond, depending on the coordination sphere of the heteroatom.

2.2.3 Formation of 6-membered Rings

The *o*-terpheynl substrates already mentioned earlier transformed to the triphenylene products **37**–**40** very smoothly with high yields (Scheme 2.7). There is no particular strain that has to be overcome; rotation around the aryl-fluoroaryl-bond sets the two involved carbon atoms already in the right position for ring formation. The reaction was not very selective regarding the methyl substituent on the ring performing the nucleophilic attack. This is another indicator for the high reactivity of the transition state and further evidence of the assumption that the rate-determining-step (r-d-s) is the abstraction of the fluoride. Otherwise a stronger preference for the sterically more favorable transition state, with the methyl group pointing away from the incipient phenyl cation, would be expected.

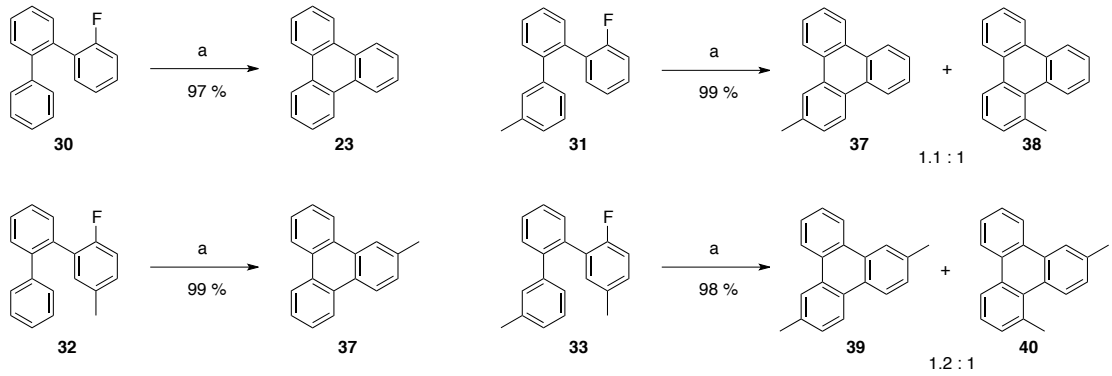

Scheme 2.7. Transformation of several fluoroterphenyl substrates to their corresponding triphenylenes. a) [iPr_3Si][$CHB_{11}H_5Cl_6$] (10 mol-%), DMDMS, PhCl, 110 °C, 8 h.

The triphenylene products are the smallest examples of a subclass of the PAH, the so-called all-benzenoid PAH (PBAH). They represent a group of PAH that only consist of complete benzene moieties. They possess exceptionally high melting points and chemical inertness. Further examples of PBAHs that were synthesized are shown in Scheme 2.8. The syntheses are based on multiple cyclizations within each of the substrates (**41**–**43**). The yields are not as high as for the triphenylene examples, despite full conversion of starting materials. The reasons for that are possibly of diverse origin. In general, the larger PAHs get, the less soluble they become and therefore become harder to handle and to purify. Compound **44** for example was purified by precipitation and washing, by which also product can be washed away. The solubility of compounds **45** and **46** is slightly better because they are not completely planar due to steric conflicts in the regions where two C–H come close. But it is also due to this feature that these compounds tend to oxidize during workup and form flat PAH by the formal loss of hydrogen, thereby reducing the yield.

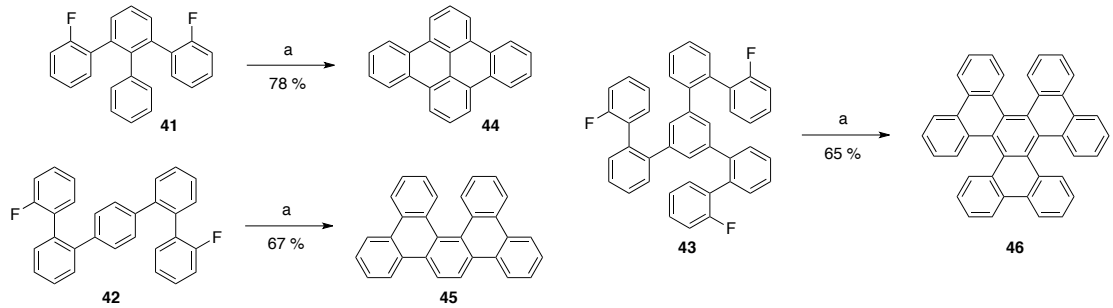

Scheme 2.8. Syntheses of other PBAHs. a) [$^{i}Pr_3Si$][$CHB_{11}H_5Cl_6$] (10 mol-%), DMDMS, PhCl, 110 °C, 8 h.

Furthermore, substrates **42** and **43** can form additional regioisomers, which leads to a lower yield. The remarkable regioselectivity observed for substrate **42** is discussed in chapter 2.5.

2.2.4 Formation of Strained Rings

Already the model substrate experiences strain upon the formation of the additional cycle, though not that much admittedly. Its synthesis is fast and high yielding, in contrast to two similar substrates, containing an anthracene core with attached fluorophenyl(s) (**47** and **48**). In the case of **47**, the lower yield is thought to come from degradation of product **49**. Examination by ^{1}H-NMR of a sample stored in $CDCl_3$ at room temperature for several days showed the formation of decomposition products of unknown nature. A large number of aromatic signals had emerged, that could not be assigned. Compound **50** is thought to be more strained and additionally a regioisomer can be formed, which was not isolated. The ring-closing of substrate **51** to indenocorannulene **52** is accompanied by more extensive bending of the already bowl-shaped corannulene. To overcome this additional barrier, the reaction time had to be doubled. The stable product was purified by flash column chromatography and could be obtained in a yield of 79 %. A summary of the described reaction is presented in Scheme 2.9.

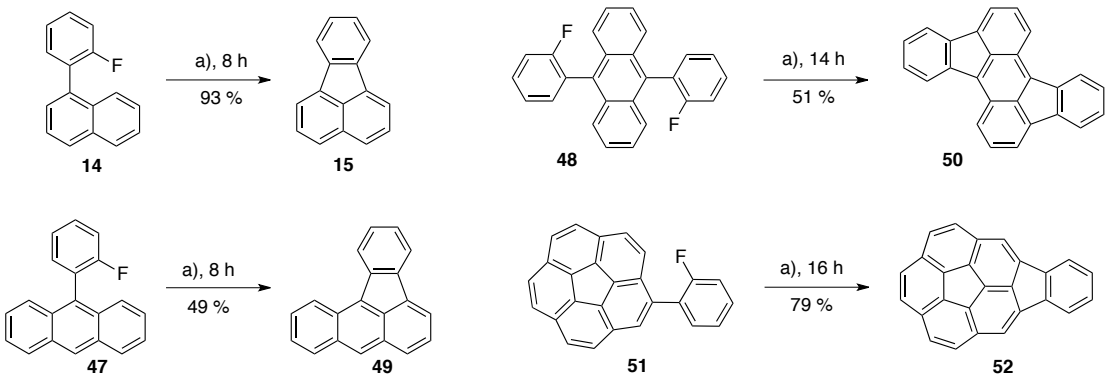

Scheme 2.9. Application of the C–F activation protocol on substrates forming strained 5-membered rings. a) [^{i}Pr$_3$Si][CHB$_{11}$H$_5$Cl$_6$] (10 mol-%), DMDMS, PhCl, 110 °C.

But there are also ring strains too high to overcome with this method. The substrates shown in Scheme 2.10 did not cyclize when the catalytic protocol with conventional heating was used.

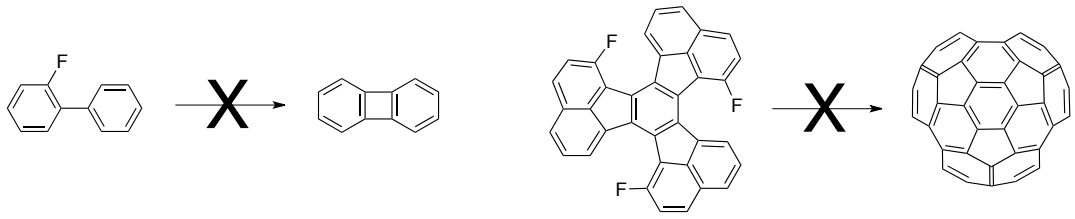

Scheme 2.10. Failed attempts to ring-close substrates to highly strained products.

2.2.5 Reduced Electron Density

Low reactivity could also be observed for substrates with reduced electron density on one of the rings involved in the coupling. Electron withdrawing groups on the fluorine-bearing ring have a more drastic effect, as described before. Substrate **35**, containing fluorobromophenyl, does not yield any product at all. Substrate **34** with a bromine substituent attached to the "attacking ring" can still be converted to product with a yield of 95 %, although with longer reaction time (Scheme 2.11). For this comparison it is assumed that the second bromine atom in compound **35** does not influence the course of the experiment. The reasons for that were discussed in chapter 2.1.5.1.

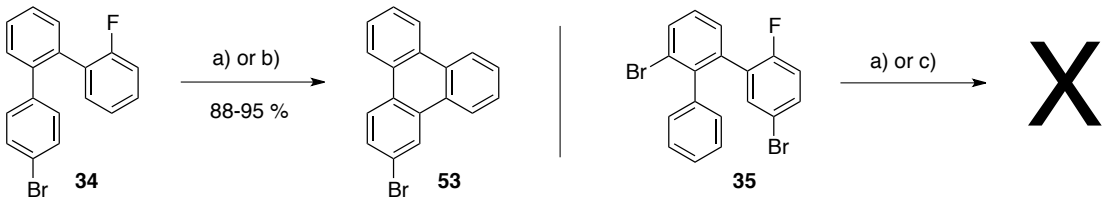

Scheme 2.11. Starting materials containing a bromine substituent on one of the rings involved in the coupling, take more time to react, or do not react at all, depending on the position of the bromine. a) [$^{i}Pr_3Si$][$CHB_{11}H_5Cl_6$] (5 mol-%), DMDMS, PhCl, 200 W MW irr., 70 min. b) [$^{i}Pr_3Si$][$CHB_{11}H_5Cl_6$] (10 mol-%), DMDMS, PhCl, 110 °C, 16 h. c) b + 24 h.

Of special interest in this category are substrates that contain further fluorine atoms; these could open up easier substrate syntheses for the preparation of larger PAHs. It is hard to draw conclusions from these experiments, since the results are not very clear. Because fluorine is much more electronegative than bromine, it is expected that substrates containing additional fluorine substituents would react even slower. This hypothesis could be confirmed by an experiment performed on substrate **54** (Scheme 2.12). It can be compared to the bromine substituted **34**. Although the substituents do not occupy the same position, they are both located on the meta-carbon with respect to the carbon undergoing the ring-closure. What could be

observed by GC-MS was the formation of product **55**, but even after stirring at 110 °C for 23 h, there was still a substantial amount of starting material present, even though two equivalents of DMDMS had been added. It was stirred for another 40 h, but at this point, both, starting material and product had transformed into higher mass products. So it seems that fluoroarene can in fact serve as the nucleophilic intramolecular coupling partner of the cyclization. And the long reaction time is in agreement with the high electronegativity of fluorine compared to bromine (in compound **34**). But what was further shown is that a fluorine substituent in the substrate that does not have a corresponding intramolecular coupling partner will react further with a different nucleophile, if there are still silyl cations present. Products of such an intermolecular coupling are compounds **56** and **57** that result from reaction with mesitylene and solvent respectively. They were identified by GC-MS and are part of Scheme 2.12, showing these side reactions.

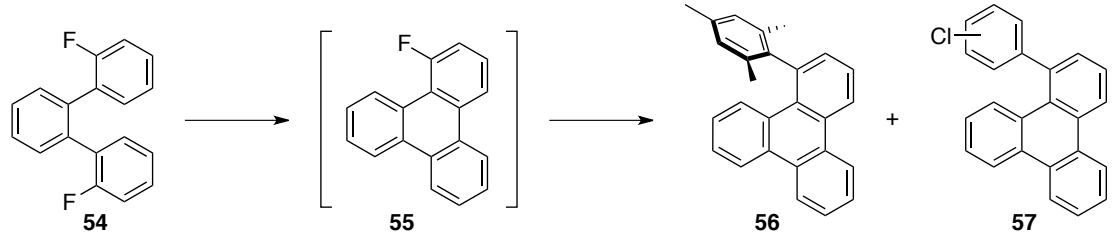

Scheme 2.12. Intramolecular coupling of two fluoroarenes leading to fluorotriphenylene as intermediate product, which reacts further if further reagent is present.

Substrates bearing two fluorine substituents at the same ring were examined too (Scheme 2.13). Since the bromine analog (substrate **35**) did not lead to product formation, it was expected that the difluorophenyl substrates did not react either. This held true when **58** was treated with the regular catalytic reaction conditions under conventional heating - no product formation was observed. But surprisingly, compound **59**, also containing a difluorophenyl, was slowly transformed to the highly insoluble **60**.

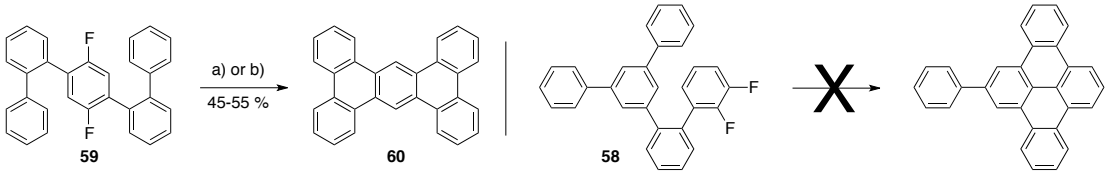

Scheme 2.13. Different outcomes of substrates bearing two fluorine atoms at the same ring. a) [$^{i}Pr_3Si$][$CHB_{11}H_5Cl_6$] (40 mol-%), DMDMS, PhCl, 110 °C, 20 h. b) [$^{i}Pr_3Si$][$CHB_{11}H_5Cl_6$] (10 mol-%), DMDMS, PhCl, 250 W MW irr., 4 h.

The successful transformation of **60** came at the cost of longer reaction time and/or increased amount of silyl cation. In the case of the non-microwave method the loading of initiator was at 40 mol-% (20 mol-% per fluorine). Microwave irradiation was operated with 250 W instead of 200 W.

The difference in reactivity between compound **58** and **59** can be rationalized by looking at the transition state. Whereas the incipient positive charge upon abstraction of the fluorine is in para position for **59**, it is ortho to the fluorine in **58**. And since the inductive effect of the electron withdrawing fluorine decreases with distance, the transition state of the latter is much more destabilized. But the reason why the para-difluorophenyl substrate yields product and the para-bromofluorophenyl does not, could not be discovered.

2.2.6 Heteroatoms and Functional Groups

Primary and secondary amines, or alcohols form covalent bonds to silicon if they are given a chance to interact with silyl cations. As mentioned in a previous chapter, the strong bond formed thereby is the driving force. As for tertiary amines or ethers, those tend to coordinate to silyl cations, absorbing part of their positive charge. This in turn leads to a less reactive silyl cation, due to its decreased cationic character. Imagining an equilibrium as shown in Scheme 2.14 on the right hand side, where most of the silyl cation is deactivated by coordination to pyridine, but still a small fraction exists as free silyl cation, it might be possible to have this minority abstract fluoride and promote intramolecular arylation.

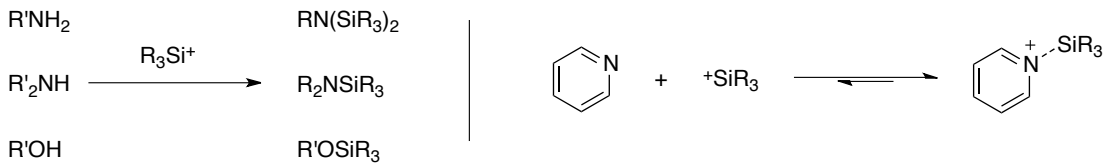

Scheme 2.14. Reactivity of amines, alcohols, and ethers towards silyl cations.

To test this hypothesis, substrate **61** was synthesized, featuring the same structure as the former model substrate, except for the nitrogen replacing a carbon atom in the fluorophenyl ring (Scheme 2.15).

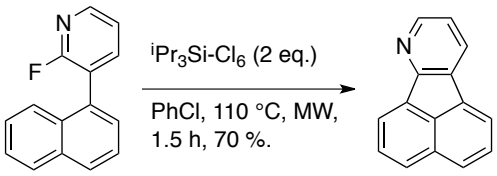

61 **62**

Scheme 2.15. Transformation of substrate **61** to product was achieved by using two equivalents of silyl cation and by application of microwave irradiation.

The C–F activation reaction of this compound was performed in PhCl-d5, in order to observe the faith of the reactants by ^{1}H-NMR. The methyl signal of the silyl cation's isopropyl groups served as reference signals and provided a deeper insight into the course of the reaction. The peaks, representing the situation in the reaction mixture during 43 h are shown in Fig. 2.5. For reasons of symmetry and due to the coupling with the C–H group, one doublet is expected for the methyl groups. At t=0, two doublets are visible. Since 1.2 equivalents of triisopropylsilyl cation were present in the mixture, the large signal is attributed to fluoropyridyl-bound silyl cation ($^{i}Pr_3Si$–py(SM)). The small signal therefore would originate from "free" or unbound cation ("$^{i}Pr_3Si^{+}$"), derived from the excess of 0.2 equiv. Whether the silylium ion is truly isolated or coordinated to solvent, fluorine, anion, or to the π-electrons of the nitrogen remains an open question. In any case, after stirring at 110 °C for 8 h this peak had vanished. Addition of another 0.8 equivalents of silyl cation made it appear again. When the reaction was given more time at 110 °C, the NMR spectrum showed a third isopropyl peak emerge. After another 24 h and a total of 45 h of heating, one could clearly see three doublets, one of them increasing on the cost of the other two. The third peak was interpreted as silyl cation coordinated to product ($^{i}Pr_3Si$–py(P)).

This reaction was then run under microwave irradiation using 1.2 equiv. of each, [$^{i}Pr_3Si$][$CHB_{11}H_5Cl_6$] and DMDMS, which led to full conversion of starting material to product within only 2 hours.

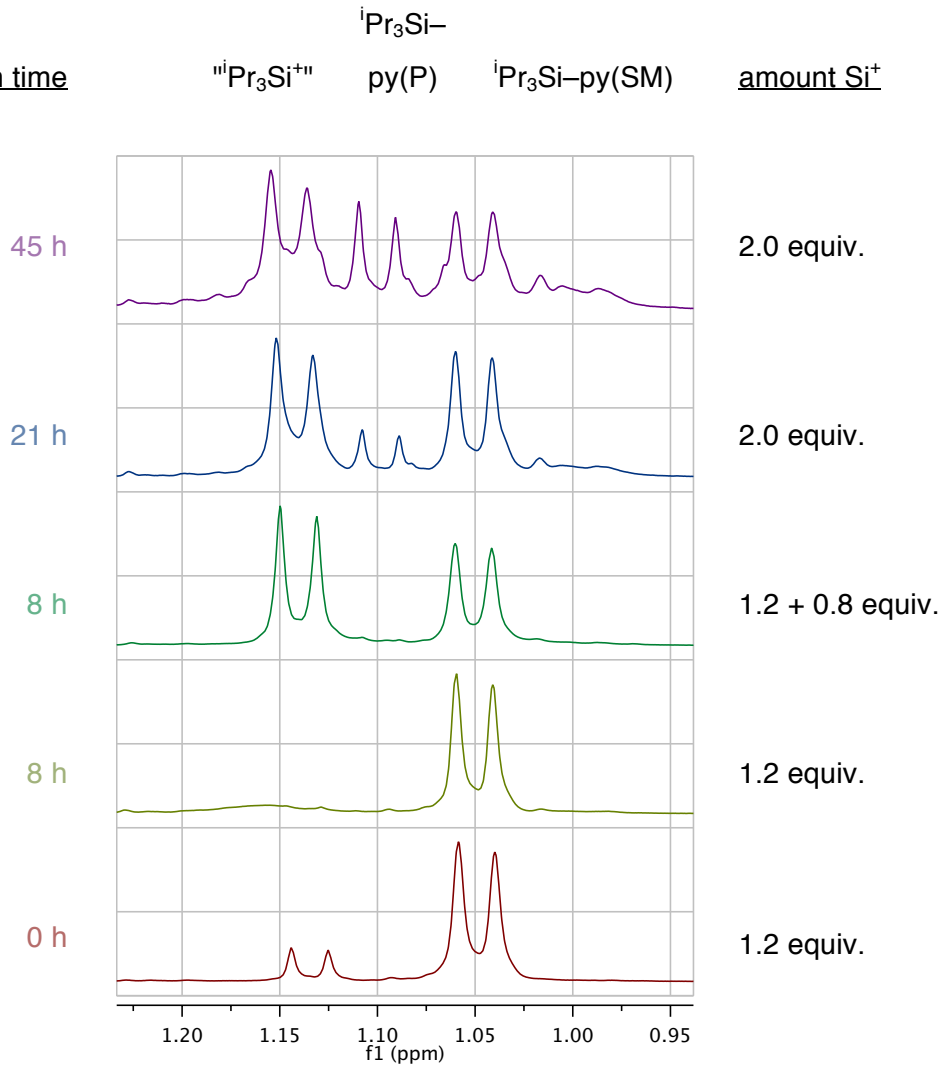

Figure 2.5. Development of the ^{1}H NMR signals of the methyl groups of $^{i}Pr_3Si^+$ during reaction that is shown in Scheme 2.15.

Although this was a huge progress, it did not proof the earlier hypothesis of the equilibrium between free and bound silyl cation, because one additional equivalent of silyl cation was used to saturate the free lonepair on the nitrogen. Therefore, the same experiment was carried out, but with only 10 mol-% of silyl cation. After stirring for 2 h under microwave irradiation, it became clear that product was forming, but very slowly. When after 10 h heating, the reaction was still far from full conversion, it was stopped. By that time product contributing to a yield of 43 % could be isolated. This shows though, that even in the presence of a strong Lewis base, the coordination to the Si^+ can be loosened by microwave irradiation to inducesilyl cation-promoted C–F bond activation.

From this knowledge, aza-indenocorannulene **63** was synthesized, which will be discussed in a separate chapter. This substrate includes all three possible hurdles

that can occur using our method: inclusion of a heteroatom, reduced electron density (caused by the nitrogen), and strain that is induced by the formation of the indenocorannulene.

Another investigation on the tolerance of functional groups was performed on oxygen-containing substrates. Since alcohols form covalent bonds to silyl cations, and well-accessible ethers would need one additional equivalent of Si^+ to represent a convenient substrate for the intramolecular arylation reaction, a very bulky silyl protecting group was introduced. The idea is that the isopropyl groups might be able to shield the oxygen lone pairs from coordination of the silyl cation.

It is known that silyl ethers are cleaved under highly acidic conditions. But because the reaction conditions described here are non-nucleophilic, the silyl cation created that way could only go back to the alcohol, and if it does not, it is just additional reagent with the ability to abstract fluoride. The other side reaction that could occur would be an exchange of silyl groups, which would not be regarded as problem. The two equilibria are depicted in Scheme 2.16.

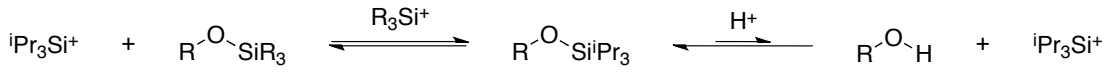

Scheme 2.16. Possible equilibria occurring in a mixture of silyl ether, silyl cation, and acid, which are the main components of our reaction conditions.

The reason for this analysis is the outcome of the reaction performed on substrate **64**, using the microwave assisted protocol (Scheme 2.17). The compound could not only be cyclized as planned, it additionally got deprotected during the course of the reaction or the workup (yet being very mild) to yield the alcohol **65**.

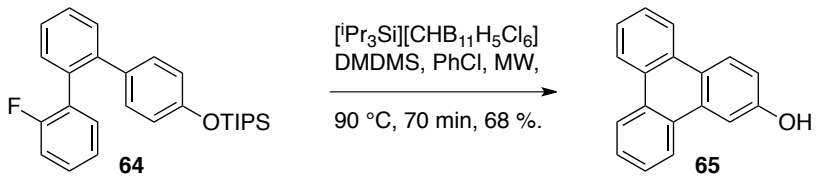

Scheme 2.17. Transformation of a substrate containing a TIPS-protected alcohol, using the catalytic method (5 mol-% silyl cation) under microwave irradiation.

The result is very surprising, because theoretically, there are not enough acidic protons (5 mol-%) in the reaction mixture to cause deprotection of almost 70 % of the starting material. Although water is added during the workup, this should not be

enough to remove one of the most resistant silyl ethers. While there are not enough acidic protons present at once, there is 1 equivalent that is generated upon transformation of starting material. If it is assumed that the equilibrium in Scheme 2.16 lies on the right-hand side, the alcohol product could be explained. For every molecule of product that is formed, a proton is liberated. If this proton is captured by the oxygen of the silyl ether (and not by DMDMS) and therefor $^{i}Pr_3Si^+$ is released, one would end up with deprotected cyclized product. This again would imply that DMDMS is not necessary for the reaction to proceed, since the starting material itself would provide the proton for cleaving the silyl ether and in that way supply the needed silane for silyl cation formation. Fortunately it is easy to test this hypothesis. The reaction from Scheme 2.17 was setup, but this time omitting DMDMS. After stirring under microwave irradiation for 70 min, two main fractions were obtained; one being starting material, the other was deprotected starting material. Compound **65** could only be observed in traces. This suggests that the equilibrium in Scheme 2.16 stays in the middle/left also during microwave irradiation, and cannot as easily be shifted like it was shown for the coordination to pyridine.

2.2.7 Overview & Outlook

The substrates that were successfully transformed are depictured in Table 2.3. They just give an idea of the possibilities provided by the intramolecular arylation method. More complex starting materials could furnish novel PAHs possessing distinct optical properties, for example. The fact that the presence of bromine, depending on the position within the starting material, does only faintly influence the course of the reaction, makes further derivatization at the position of the halogen (e.g. cross-coupling reactions) easily achievable. Also the option of treating substrates bearing a pyridine ring or a TIPS-protected hydroxy group broadens the scope of accessible functionalized PAHs.

Table 2.3. Overview of substrates and corresponding products that were transformed using the intramolecular arylation method.

Substrate	Product	Yield	Substrate	Product	Yield
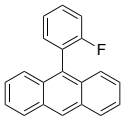	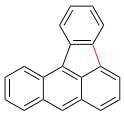	51 %	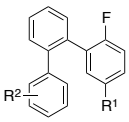 R^1=R^2=H R^1=Me, R^2=H R^1=H, R^2=Me R^1=R^2=Me R^1=H, R^2=Br	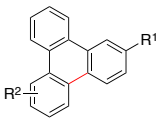	97 % 99 % 99 % 98 % 94 %
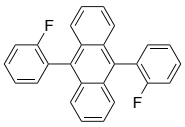	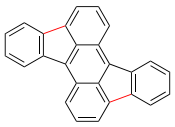	49 %	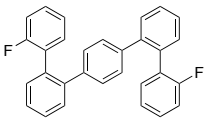	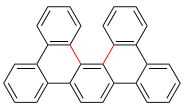	67 %
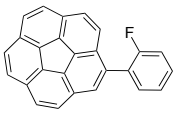	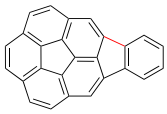	79 %	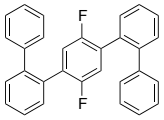	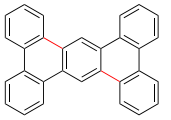	60 %
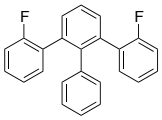	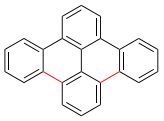	78 %	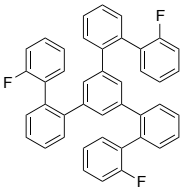	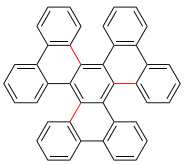	65 %
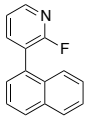	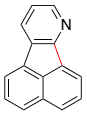	75 %	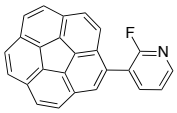	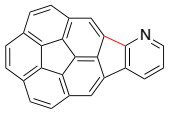	24 %
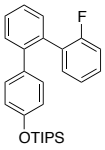	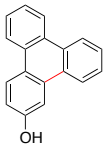	68 %	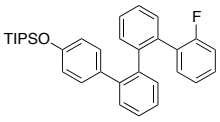	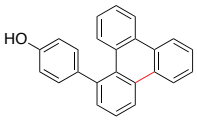	60 %

2.3 Synthesis of Aza-indenocorannulene

From the results obtained in the former chapter, the synthesis of the first aza-indenocorannulene seemed feasible. The challenge is harder though, because as for compound **61** there is a heteroatom within the substrate that, on one hand, deactivates silyl cations and on the other hand reduces the electron density in the fluoropyridyl and thereby destabilizes the transition state. Reported examples of 1,2-pyridynes, which would represent a possible reaction intermediate could not be found. But additionally to low electron density and presence of a heteroatom, upon

formation of the indeno-fused product **63**, there is also a strain that is introduced, which further slows down the reaction, as seen in the synthesis of the all-hydrocarbon indenocorannulene **52**.

The synthesis of **63** is based on a boronic ester derivative of corannulene (**68**), synthesized in our group,[78] and its Palladium-catalyzed coupling with 3-bromo-2-fluoropyridine (Scheme 2.18). The Suzuki coupling was performed in a THF/water mixture at 70 °C and afforded corannulene derivative **69** in 71 % yield. The conditions that worked best for the intramolecular arylation reaction involved the usage of 1.2 equivalents of silyl cation and an additional equivalent of DMDMS. The low yield of 26 % can be partially explained by the formation of byproducts stemming from intermolecular coupling of substrate with mesitylene and chlorobenzene. In an attempt to reduce these side products, DMDMS was omitted and 2 equivalents of silyl cation were added instead. This approach did not improve the yield though; also addition of base (2,6-di-tert-butylpyridine) did not have a positive effect.

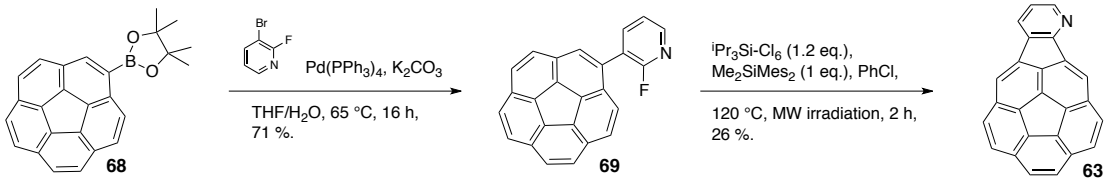

Scheme 2.18. Reaction scheme for the synthesis of aza-indenocorannulene, starting from Bpin-corannulene.

Since corannulene possesses a bowl-shaped structure its mono-substitution would lead to a chiral compound. This holds true for very low temperatures. But in ambient conditions the bowl is able to flip due to an estimated inversion barrier of only around 48 kJ/mol.[79] But by connecting two of corannulene's CH carbons as done in indenocorannulene, the inversion barrier is more than doubled. Therefore, bowl-to-bowl inversion does no longer occur at room temperature. In our case, where an indene carbon is replaced by a nitrogen atom, the plane of symmetry present in regular indenocorannulene is broken, leaving behind two enantiomers. The presence of the two enantiomers could be demonstrated with an NMR experiment, using a chiral shift reagent. By adding one equivalent of (*R*)-(-)-Mandelic acid to a solution of **63** in $CDCl_3$, almost all the proton signals split into two, due to the formation of diastereomeric ion pairs of **63** with the acid. The proton signals obtained by ^1H NMR spectroscopy are shown in Figure 2.5 and 2.6 respectively. The signals of the

racemic mixture without addition of chiral shift reagent are shown on top, the spectra after addition of the chiral acid are shown on the bottom.

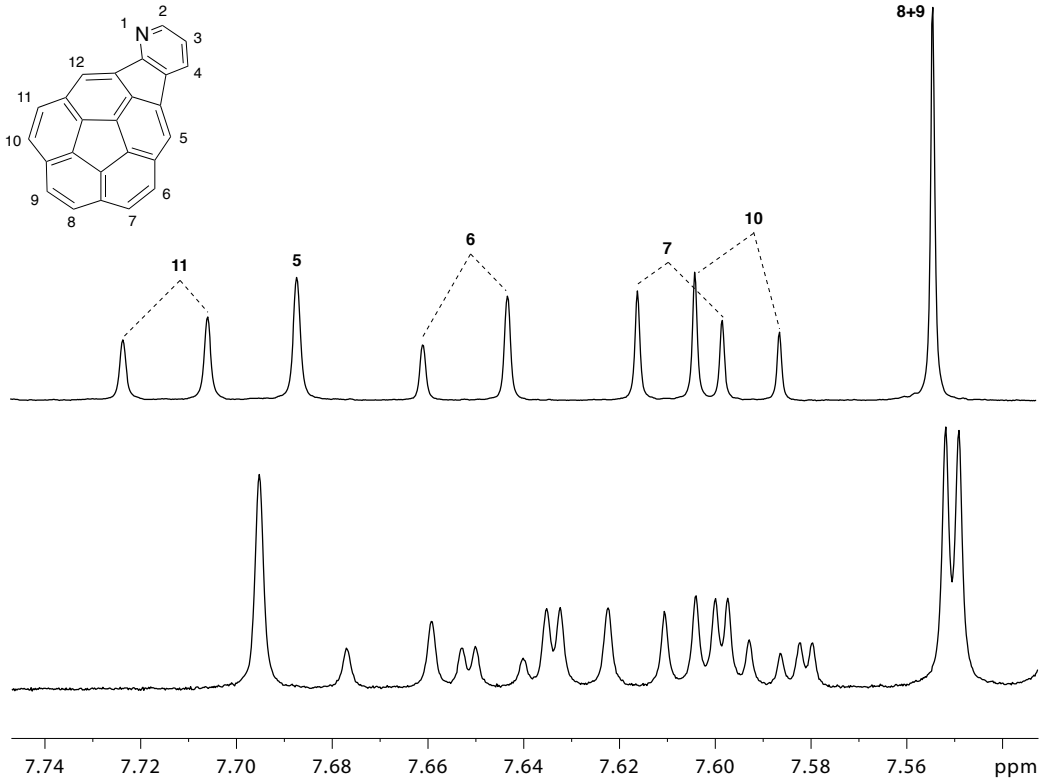

Figure 2.5. ^{1}H-NMR signals of the corannulene part of **63** with (bottom) and without (top) (R)-(-)-mandelic acid as chiral shift reagent.

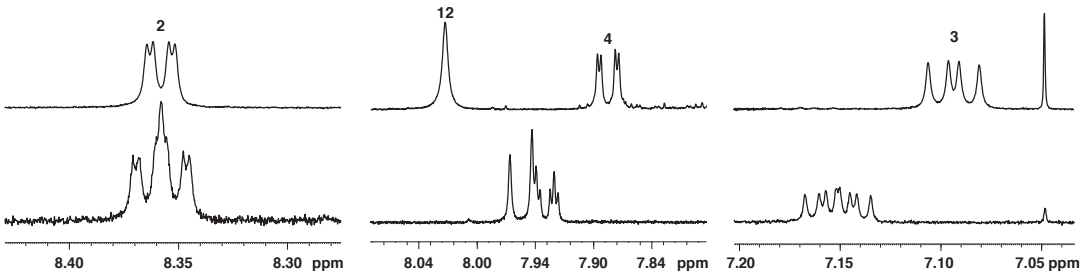

Figure 2.6. ^{1}H-NMR signals of the pyridine signals (2–4) of **63** and one corannulene signal (12), before (top) and after addition of (R)-(-)-mandelic acid as chiral shift reagent.

The two enantiomers could be separated by chiral HPLC in the laboratory of T. S. Balaban at the University of Marseille. Additionally they measured electronic circular dichroism (ECD) spectra. A paper will be drafted once all the data is collected.

First attempts of recrystallizing compound **63** failed. Experiments involving the recrystallization of the diastereomeric salts of the enantiomers of **63**–H^+ and (*R*)-(-)-mandelate were not successful either. During the process of recrystallization attempts, a trace impurity could be isolated, which was not observed in the NMR experiments. It results from the coupling of the starting material with a hexachlorocarborane - its crystal structure is shown in Figure 2.7. The dots indicate a second conformation that is comprised of rotation of the C(cor)–C(py) bond and inversion of the corannulene bowl. What the crystal structure shows, is the replacement of fluorine from the substrate with a chlorine atom and the attachment of pentachlorocarborane to the pyridyl moiety by a nitrogen-boron bond.

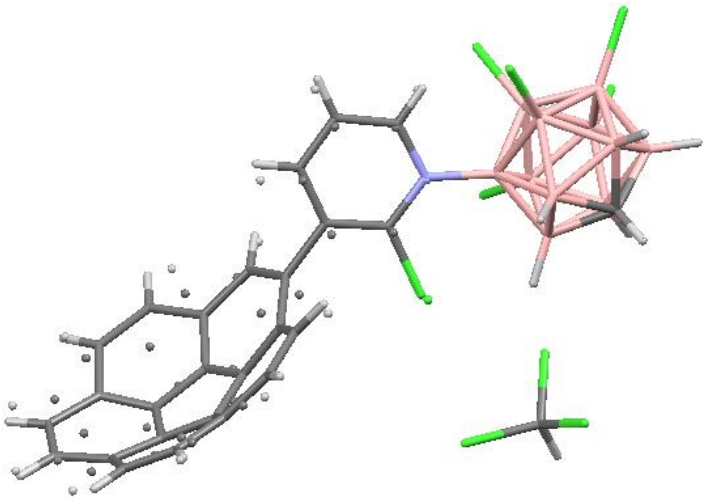

Figure 2.7. Crystal structure of the byproduct found from the azaindenocorannulene synthesis; a coupling product of the starting material and a hexachlorocarborane anion. The dots illustrate the second confirmation that was found.

The overall molecule is neutral, but it possesses a zwitterionic character due to a formal positive charge on the nitrogen atom and a widely distributed negative charge on the carborane moiety. This byproduct can be interpreted as the outcome of an insertion of the intermediate pyridyl cation's C=N bond into the B–Cl bond of the carborane. Interestingly, this reactivity strongly resembles the C–H insertion described in Chapter 3. In both cases the partially negatively charged atom (which is the more electronegative atom except for the C–C bond in the phenyl cation) of each of the two involved bonds, ends up with the atom containing the partially positive charge. In the example at hand, this means that nitrogen forms a bond with boron, and carbon bonds with chlorine. With other substrates that were subjected to these reaction conditions, this byproduct was not observed. But this does not mean that it did not form, because it was not looked for specifically. For substrates that do not

contain a fluoropyridyl moiety, the corresponding byproduct would be negatively charged, and would therefore be stuck on the column upon purification.

2.3.1 Outlook

Due to the possibility of separation by chiral HPLC, the two enantiomers can be analyzed individually. The already mentioned CD spectroscopy that was performed shows mirror image spectra for the enantiomers. And by combining electronic and vibrational circular dichroism (ECD and VCD), the absolute configuration can be determined. Because of its high rigidity and low rotational degree of freedom, the azaindenocorannulene represents a very good example for this particular structure determination method.

2.4 Bis(2,2'-biphenylyl)ammonium Ion - a Tertiary Amine as Nucleophile

From the promising results obtained with the fluoropyridine substrates, it became clear that inclusion of heteroatoms does not categorically preclude the intramolecular arylation reaction from happening. And since nitrogen is a good nucleophile, the idea of using it as intramolecualr coupling partner with fluoroarene was intriguing. Selection of a tertiary amine was practical due to several reasons. With three substituents and sp^3 hybridization, the nitrogen lonepair is not so well accessible anymore. This would facilitate presence of the free form of the silyl cation, compared to coordination to nitrogen. Additionally, the fact that formation of product leads to an ammonium ion further reduces possibilities of Si–N complexes. Whereas for secondary or primary amines, addition of a base might be sufficient to induce a nucleophilic aromatic substitution reaction at the fluoroarene, for a tertiary amine this alternative is lacking. Therefore, substrate **70** was synthesized in order to create the tetraarylammonium ion **71** (an alternative procedure was described by Hellwinkel and Seifert[80]). The starting point was carbazole, which was reacted with bromo-iodobenzene to afford a mixture of bromo- and iodophenylcarbazole (Scheme 2.19). Of these two substrates only the iodo compound reacted to give **70**.

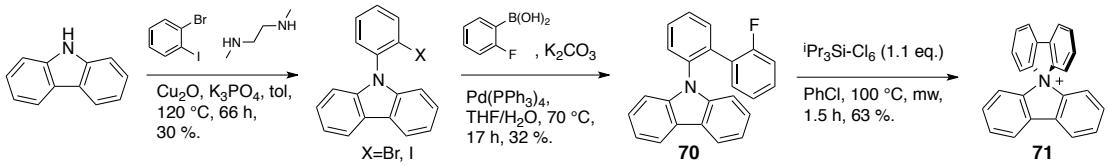

Scheme 2.19. Synthesis of the tetraarylammonium salt **71**.

The final product was obtained by addition of 1.1 equivalent of silyl cation and stirring for 1.5 h under microwave irradiation. The ammonium ion with its carborane counterion was purified by flash column chromatography under very polar conditions. Also a substantial amount of byproduct was formed, which could be identified as azepine **72**. This product is derived from the nucleophilic attack of the carbazole's benzene moiety, *i.e.* the regular reactivity, creating a 7-membered ring.

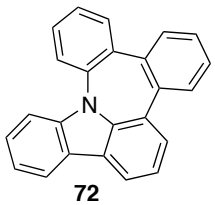

72

What is remarkable in this reaction is that only 1.1 equivalents of silyl cation were necessary for full transformation of the starting material. This corresponds to an excess of only 0.1 equivalent, compared to an excess of at least 1 equivalent for the fluoropyridyl substrates. It is not clear yet what might be the reason for only such a small influence of the nitrogen atom. Steric shielding by the aromatic moieties, or the relatively low electron density on the nitrogen are possible explanations. The first one is probably not a very likely reason, because the steric influence of flat substituents is usually not that high. Latter is caused by the resonance effect of the attached aryl rings, leading to distribution of the lone pair electrons among the arenes (already carbazole has a pKa of 19.9 (deprotonation of N–H), which is very low for an amine). This could effect a weaker coordination of silyl cation to the nitrogen. Another perspective can be gained by focusing on the small excess of silyl cation. If the 0.1 equivalent can activate a C–F bond, the starting material would form an ammonium ion. This means that nitrogen binding sites are depleted and prior bound or deactivated silyl cation would become free. If this holds true, addition of only 1

equivalent to the reaction mixture should result in significantly slower product formation.

Two polymorphic crystal structures could be obtained; they are depicted in Figure 2.8. They are both of orthorhombic symmetry, with one showing columns of carborane with the ammonium ion distributed around it (left), and the other one consisting of diffuse arrays of cation and of anion (right).

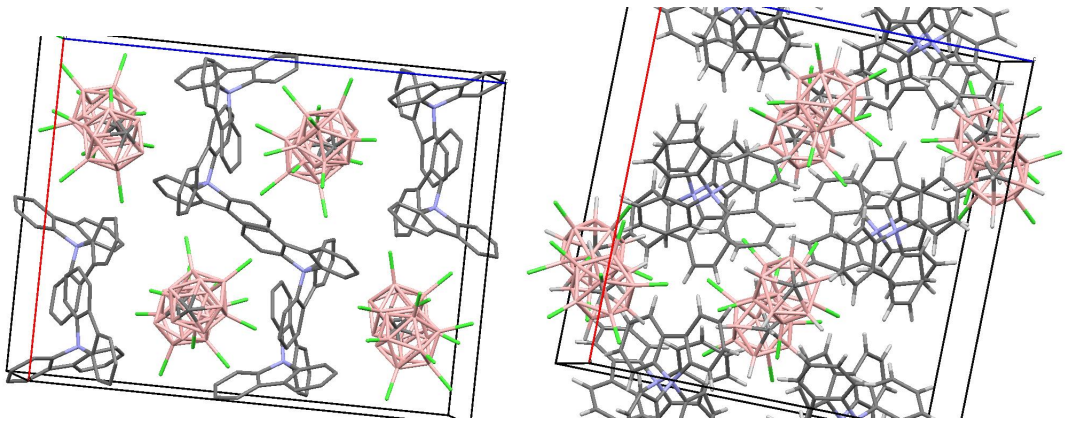

Figure 2.8. Two enantiomorphic crystal structures of tetraarylammonium carborane.

Further advancement of the project should go towards anion exchange. By recovery of the hexachlorocarborane, the synthesis of the tetraarylammonium ion becomes much more economic. Recrystallization of **71** with its borate counterpart ($[B(C_{12}H_8)_2]^-$) and analysis of its crystal structure would be particularly desirable. Furthermore, the synthesis of the tetraarylammonium salt provides a possibility to generate chiral cations by substitution of the distinct arenes of the precursors. One can also consider tuning the reaction conditions to enhance the formation of the azepine byproduct, if there is an interest in such a compound.

2.5 Acene vs Helicene

The regioselectivity of the intramolecular arylation is usually determined by the position of the fluorine atom. But because the nucleophilic arene is not activated in any kind, a mixture of products can result, if there is more than one possible reaction site, either caused by the presence of multiple coupling partners or by rotation of the arene. This could already be observed in the case of the terphenyl substrates that were examined regarding to the influence of electron density of the involved arenes.

Subjected to the catalytic reaction protocol, substrates **31** and **33** transformed to product mixtures containing both, ortho- and para methyl groups (with respect to the newly formed C–C bond). The preference for para product can be anticipated considering a stronger steric repulsion induced by the o-methyl group compared to the p-methyl group in the corresponding transition states. The only very small excess of para product is remarkable and demonstrates only a minor influence towards selectivity caused by the methyl group. The stabilities of the Wheland intermediates that are formed after fluoride abstraction and intramolecular arylation are thought to be very similar since resonance structures of both regioisomers exhibit stabilization by a positive charge in benzylic position and at a tertiary carbon (Figure 2.9). This should therefore not have a strong influence on the ratio of products.

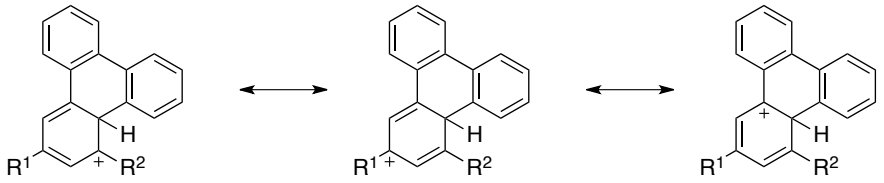

37: R^1=Me, R^2=H
38: R^1=H, R^2=Me

Figure 2.9. Resonance structures of the two possible reaction intermediates - no matter which of the two possible isomers is formed, they possess carbocations that are equally stabilized.

A much more surprising outcome related to regioselectivity can be observed applying the catalytic reaction protocol to substrate **42** (Scheme 2.20). The major product from this reaction is not the symmetric phenanthro[9,10-*b*]triphenylene (**60**), but the highly twisted dibenzo[5]helicene (**45**). This selectivity is not expected, because the major product formed is essentially higher in energy than the acene (linearly fused polybenzene). Insert values! Despite that discrepancy, similar results were also obtained by other groups using the Scholl reaction.[59] Although the discussion of the mechanism in this chapter is based on our method using silyl cations, there might be similarities to the reported examples.

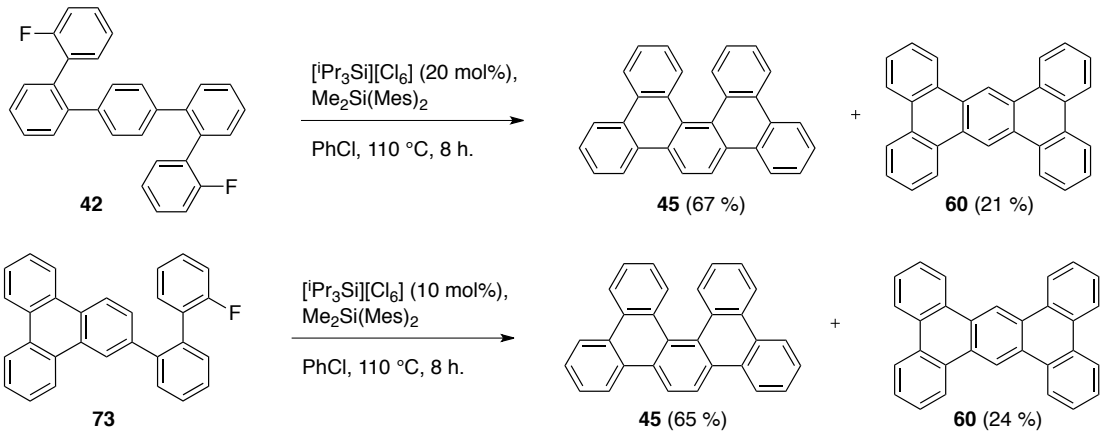

Scheme 2.20. Product distribution is not affected by the number of cyclizations necessary - they are thought to happen independently.

Because the regioisomer, which is higher in energy, is formed preferably, an explanation cannot be sought by consulting thermodynamic factors. In this regard, the reaction leading to the major isomer would not be favorable. But not only the energy of the product, also the energy of the transition state has an influence on the outcome of the reaction. Two possible transitions states are depicted in Figure 2.10. It is suggested that the transition state leading to the dibenzohelicene is lowered due to a favorable interaction between the silyl cation and electrons of the triphenylene π-system. π–Si^+ coordination is not a new phenomenon and has been reported for many examples.[11, 12b, 81] This interaction could reduce the energy of one transition state, and since such a geometry is not accessible in the transition state leading to the acene, the first pathway would be preferred.

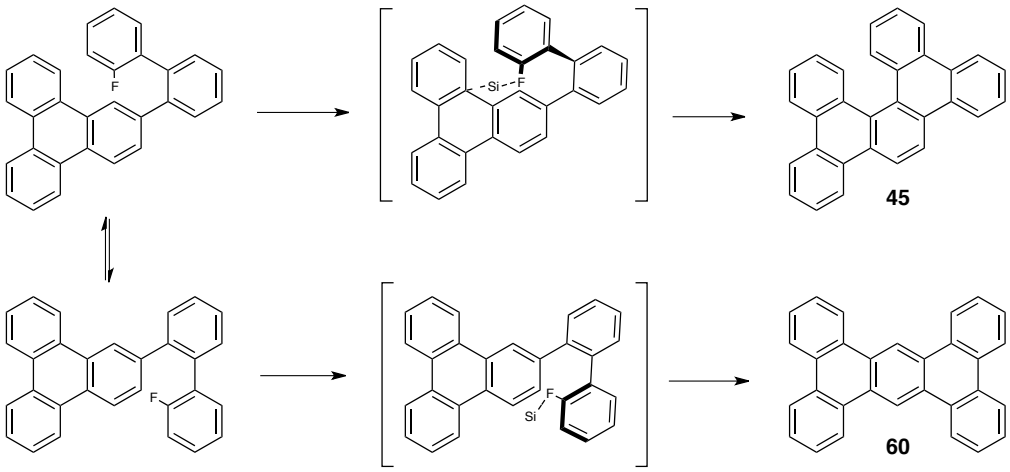

Figure 2.10. Suggested reaction pathways that lead to the helicene **45** and acene **60**. The upper transition state would experience a stabilization by coordination of the silyl cation to the triphenylene π-system.

For this hypothesis it is assumed that the two cyclizations happen independently. And indeed, performing the reaction on substrate **73**, which has one triphenylene group already cyclized, results in a very similar distribution of regioisomers (Scheme 2.20). The involvement of simple substituent effects that direct the position of electrophilic attack was considered not to be significant. The reason for that lies in the similarity of the two positions. If the triphenylene is simplified as two individual phenyl groups (ortho/para-directing), both positions of electrophilic attack exhibit one phenyl group in favorable ortho or para position, and one in unfavorable meta position (Figure 2.11). Therefore it is assumed that the two sites for electrophilic substitution are very similar, if not the ortho position slightly disfavored. So the substituent effect shouldn't have an influence on the product distribution.

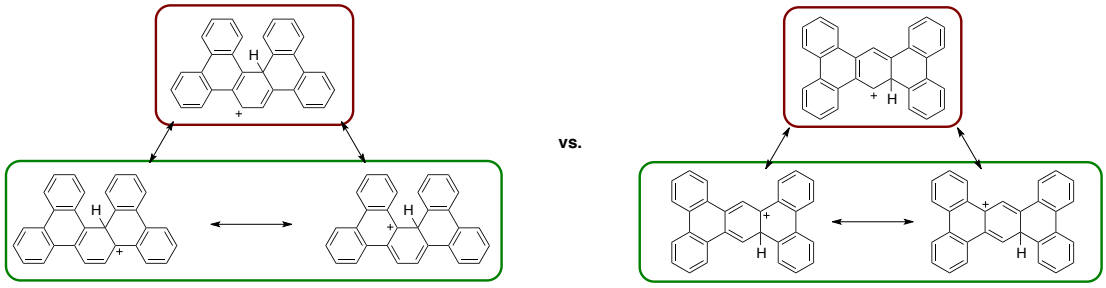

Figure 2.11. Comparison of the intermediate carbocations leading to the two observed isomers. Both reactive intermediates posses two more stable (green) and one less stable (red) resonance structure.

To find support for the Si^{+}–π coordination theory, the synthesis of a different substrate is required. The idea was to synthesize two substituted derivatives of **73**; one bearing an electron withdrawing group on the triphenylene, the other one an electron donating group. An increased electron density on the triphenylene should result in a higher amount of helicene, due to easier coordination of the silyl cation and thereby lowering the energy of the transition state. According to this hypothesis, a decreased electron density should then lead to a shift of product distribution towards the acene.

In an attempt to increase the electron density on that particular benzene moiety, substrate **74** was synthesized. It bears an additional methyl group that should provide the ring's π-system with a slightly higher electron density, in order to shift the outcome of the intramolecular arylation reaction towards the formation of the helicene. Analysis of the product mixture showed no big effect caused by the methyl group. By ^{1}H-NMR spectroscopy a very similar ratio of helicene to acene as in the

non-methylated product could be observed. This leads to the conclusion that either the proposed mechanism is not in agreement with the real process, or the influence of the methyl group is just too low. It would therefore be interesting to see what changes are caused by a chlorine substituent at the position of the methyl group. Unfortunately, the corresponding substrate could not be synthesized yet. But due to the strong electron withdrawing effect of chlorine, caused by its high electronegativity, a larger impact on the product ratio is expected.

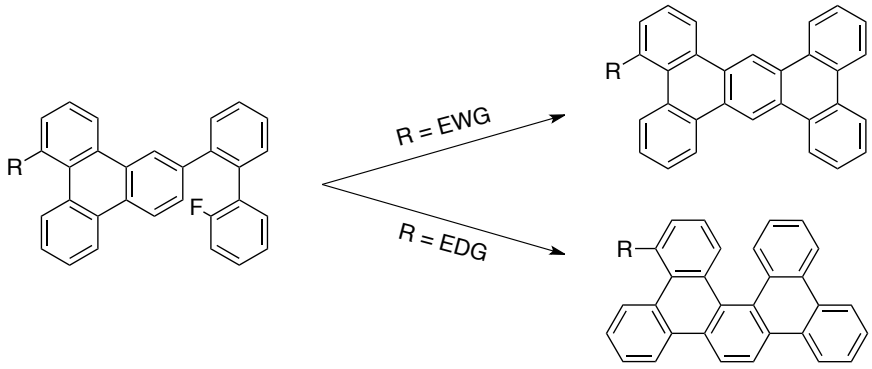

Scheme 2.21. According to the proposed transition state in Figure 2.10, an electron withdrawing group (EWG) should favor the formation of the acene, an electron donating group (EDG) should favor the formation of the helicene.

Apart from the mechanistic studies, one of the products of the reaction, the dibenzo[5]helicene, was utilized in a 2D crystallization experiment.[82] Therefore the compound was adsorbed on a gold surface (Au(111)) and the resulting layer was analyzed by scanning tunneling microscopy. It could be observed that the two enantiomeric forms of the helicene (P and M) formed homochiral domains, i.e. areas of ordered helicene of only one chirality - a novel finding for apolar helicenes. Furthermore, formation of one enantiomorph could be suppressed by addition of enantiomerically pure heptahelicene. The interested reader is referred to the publication in JACS (dx.doi.org/10.1021/ja402012j).

2.5.1 Syntheses of the Starting Materials

Substrate **73** was synthesized by a series of Negishi couplings, starting from 2-bromo-1-fluorobenzene, which was reacted with 1-bromo-2-iodobenzene to result in biphenyl **75** (Scheme 2.22). Cross-coupling with 1-bromo-4-iodobenzene afforded the *o*-terphenyl **34**, which was then subjected to the reaction conditions of the

intramolecular arylation, using triisopropylsilyl cation and DMDMS. Another Negishi coupling yielded the intermediate (**73**) of the reaction presented in this chapter.

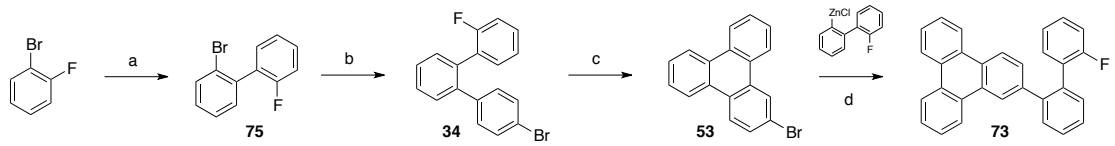

Scheme 2.22. Synthesis of the reaction intermediate **73**. a) 1. n-BuLi, $ZnCl_2$, –78 to r.t., THF 2. 1-bromo-2-iodobenzene, $Pd(PPh_3)_4$, 70 °C, 90 %. b) 1. n-BuLi, $ZnCl_2$, –78 to r.t., THF 2. 1-bromo-4-iodobenzene, $Pd(PPh_3)_4$, 70 °C, 52 %. c) $[^iPr_3Si][CHB_{11}H_5Cl_6]$, DMDMS, PhCl, 110 °C, 15 h, 94 %. d) Pd-PEPPSI-iPr, THF, 80 °C, 74 %.

Substrate **74** was synthesized starting from 2,6-dibromoaniline (Scheme 2.23). By performing a Sandmeyer reaction, the iodo-derivative **76** was obtained, which was subjected to Suzuki cross-coupling conditions to yield biphenyl **77**. Methylation thereof was achieved by treatment with *n*-BuLi followed by addition of iodomethane, to yield **78**. Two consecutive Negishi couplings resulted in formation of quaterphenyl **79**. Application of the intramolecular arylation reaction protocol with silyl cation and DMDMS resulted in the substituted triphenylene **80**. The reason why the cyclization reaction was performed at this stage and not one step earlier is the bromine atom on the fluoroarene of compound **81**, which drastically reduced the rings reactivity towards fluoride abstraction. In the final step, again, a Suzuki coupling was performed to result in substrate **74**.

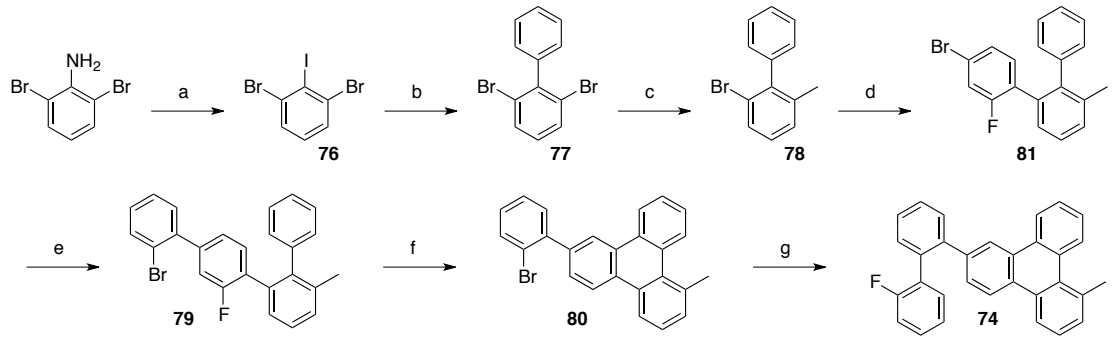

Scheme 2.23. Synthesis of the methylated reaction intermediate **74**. a) 1. HCl, $NaNO_2$, H_2O, 0 °C 2. KI, H_2O, 0 °C to r.t., 67 %. b) $PhB(OH)_2$, K_2CO_3, Pd-PEPPSI-iPr, dioxane, 90 °C, 38 h, 46 %. c) 1. n-BuLi, THF, –78 °C 2. MeI, 68 %. d) 1. n-BuLi, $ZnCl_2$, –78 to r.t., THF 2. 4-bromo-1-fluoro-2-iodobenzene, $Pd(PPh_3)_4$, 70 °C, 59 %. e) 1. n-BuLi, $ZnCl_2$, –78 to r.t., THF 2. 1-bromo-2-iodobenzene, $Pd(PPh_3)_4$, 70 °C, 46 %. f) $[^iPr_3Si][CHB_{11}H_5Cl_6]$, DMDMS, PhCl, 90°C, MW, 1 h, 88 %. g) 2-Fluorophenylboronic acid, K_2CO_3, $Pd(PPh_3)_4$, THF/H_2O, 70 °C 50 h, 34 % (50 % rSM).

2.6 Towards an Intermolecular Coupling Protocol

Considering the observed byproduct in the microwave-assisted reaction (mesitylated starting material), the development of an intermolecular aryl-aryl coupling reaction protocol seems feasible. But the task also bears many challenges. In this chapter some preliminary results towards the intermolecular coupling between fluoroarenes and arenes are presented and difficulties in the realization of such a method are discussed.

Some critical issues that have to be dealt with in order to design a reliable coupling protocol involving fluoroarenes and silyl cations are given by the following keywords.

Selectivity

A coupling partner like toluene for example, contains three different reaction sites. Is it possible to establish reaction conditions at which one single product is obtained? And how can one assure that the product itself does not react again with a fluoroarene, to result in oligomers or polymers?

Solvent

A solvent like chlorobenzene represents a possible coupling partner too. It might not be very reactive, due to the ring's electron deficiency, but the high concentration partially makes up for that. Neat reactions on the other hand might deactivate the silyl cation towards C–F activation by complexation of Si^+ to the arene coupling partner.

Nucleophile

An arene, which is used as nucleophile in the intramolecular coupling, is not very reactive, but this is not necessary, if the two reactants are already in the right position. But that is not the case in the intermolecular coupling, therefore an arene activated towards nucleophilic attack might be considered, keeping in mind that certain substituents can interfere with the silyl cation again.

A first very simple setup showed an unexpected outcome (Scheme 2.24). 3,5-dimethylfluorobenzene was heated with toluene or xylene, applying the catalytic reaction conditions at 110 °C. But instead of reacting with the provided coupling partner, coupling product of fluoroarene and mesitylene was found by GC-MS. This implied that abstraction of mesitylene directly from DMDMS had occurred. Indeed,

performing the same reaction, but omitting the intended coupling partner also results in defluoromesitylated starting material.

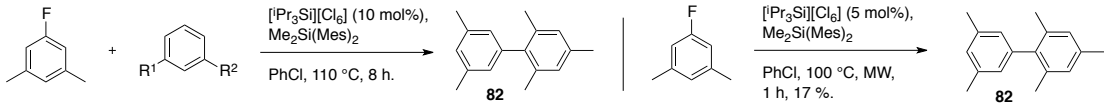

Scheme 2.24. First attempts of intermolecular coupling resulted in mesitylation of the fluoroarene.

But on the other hand, providing mesitylene as coupling partner and using TIPSPh as silane also resulted in the mesityl product. So it seems that not only silicon bound arenes can act as coupling partner, but also dissolved ones. The determining factor appears to be the electron density (i.e. the nucleophilicity) of the aromatic ring. This assumption can be tested by an experiment using deuterium-labeled mesitylene. By comparing the ration between non-deuterated product (from coupling with DMDS) and deuterated product (from coupling with mesitylene-d12 from solution), a statement on the effect of the silicon substituent on the mesitylene can be made.

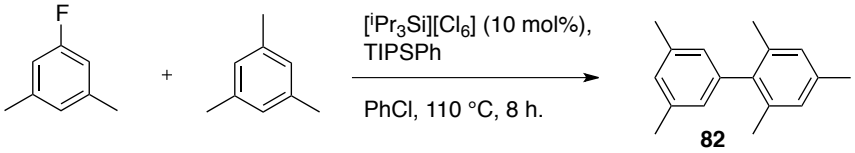

Scheme 2.25. Also the reaction with mesitylene in solution and TIPSPh as silane resulted in the same product (**82**).

But irrespective of the outcome, so far the conversion was rather low and the method needs drastic improvements in order to be able to compete with conventional methods. As already shown in the introduction, for strong nucleophiles (deprotonated amines, alcohols, or thiols) simple nucleophilic aromatic substitution works very well on fluoroarenes. For cross-coupling reactions, several strategies involving transition metals have proven useful. Therefore, further investments into the development of a silyl cation promoted intermolecular coupling reaction are questionable.

3 C–H Insertion Reaction

As we have seen in the previous chapter, a silyl cation can be used to cleave a C(Ar)–F bond and the incipient phenyl cation is attacked intramolecularly by a proximal aryl moiety. If the ring to be formed generates too much strain, the reaction is either very slow or does not proceed at all. But having a methyl group in close distance to the fluoroarene, the potential of this reaction can be directed towards another mechanism. This is best demonstrated with 2-fluoro-2'-methylbiphenyl (**83**). Whereas the already reported reactivity, which would lead to a highly strained 4-membered ring, does not occur, bond formation between phenyl and methyl does, affording fluorene (**84**) as the product. The thereby liberated proton is captured again by DMDMS, which upon protodesilylation, regenerates the silyl cation (Scheme 3.1).

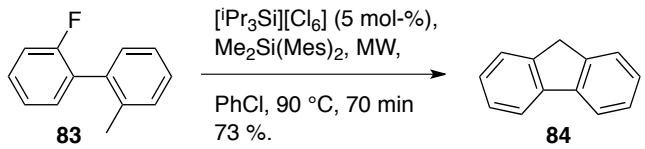

Scheme 3.1. Synthesis of fluorene by C–F activation/C–H insertion cascade, using silyl cations.

A similar reactivity was also observed for diazonium analogues (E.g. compound **85** in Scheme 3.2). These diazoniumbiphenyls are decomposed either thermally or under acidic conditions. The thereby generated phenyl cation forms a five-membered ring with an ortho alkyl substituent from the other ring of the biphenyl system, analogous to our reaction. The first observation of this kind was made by Mascarelli et al. in 1933,[83] and it was speculated about the mechanism since. One of the most persistent theories is the one of a Hydride shift from the methyl group to the phenyl cation, resulting in a benzyl cation, which can undergo intramolecular electrophilic aromatic substitution. This mechanism has been reasoned by the evidence of a benzyl alcohol **86**, generated from the reaction of the benzyl cation with water (Scheme 3.2).[84] This quenched intermediate was only isolated with a yield of 8 % though. And if these 8 % really had had formed the fluorene derivative is another question.

In a study involving a substrate containing a trifluormethyl instead of a simple methyl group, the corresponding fluoride shift from CF_3 to the arene could be observed, due to partial fluorination of position 4 in the fluorene product.[85] But one has to consider

that these results cannot simply be transferred to the compounds presented here. The differences in behavior of hydrogen and fluorine are considered too grave.

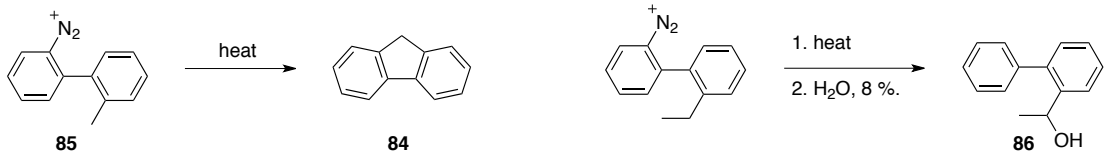

85 84 86

Scheme 3.2. Reactions that led to the idea of a hydride transfer mechanism.

What was further interpreted as evidence for a H^- shift mechanism was the observation of the corresponding reaction intermediate in the denitrogenation of diazonium-N,N-dibenzylbenzamide **87**, which is shown in Scheme 3.4.[86] The presence of the imminium ion **88**, the result of a hydride shift from the methyl group to the phenyl cation, could be proven. Yet in that study it was not supposed that this reactive carbocations would undergo ring closure, but rather be hydrolized and therby lead to benzaldehyde (**89**) and benzamide **90**. The also observed phthalimidine **91** was proposed to be generated by an insertion mechanism.[87] This was justified by exclusion of other paths, e.g. the hydride shift.

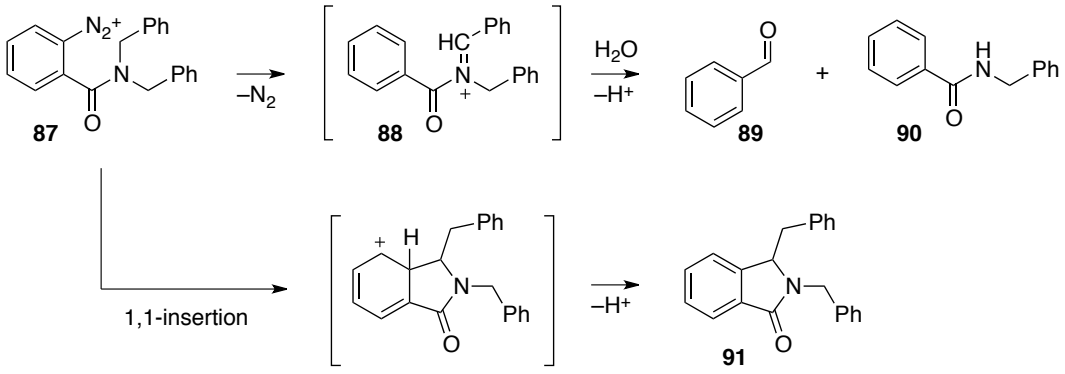

87 88 89 90 91

Scheme 3.3. Studies by Cohen and Lipowitz showed the intermediate formation of imminium ion **88** by hydride transfer. But the mechanism leading to ring-closed product **91** was suggested to be a 1,1-insertion.

In a different publication a pentacoordinated carbocation was considered as an intermediate for the Mascarelli reaction.[88] Product formation would occur from the loss of the proton from this cation. Another theory includes a Zwitterion intermediate[89] that is thought to be formed by abstraction of a benzylic proton. None of these suggestions were proven with clear evidence though. Both proposed reaction intermediates are shown in Figure 3.1.

Figure 3.1. Two proposed intermediates that were thought to be responsible for the formation of fluorine from 2-diazonium-2'-methylbiphenyl; pentacoordinated carbocation[88] (left) and zwitterion[89] (right).

It is assumed that the fluoroarenes presented herein react in a similar fashion as the diazonium compounds. So to contribute to this 80-year-lasting discussion, a deuterated analog of the 1-fluoro-1'-methylbiphenyl was synthesized to observe the faith of the methyl protons. MS and NMR analysis showed that most product molecules still possessed all three deuterium atoms. Only a small fraction ended up being captured as D^+, by the base (DMDMS) supposedly. In contrast to what has been proposed previously, Deuterium distribution (see square in Figure 3.4) within the product now suggests a different mechanism as the predominant pathway. A 1,2 insertion of the phenyl cation into the carbon deuterium bond followed by elimination of a proton would result in deuteration of product in position 1. A possible explanation of finding deuterium at position 2 is also given in Scheme 3.4. A hydride or a deuteride shift after the insertion would lead to the more stable cation **92** (conjugated with the other benzene ring of fluorene). The energy difference in favor of the product of a hydride/deuteride shift (**92**, compared to **93**) was claculated to be 33 kJ/mol.* Taking into account that a hydride shift occurs more readily than a deuteride shift, one would end up with a pronounced deuteration at position 1, but also deuteration at position 2.

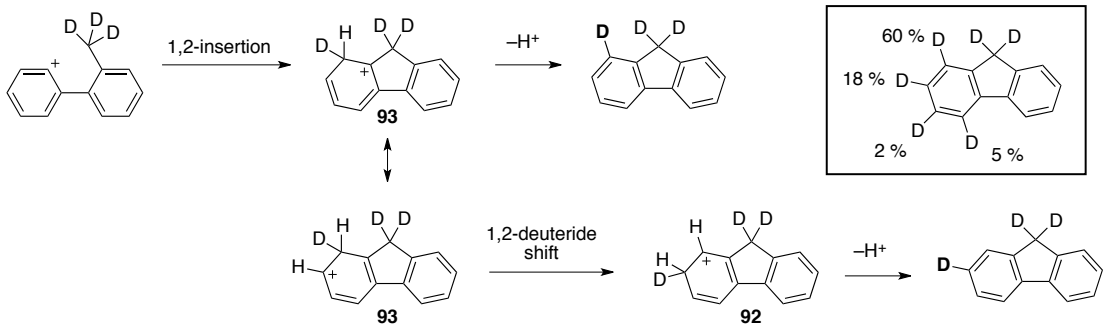

Figure 3.4. Possible explanation for the finding of deuterium distribution; pathways leading to the major products, 1- and 2-substituted fluorene respectively.

* For details on the calculations, see the experimental part.

Considering a mechanism that involves an intramolecular hydride transfer, deuteration of position 4 or no deuteration would be expected. In fact, there is a small fraction of product that is deuterated in this position. Thus, the hydride transfer mechanism cannot be excluded completely although not being very likely. This is also suggested by another experiment performed with 2-fluoromethylbiphenyl (**94**). Subjected to the reaction conditions used on **83** (although at room temperature due to the high reactivity[48]), no formation of fluorene was observed, but only substitution of fluorine by mesitylene, resulting in **95**. Admittedly one can still argue that fluorene might form at high temperatures.

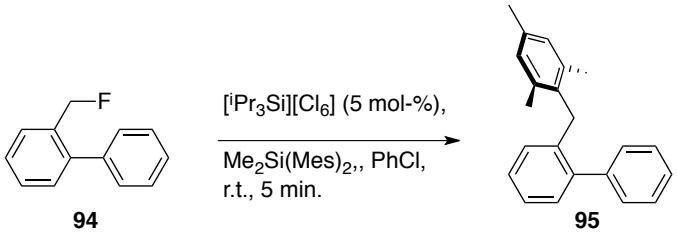

94 **95**

Scheme 3.3. Fluorene was not obtained when **94** was subjected to the CF activation reaction conditions. The intermediate benzylic carbocation was mesitylated.

In the example reaction showed in the beginning, CH insertion occurred exclusively, because of the high strain of four-membered rings (product of the intramolecular arylation). In substrates where both reaction pathways are probable, a distribution of the two different products can be observed. Whereas 1-(2-fluorophenyl)-2-methylnaphthalene (**96a**) gave the product of arene-fluoroarene coupling as major compound (**97a**), for substrates **96b** and **96c**, the ratio was shifted towards the C–H insertion product (**98b-c**). The reactions and ratios are summarized in Scheme 3.4. The composition of the product mixtures stemming from fluoroarene-arene coupling (**97a-c**) and C–H insertion (**98a-c**) were calculated by ^{1}H-NMR. The reason for the specific selectivities is thought to arise from the various C–H bond strengths of the involved methyl group. In the case of substrate 96a the carbon-hydrogen bond of a primary methyl group has to be broken in order to obtain a C–H insertion. For substrates 96b and 96c the hydrogen is attached to a tertiary methyl group. The fact that the latter C–H bond is weaker compared to the first (iPr vs Me), matches the observed ratios, which are shifted towards C–H insertion in case of the weaker C–H bonds.[90] A faster insertion into the isopropyl C–H bond compared to the methyl C–H bond is the consequence. What also has to be mentioned is that in the second reaction of Scheme 3.4, no formation of a six-membered ring could be observed (reaction with CH_3 instead of CH).

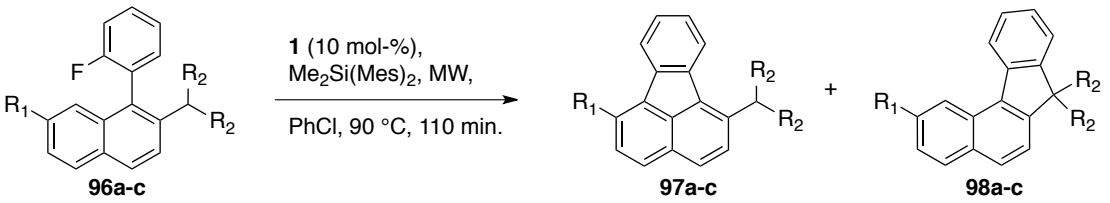

Product distribution:	a)	R^1=H, R^2=H	1.8 : 1.0
	b)	R^1=H, R^2=Me	1.0 : 1.5
	c)	R^1=^{i}Pr, R^2=Me	1.0 : 1.6

Scheme 3.4. Variations in the distribution of products due to different preferences toward intramolecular arylation and C–H insertion.

So far only insertion into C–H bonds of benzylic carbons were observed. But applying the reaction conditions on 2-fluoro-2'-tert-butylbiphenyl (**99**) yields ring-closed product **100** (9-hydro-10-dimethylphenanthrene). The formation thereof is slower than that of the model compound. This observation matches the increased C–H bond strength in an aliphatic methyl group (bond dissociation energy (BDE): ~420 kJmol^{-1})[91], compared to a benzylic CH_3 (BDE: 375 kJmol^{-1})[91].

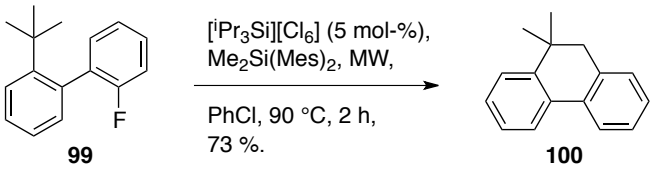

Scheme 3.5. CH insertion into a non-benzylic C–H bond was achieved with substrate **99**, resulting in product **100**.

The stepwise activation of two generally very stable functional groups (F, Me) opens up new possibilities for the synthesis of small polyaromatic hydrocarbons and provides access to a greater variety of products, which was demonstrated on a corannulene derivative (Scheme 3.6). Installing two fluorophenyl groups on dibromodimethyl corannulene substrate **101** under Suzuki cross coupling conditions provided starting material **102** for the newly introduced method. Due to the increased distance between methyl and fluoroarene the reaction proceeded slowly compared to the biphenyl substrate. Also different reaction conditions were chosen in order to facilitate a smooth transition to product **103**. UV/Vis and luminescence spectra were measured for this compound

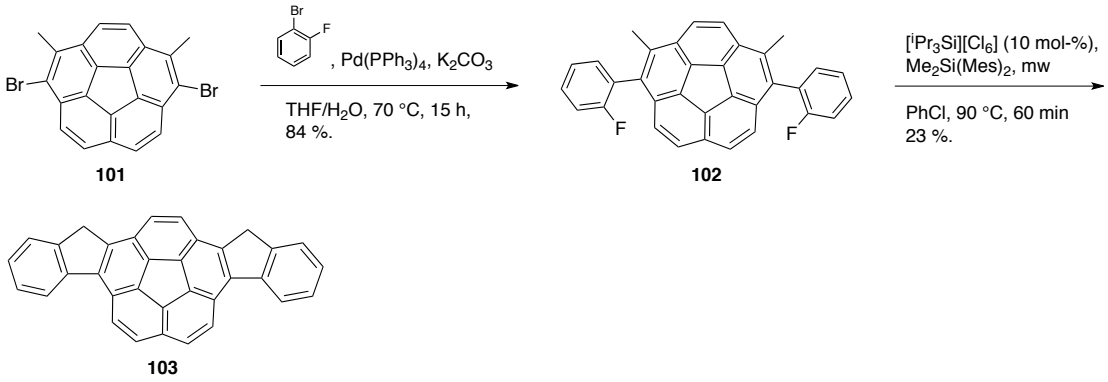

103

Scheme 3.6. Synthetic pathway leading to a novel corannulene derivative.

4 Experimental Part

Materials and Methods

Reaction Conditions and Chemicals

The C–F activation reactions were set up in an MBraun glovebox under a nitrogen atmosphere with O_2, H_2O < 0.1 ppm. The reaction mixture was heated outside the glovebox, but still under a nitrogen atmosphere. The microwave-assisted version of the reaction was also set up in the glovebox using a microwave tube. The tube was eqipped with a regular cap and heated using a CEM Discover microwave reactor.
All glassware was dried at 150 °C for at least 12 hrs and allowed to cool in vacuo.
The substrates and reagents used for the C–F activation reactions were synthesized and purified in our group (exceptions in Table 4.1). 2,6-Di-tert-butylpyridine was further purified by filtration through dry aluminum oxide. The solvents were of pro analysis grade and were additionally purified (see Table 1 for suppliers). Chlorobenzene was distilled from CaH_2 or passed through activated alumina and stored over molecular sieves. Pentane was purified by washing with conc. H_2SO_4, followed by washing with a basic aqueous $KMnO_4$ solution (1 g in 50 mL of 1 M aq. NaOH), followed by distillation from CaH_2. All solvents were stored over 3 Å molecular sieves. For work-up and purification outside the glovebox, distilled solvents of technical grade were used.

Table 4.1. Suppliers and grade of used chemicals.

Compound	Quality	Supplier
benzene	≥99.5%	Fluka
chlorobenzene	puriss.	Fluka
pentane	99+%	Acros
tris(o-tolyl)phosphine	99%	Acros

2,6-di-tert-butylpyridine	97%	Acros
2-fluorophenylboronic acid	97%	Apollo
dichlorodimethylsilane	99+%	Acros
2-bromomesitylene	99%	Alpha Aesar

Instruments

Melting points were measured with a Büchi Melting Point P-540 apparatus and are uncorrected.

NMR spectra were recorded on Bruker AV-400 (^{1}H, ^{13}C, ^{19}F, ^{29}Si), and Bruker AV-500 (^{1}H, ^{13}C) instruments. ^{13}C and ^{29}Si NMR spectra are proton decoupled. Data are reported as follows: chemical shift in ppm, multiplicity (s = singlet, d = doublet, t = triplet, q = quadruplet, m = multiplet, dd = doublet of doublet, dt = doublet of triplet, etc.), coupling constant ^{n}J in Hz, and integration. The signals were referenced against solvent peaks (^{1}H: residual $CHCl_3$ 7.26 ppm, residual C_6HD_5 7.16 ppm; ^{13}C: $CDCl_3$ 77.16 ppm, C_6D_6 128.0 ppm) or external standards (^{29}Si: $SiMe_4$ in C_6D_6 0 ppm, ^{11}B: $BF_3{\cdot}Et_2O$ capillary in acetone-d_6 0 ppm, ^{19}F: CCl_3F in $CDCl_3$ 0 ppm).

Infrared spectra were recorded on a Jasco FT/IR-410 spectrophotometer. Compounds were measured as solids or oils (neat). Absorption bands are given in wave numbers (cm^{-1}), and the intensities are characterized as follows: s = strong (0–33% transmission), m = medium (34–66% transmission), w = weak (67–100% transmission).

Mass spectra were recorded by the Laboratory for Mass Spectroscopy of the Organic Chemistry Institute of the University of Zurich on a Finnigan MAT95 instrument or on a Finnigan Trace DSQ GC-MS. Data are reported as follows: m/z (% relative intensity).

X-ray structure analyses were performed by the X-ray Crystallography Facility of the Institute of Organic Chemistry at the University of Zurich.

Computational Methods

All structure and property calculations were carried out using the GAMESS[92] and Gaussian03[93] software packages, employing both density functional theory (B98)[94] as well as conventional second order Møller-Plesset perturbation theory (MP2).[95] Full geometry optimizations were performed and uniquely characterized via second derivatives (Hessian) analysis to determine the number of imaginary frequencies (0=minima; 1=transition state) and zero point corrections. Dunning's double-z polarized basis sets,[96] denoted DZ(2df,pd) (geometry) and DZ+(2df,pd) (properties) were both employed. An ultrafine grid was used for all computations. From the fully optimized structures, single point MP2[95] energies were carried out for accurate energetics, and contributions from solvent environment were including using the COSMO solvation method[97] and Klamt radii. Effects of the solvent are essential for determining accurate energetics for the reaction process. NMR computations were performed with the class II NMR method, CSGT,[98] and calibrated to TMS. Molecular orbital contour plots, used as an aid in the analysis of results, were generated and depicted using WEBMO, and QMViev.[99]

Procedures and Characterization

General procedure A for the intramolecular Friedel–Crafts aryl coupling using conventional heating

Arylfluoride (1.0 equiv.), dimethyldimesitylsilane (1.2 equiv.) and triisopropylsilylium carborane (0.1 equiv.) were dissolved in chlorobenzene to give a 0.1 M clear solution. The reaction mixture was heated to 110 °C and stirred for 8 h under nitrogen atmosphere. After cooling to room temperature, the mixture was diluted with EtOAc (2 mL) and some drops of water were added to quench the reaction. The solvents were evaporated under reduced pressure and the residue was subjected to silica gel flash column chromatography using dry charge.

General procedure B for the intramolecular Friedel–Crafts aryl coupling using microwave irradiation

A microwave tube was charged with arylfluoride (1.0 equiv.), dimethyldimesitylsilane (1.2 equiv.) and triisopropylsilylium carborane (5 mol-%) inside the glovebox. The compounds were dissolved in chlorobenzene to give a 0.1 M clear solution. The reaction mixture was heated at 200 W with cooling turned on (Max. Power) for 40 to 120 min. Usually a temperature of around 90 °C was reached towards the end of the reaction time. After cooling to room temperature, the mixture was diluted with EtOAc (2 mL) and some drops of water were added to quench the reaction. The solvents were evaporated under reduced pressure and the residue was subjected to silica gel flash column chromatography using dry charge.

General procedure C for the Suzuki cross-coupling reactions using THF/H_2O

A 2-neck flask equipped with a cooler was purged with 3 cycles of vac./N_2. It was charged with haloarene (1.00 equiv.), boronic acid (1.50 equiv.), Palladium catalyst (2 mol-%), K_2CO_3 (3 equiv.), and degassed solvent (THF/H_2O 9:1, ~10 mL/mmol haloarene). The mixture was heated to 70 °C and stirred for 14 h. After cooling the solution to room temperature, sat. aq. sol. of $NaHCO_3$ was added. The aqueous phase was extracted with DCM three times and the combined organic layers were dried over $MgSO_4$, filtered and concentrated *in vacuo*. The residue was purified by flash column chromatography.

General procedure D for the Suzuki cross-coupling reactions using tol/EtOH/H_2O

To a 0.25 M solution of aryl bromide (1.00 equiv.) in degassed toluene/EtOH/H_2O (10/4/1) fluoroarylboronic acid (1.05 equiv.), potassium carbonate (3.00 equiv.) and $Pd(PPh_3)_4$ (0.01 equiv.) were added. The reaction mixture was heated to 90 °C and stirred for 14 h under nitrogen atmosphere. After cooling the solution to room temperature, water was added. The aqueous phase was extracted with EtOAc three times and the combined organic layers were dried over $MgSO_4$, filtered and

concentrated *in vacuo*. The residue was purified by flash column chromatography to obtain the desired product.

General procedure E for Negishi cross-coupling reactions

To a solution of haloarene (1.1 equiv.) in THF (degassed, ~10 mL/mmol haloarene) *n*-BuLi (1.6 M in hexanes, 1.15 equiv.) was added slowly at –78 °C. After stirring for 30 min a solution of freshly dried $ZnCl_2$ (1.2 equiv., dried under vacuum at 600 °C for 1 min) in THF (as little as possible) was added. The solution then usually turned from slightly yellow to colorless. After warming to room temperature, the solution was transferred to a flask charged with the haloarene coupling partner, Palladium catalyst, and THF (couple of mL). The mixture was heated to 70 °C and stirred for 14 h. After cooling the solution to room temperature, sat. aq. sol. of $NaHCO_3$ was added. The aqueous phase was extracted with DCM three times and the combined organic layers were dried over $MgSO_4$, filtered and concentrated *in vacuo*. The residue was purified by flash column chromatography to obtain the desired product

Triisopropylsilylium 7,8,9,10,11,12-Cl_6-*closo*-carborate (2)

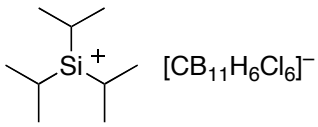

The reaction was run in the glovebox. To a suspension of trityl hexachlorocarborane (250 mg, 0.42 mmol) in chlorobenzene (1.5 mL) an excess of triisopropylsilane (30 drops) was added and the mixture was stirred at room temperature for 3 h. The suspension was concentrated to about 20 % of its original volume and the residue was washed with pentane four times to give the product **2** as a slightly yellow solid (200 mg, 90 %).

^{1}H NMR (400 MHz, C_6D_6): δ = 1.64 (s (broad), 1H), 1.19 (sept., J = 7.6 Hz, 3H), 0.70 (d, J = 7.6 Hz, 18H).
For full characterization see [100].

Mesitylenium 7,8,9,10,11,12-Cl_6-*closo*-carborate

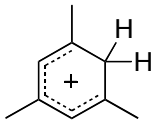

$[CB_{11}H_6Cl_6]^-$

For procedure and characterization check [101].

Dimethyldimesitylsilane (DMDMS)

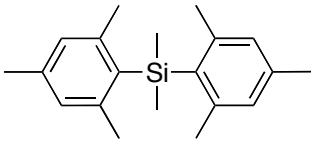

A solution of 2-bromomesitylene (4.7 mL, 30 mmol) in THF (20 mL) was cooled to –78 °C. Thereto *n*-BuLi (1.52 M in hexane, 20 mL, 30 mmol) was added over a period of 25 min. Precipitate started to form. After stirring for 1 h dichlorodimethylsilane (1.8 mL, 15 mmol) was added and the mixture was kept at –78 °C for 90 min, before it was allowed to warm to room temperature and stirred for 1 h. The resulting suspension was diluted with EtOAc and water. The aqueous phase was extracted with EtOAc three times. The combined organic layers were dried over MgSO4, filtered and concentrated *in vacuo*. Flash column chromatography (pure hexane) afforded the desired product DMDMS as colorless crystals (2.25 g, 50 %).

R_f (hexane) = 0.25.

M.p.: 74–76 °C.

^{1}H-NMR (500 MHz, $CDCl_3$): δ = 6.75 (s, 4H), 2.24 (s, 12H), 2.22 (s, 6H), 0.66 (s, 6H).

^{13}C-NMR (125.8 MHz, $CDCl_3$): δ = 143.28, 138.29, 135.15, 129.27, 24.18, 21.08, 6.18.

^{29}Si-NMR (79.5 MHz, $CDCl_3$): δ = –10.0.

IR (neat, cm^{-1}): 3025*w*, 2962*w*, 2947*w*, 2916*w*, 1604*m*, 1541*w*, 1449*m*, 1405*m*, 1374*w*, 1259*w*, 1251*w*, 1062*w*, 1025*w*, 849*m*, 834*s*, 815*s*, 768*m*, 714*w*, 673*m*, 607*m*, 550*m*.

MS (EI): *m/z* (%): 296.1 (2), 281.1 (19), 176.1 (100), 161.0 (100).

HR-MS (EI): *m/z*: Calculated for $C_{20}H_{28}Si$: 296.1960; measured: 296.1960.

1-(2-Fluorophenyl)naphthalene (14)

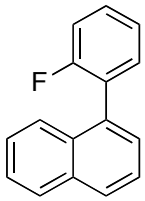

14 was synthesized according to the general procedure E, using 1-bromonaphthalene (1.04 g, 5.0 mmol), *n*-BuLi (2.5 M in hexanes, 2.1 mL, 5.2 mmol), $ZnCl_2$ (745 mg, 5.5 mmol), $Pd(PPh_3)_4$ (60 mg, 0.05 mmol), and 1-bromo-2-fluorobenzene (797 mg, 4.5 mmol). The reaction mixture was stirred at 65 °C for 14 h and FC (SiO_2, hex/DCM 99:1 to 95:5) followed by Kugelrohr distillation afforded the desired product as colorless crystals (755 mg, 67 %).

R_f (hexane) = 0.24.

^{1}H-NMR (500 MHz, $CDCl_3$): δ = 7.92–7.87 (m, 2H), 7.68–7.63 (m, 1H), 7.54 (dd, *J* = 8.3, 7.3 Hz, 1H), 7.51–7.47 (m, 1H), 7.47–7.38 (m, 4H), 7.26 (td, *J* = 8.0, 8.0, 1.0 Hz, 1H), 7.23–7.18 (m, 1H)

^{13}C-NMR (125.8 MHz, $CDCl_3$): δ = 160.22 (d, $^1J_{C–F}$ = 246.6 Hz), 134.03, 133.67, 132.53 (d, $^3J_{C–F}$ = 3.5 Hz), 131.92, 129.58 (d, $^3J_{C–F}$ = 8.1 Hz), 128.53, 128.42, 128.13 (d, $^2J_{C–F}$ = 16.4 Hz), 127.81, 126.35, 126.02, 125.96, 125.42, 124.21 (d, $^4J_{C–F}$ = 3.8 Hz), 115.83 (d, $^2J_{C–F}$ = 22.4 Hz).

^{19}F-NMR (376.5 MHz, $CDCl_3$): δ = –114.12.

IR (neat, cm^{-1}): 3059*w*, 1578*w*, 1508*w*, 1491*m*, 1460*w*, 1447*w*, 1396*w*, 1248*w*, 1214*m*, 1098*w*, 1033*w*, 1018*w*, 843*w*, 798*m*, 775*s*, 755*s*, 616*w*, 537*w*, 517*w*.

MS (EI): *m/z* (%): 222.1 (100), 220.1 (50), 202.1 (12), 110.0 (20).

HR-MS (EI): *m/z*: Calculated for $C_{16}H_{11}F$: 222.0845; measured: 222.0840.

Fluoranthene (15)

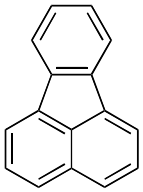

15 was synthesized according to the general procedure B, using **14** (36 mg, 0.162 mmol), [$^{i}Pr_3Si$][$CHB_{11}H_5Cl_6$] (5 mg, 0.010 mmol), and DMDMS (62 mg, 0.209 mmol). The reaction mixture was subjected to microwave irradiation (200 W) for 40 min, in which a temperature of around 85 °C was reached. FC (hex/DCM 98:2 to 96:4) gave the product as white solid (28 mg, 85 %).

M.p.: 100–105 °C.

^{1}H-NMR (500 MHz, $CDCl_3$): δ = 7.95 (d, *J* = 7.0 Hz, 2H), 7.94–7.90 (m, 2H), 7.85 (d, *J* = 8.0 Hz, 2H), 7.65 (dd, *J* = 8.0, 7.0 Hz, 2H), 7.41–7.37 (m, 2H).

^{13}C-NMR (125.8 MHz, $CDCl_3$): δ = 139.58, 137.10, 132.52, 130.12, 128.11, 127.69, 126.80, 121.68, 120.21.

IR (neat, cm^{-1}): 3051*w*, 3039*w*, 1942*w*, 1879*w*, 1815*w*, 1688*w*, 1602*w*, 1454*m*, 1439*m*, 1426*m*, 1183*w*, 1135*w*, 970*w*, 939*w*, 911*w*, 825*m*, 773*s*, 748*s*, 617*m*.

MS (EI): *m/z* (%): 202.1 (100), 200.0 (30), 101.0 (32).

2-Fluoro-1,1':2',1''-terphenyl (30)

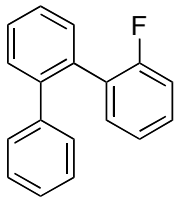

30 was synthesized according to the general procedure A to result in a colorless oil with a yield of 99 %.

R_f (hexane) = 0.19.

^{1}H-NMR (500 MHz, $CDCl_3$): δ = 7.46–7.37 (m, 4H), 7.22–7.08 (m, 7H), 7.00 (td, J = 7.5, 7.5, 1.2 Hz, 1H), 6.94–6.87 (m, 1H).

^{13}C-NMR (125.8 MHz, $CDCl_3$): δ = 159.68 (d, $^1J_{C–F}$ = 246.4 Hz), 141.83, 141.43, 134.55, 132.28 (d, $^3J_{C–F}$ = 3.5 Hz), 131.12, 130.30, 129.37, 129.28 (d, $^2J_{C–F}$ = 15.7 Hz), 128.96 (d, $^3J_{C–F}$ = 7.9 Hz), 128.31, 127.92, 127.30, 126.74, 123.82 (d, $^4J_{C–F}$ = 3.6 Hz), 115.54 (d, $^2J_{C–F}$ = 22.4 Hz).

^{19}F-NMR (500 MHz, $CDCl_3$): δ = –115.15.

IR (neat, cm^{-1}): 3058*w*, 3023*w*, 1506*w*, 1493*w*, 1472*m*, 1444*w*, 1433*w*, 1010*w*, 825*w*, 752*s*, 743*s*, 699*s*, 614*w*, 571*w*, 549*w*, 512*w*.

MS (EI): *m/z* (%): 248.1 (100), 228.1 (37), 226.1 (29).

HR-MS (EI): *m/z*: Calculated for $C_{18}H_{13}F$: 248.1001; measured: 248.0999.

Triphenylene (23)

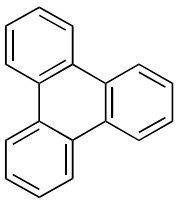

23 was synthesized according to the general procedure A, using **30** (50 mg, 0.203 mmol), [*i*Pr$_3$Si][CHB$_{11}$H$_5$Cl$_6$] (10 mg, 0.020 mmol) and DMDMS (72 mg, 0.244 mmol). The mixture was heated at 110 °C for 8 h. Flash column chromatography (SiO_2, hex/DCM 99:1) afforded the product as colorless needles (45 mg, 97 %).

R_f (hexane) = 0.14.

M.p.: 194–197 °C.

^{1}H-NMR (500 MHz, $CDCl_3$): δ = 8.67–8.63 (m, 6H), 7.67–7.63 (m, 6H).

^{13}C-NMR (125.8 MHz, $CDCl_3$): δ = 129.92, 127.36, 123.44.

IR (neat, cm^{-1}): 2956*w*, 2916*w*, 1433*m*, 1242*w*, 739*s*, 618*w*.

MS (EI): *m/z* (%): 228 (100), 226.1 (44), 114.0 (40).

2-Fluoro-5-methyl-1,1':2',1''-terphenyl (32)

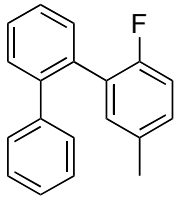

32 was synthesized according to the general procedure C, using 2-bromobiphenyl (500 mg, 2.1 mmol), 2-fluoro-5-methylphenylboronic acid (346 mg, 2.3 mmol), K_2CO_3 (888 mg, 6.4 mmol), and Pd(PPh$_3$)$_4$ (10 mg). The reaction mixture was stirred at 90 °C for 18 h. FC (SiO_2, hexane) afforded the desired product as colorless oil (463 mg, 82 %).

R_f (hexane) = 0.16.

^{1}H-NMR (500 MHz, $CDCl_3$): δ = 7.46–7.36 (m, 4H), 7.22–7.12 (m, 5H), 6.99–6.92 (m, 2H), 6.77 (dd, *J* = 9.5, 8.5 Hz, 1H), 2.23 (s, 3H).

^{13}C-NMR (125.8 MHz, $CDCl_3$): δ = 157.81 (d, $^1J_{C-F}$ = 243.9 Hz), 141.81, 141.55, 134.79, 133.15 (d, $^4J_{C-F}$ = 3.6 Hz), 132.57 (d, $^3J_{C-F}$ = 3.4 Hz), 131.09, 130.22, 129.36

(d, $^{3}J_{C-F}$ = 7.8 Hz), 129.32, 128.83 (d, $^{2}J_{C-F}$ = 16.0 Hz), 128.21, 127.88, 127.27, 126.69, 115.12 (d, $^{2}J_{C-F}$ = 22.5 Hz), 20.74.

^{19}F-NMR (376.5 MHz, $CDCl_3$): δ = –120.43.

IR (neat, cm^{-1}): 3058*w*, 3026*w*, 2922*w*, 1497*m*, 1474*m*, 1434*w*, 1242*w*, 1219*m*, 1009*w*, 882*w*, 814*m*, 781*w*, 761*m*, 743*s*, 699*s*.

MS (EI): *m/z* (%): 262.1 (100), 247.1 (47), 242.1 (41), 227.1 (16).

HR-MS (EI): *m/z*: Calculated for $C_{19}H_{15}F$: 262.1158; measured: 262.1157.

2-Methyltriphenylene (37)

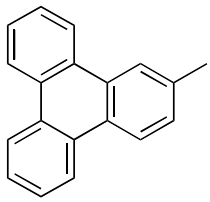

37 was synthesized according to the general procedure A, using **32** (50 mg, 0.189 mmol), [*i*Pr_3Si][$CHB_{11}H_5Cl_6$] (10 mg, 0.019 mmol) and DMDMS (67 mg, 0.227 mmol). The mixture was heated at 110 °C for 8 h. Flash column chromatography (SiO_2, hex/DCM 99:1) afforded the product as colorless crystals (47 mg, 99 %).

R_f (hexane) = 0.13.

M.p.: 99–101 °C.

^{1}H-NMR (500 MHz, $CDCl_3$): δ = 8.66–8.57 (m, 4H), 8.53 (d, *J* = 9.0 Hz, 1H), 8.43 (s, 1 H), 7.66–7.59 (m, 4H), 7.49–7.47 (m, 1H), 2.60 (s, 3H).

^{13}C-NMR (125.8 MHz, $CDCl_3$): δ = 137.03, 130.04, 129.90, 129.84, 129.54, 128.84, 127.62, 127.31, 127.24, 127.22, 126.92, 123.46, 123.44, 123.40, 123.38, 123.83, 22.01.

IR (neat, cm^{-1}): 3080*w*, 3025*w*, 2916*w*, 1617*w*, 1507*w*, 1492*w*, 1437*m*, 1244*w*, 1052*w*, 815*m*, 771*w*, 748*s*, 717*s*, 629*w*, 617*w*, 585*w*, 444*w*, 419*w*.

MS (EI): 242.2 (100), 239.1 (48), 121.0 (24).

2-Fluoro-3''-methyl-1,1':2',1''-terphenyl (31)

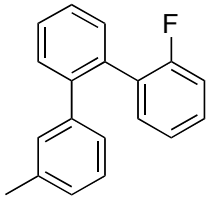

31 was synthesized according to the general procedure C to result in a colorless oil with a yield of 66 %.

R_f (hexane) = 0.17.

^{1}H-NMR (500 MHz, $CDCl_3$): δ = 7.45–7.37 (m, 4H), 7.22–7.15 (m, 1H), 7.10 (td, J = 9.5, 9.5, 2.0 Hz, 1H), 7.07–6.87 (m, 6H), 2.22 (s, 3H).

^{13}C-NMR (125.8 MHz, $CDCl_3$): δ = 159.72 (d, $^1J_{C–F}$ = 246.3 Hz), 141.88, 141.31, 137.46, 134.52, 132.30 (d, $^3J_{C–F}$ = 3.5 Hz), 131.08, 130.27, 130.16, 129.39 (d, $^2J_{C–F}$ = 15.9 Hz), 128.88 (d, $^3J_{C–F}$ = 8.1 Hz), 128.26, 127.71, 127.45, 127.17, 126.46, 123.77 (d, $^4J_{C–F}$ = 3.6 Hz), 115.50 (d, $^2J_{C–F}$ = 22.4 Hz), 21.50.

^{19}F-NMR (376.5 MHz, $CDCl_3$): δ = –115.26.

IR (neat, cm^{-1}): 3057*w*, 3031*w*, 2922*w*, 2856*w*, 1605*w*, 1583*w*, 1490*w*, 1472*w*, 1438*w*, 1240*w*, 1207*w*, 1106*w*, 822*w*, 791*w*, 751*s*, 704*m*, 561*w*.

MS (EI): *m/z* (%): 262.1 (100), 247.1 (53), 242.1 (22), 227.1 (17).

HR-MS (EI): *m/z*: Calculated for $C_{19}H_{15}F$: 262.1158; measured: 262.1156.

Mixture of 1-methyltriphenylene (38) and 2-methyltriphenylene (37)

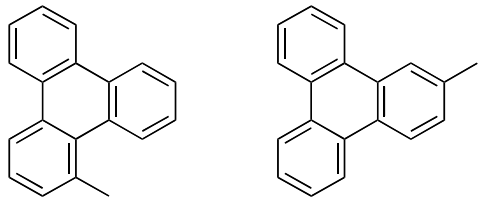

37 and **38** were synthesized according to the general procedure A, using **31** (18 mg, 0.069 mmol), [*i*Pr_3Si][$CHB_{11}H_5Cl_6$] (3.5 mg, 0.007 mmol) and DMDMS (24 mg, 0.082 mmol). The mixture was stirred at 110 °C for 8 h. Flash column chromatography (SiO_2, hex/DCM 95:5) afforded the product as colorless oil (17 mg, 99 %).
The two conformers could not be separated. The characterization of 2-methyltriohenylene was described above, therefore only the NMR signals for 1-methyltriphenylene are noted here.

^{1}H-NMR (500 MHz, $CDCl_3$): δ = 8.62–8.56 (m, 4H), 8.52 (d, J = 7.5 Hz, 1H), 7.66–7.59 (m, 3H), 7.59–7.48 (m, 3H), 2.03 (s, 3H).

^{13}C-NMR (125.8 MHz, $CDCl_3$): δ = 135.50, 131.78, 131.41, 131.12, 130.81, 130.51, 130.52, 130.07, 128.67, 127.41, 127.26, 126.73, 126.42, 125.70, 123.79, 123.38, 123.17, 121.18, 26.81.

MS (EI): 242.2 (100), 239.1 (48), 121.0 (24).

2-Fluoro-3'',5-dimethyl-1,1':2',1''-terphenyl (33)

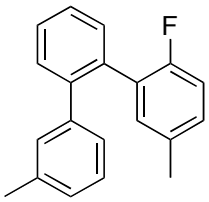

33 was synthesized according to the general procedure C, using 2-bromo-3'-methylbiphenyl (90 %, 498 mg, 1.81 mmol), 2-fluoro-5-methylphenylboronic acid (295 mg, 1.90 mmol), K_2CO_3 (752 mg, 5.44 mmol), and $Pd(PPh_3)_4$ (10 mg). The reaction mixture was stirred at 90 °C for 14 h. FC (SiO_2, hexane) afforded the desired product as colorless oil (294 mg, 59 %).

R_f (hexane) = 0.16.

^{1}H-NMR (500 MHz, $CDCl_3$): δ = 7.44–7.34 (m, 4H), 7.08–7.03 (m, 1H), 7.0–6.88 (m, 5H), 6.77 (dd, J = 12.0, 10.5 Hz, 1H), 2.23 (s, 3H), 2.22 (s, 3H).

^{13}C-NMR (125.8 MHz, $CDCl_3$): δ = 157.84 (d, $^1J_{C–F}$ = 243.7 Hz), 141.86, 141.42, 137.39, 134.77, 133.06 (d, $^4J_{C–F}$ = 3.6 Hz), 132.56 (d, $^3J_{C–F}$ = 3.4 Hz), 131.04, 130.19, 130.09, 129.28 (d, $^3J_{C–F}$ = 7.8 Hz), 128.94 (d, $^2J_{C–F}$ = 16.1 Hz), 128.15, 127.65, 127.40, 127.14, 126.39, 115.08 (d, $^2J_{C–F}$ = 22.4 Hz), 21.53, 20.74.

^{19}F-NMR (376.5 MHz, $CDCl_3$): δ = –120.50.

IR (neat, cm^{-1}): 3056*w*, 3027*w*, 2921*w*, 1503*m*, 1473*m*, 1439*w*, 1246*w*, 1220*m*, 1124*w*, 1038*w*, 885*w*, 813*m*, 791*m*, 753*s*, 723*w*, 704*m*, 623*w*, 535*w*, 444*w*.

MS (EI): *m/z* (%): 276.1 (100), 261.1 (40), 256.1 (45), 246.1 (25), 241.1 (16).

HR-MS (EI): *m/z*: Calculated for $C_{20}H_{17}F$: 276.1314; measured: 276.1311.

Mixture of 2,7-dimethyltriphenylene (39) and 2,5-dimethyltriphenylene (40)

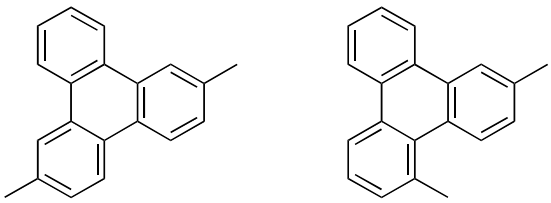

39 and **40** were synthesized according to the general procedure A, using **33** (63 mg, 0.228 mmol), [*i*Pr_3Si][$CHB_{11}H_5Cl_6$] (12 mg, 0.023 mmol) and DMDMS (81 mg, 0.274 mmol). The mixture was stirred at 110 °C for 8 h. Flash column chromatography (SiO_2, hex/DCM 95:5) afforded the product as colorless oily solid (57 mg, 98 %). The two conformers could not be separated.

^{1}H-NMR (500 MHz, $CDCl_3$): δ = 2,7-dimethyltriphenylene: 8.65–8.61 (m, 2H), 8.49 (d, J = 8.0 Hz, 2H), 8.42 (s, 2H), 7.65–7.57 (m, 2H), 7.50–7.43 (m, 2H), 2.59 (s, 3H). 2,5-dimethyltriphenylene: 8.60–8.55 (m, 2H), 8.52–8.49 (m, 2H), 8.42 (s, 1H), 7.65–7.57 (m, 2H), 7.50–7.43 (m, 2H), 7.39 (d, J = 9.0 Hz, 1H), 3.03 (s, 3H), 2.59 (s, 3H).

^{13}C-NMR (125.8 MHz, $CDCl_3$): δ = 2,7-dimethyltriphenylene: 136.53, 129.95, 129.52, 128.77, 127.72, 127.09, 123.41, 123.39, 123.17, 22.05; 2,5-dimethyltriphenylene: 136.35, 135.24, 131.73, 131.16, 131.08, 130.64, 130.56, 129.99, 128.58, 128.53, 127.28, 127.16, 126.03, 123.80, 123.49, 123.14, 121.19, 26.86, 21.84 (one signal missing).

2-Fluoro-3'-(2-fluorophenyl)-1,1':2',1''-terphenyl (41)

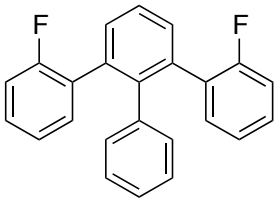

41 was synthesized according to the general procedure C, using 2,6-dichlorodiphenyl (150 mg, 0.67 mmol), 2-fluorophenylboronic acid (209 mg, 1.49 mmol), K_2CO_3 (474 mg, 3.43 mmol), and Pd-PEPPSI-iPr (9 mg, 0.01 mmol). The reaction mixture was stirred at 70 °C for 16 h. FC (hex/DCM 98:2 to 95:5) gave the desired product as colorless crystals (108 mg, 47 %).

M.p.: 95 °C.

^{1}H NMR (400 MHz, $CDCl_3$): δ = 7.52–7.41 (m, 4H), 7.18–7.10 (m, 2H), 7.06 (dd, J = 7.5, 7.5, 1.9 Hz, 2H), 6.98–6.85 (m, 9H).

^{13}C-NMR (101 MHz, $CDCl_3$): δ = 159.66 (d, $^1J_{C–F}$ = 245.8 Hz), 141.52, 139.21, 135.95, 132.27 (d, $^3J_{C–F}$ = 3.5 Hz), 130.59, 130.52, 129.45 (d, $^2J_{C–F}$ = 16.2 Hz), 128.82 (d, $^3J_{C–F}$ = 8.0 Hz), 126.98, 126.26, 123.44 (d, $^4J_{C–F}$ = 3.6 Hz), 115.27 (d, $^2J_{C–F}$ = 22.4 Hz).

^{19}F-NMR (376.5 MHz, $CDCl_3$): δ = –114.64.

IR (neat, cm^{-1}): 3058*w*, 3035*w*, 1579*w*, 1496*m*, 1458*m*, 1446*m*, 1428*m*, 1258*w*, 1242*w*, 1221*m*, 808*w*, 754*s*, 700*s*, 547*w*.

MS (EI): *m/z* (%): 342.1 (100), 322.1 (11), 321.1 (22), 320.1 (18).

HR-MS (EI): *m/z*: Calculated for $C_{24}H_{16}F_2$: 342.12177; measured: 342.12173.

Dibenzo[*f,g*:*o,p*]naphthacene (44)

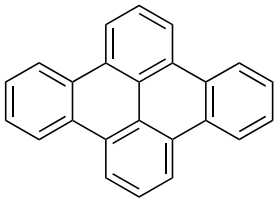

44 was synthesized according to the general procedure A, using 2,6-bis(2-fluorophenyl)biphenyl (19 mg, 0.055 mmol), [$^{i}Pr_3Si$][$CHB_{11}H_5Cl_6$] (6 mg, 0.011 mmol), and DMDMS (39 mg, 0.133 mmol). The reaction mixture was stirred at 110 °C for 8 h. Precipitation and washing with MeOH resulted in the desired product as slightly yellow powder (14 mg, 83 %).

^{1}H-NMR (500 MHz, $CDCl_3$): δ = 8.95 (d, J = 8.0 Hz, 4H), 8.8–8.83 (m, 4H), 8.08 (t, J = 7.9 Hz, 2H), 7.78–7.73 (dd, J = 6.3, 3.3 Hz, 4H).

^{13}C-NMR (125.8 MHz, $CDCl_3$): δ = 130.20, 129.79, 127.73, 126.61, 124.13, 123.89, 121.56.

HR-MS (EI): *m/z*: Calculated for $C_{24}H_{14}$: 302.10900; measured: 302.10914.

2,2''''-Difluoro-1,1':2',1'':4'',1''':2''',1''''-quinquephenyl (42)

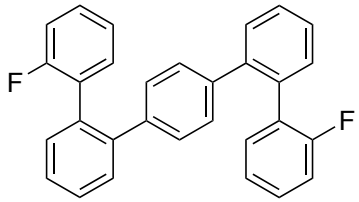

42 was synthesized according to the general procedure E, using 2-fluoro-2'-bromobiphenyl (599 mg, 2.39 mmol), *n*-BuLi (1.1 mL, 2.5 M in hexane, 2.75 mmol), $ZnCl_2$ (386 mg, 2.83 mmol), 1,4-diiodobenzene (360 mg, 1.09 mmol), and Pd-PEPPSI-*i*Pr (21 mg, 0.03 mmol). The reaction mixture was heated at 70 °C for 13 h. Flash column chromatography (Hex/DCM 98:2 to 90:10) afforded the desired product as a white solid (276 mg, 61 %).

R_f (silica, Hex/DCM 9:1) = 0.17.

M.p.: 175–178 °C.

^{1}H-NMR (500 MHz, $CDCl_3$): δ = 7.46–7.37 (m, 8H), 7.22–7.16 (m, 2H), 7.07 (ddd, *J* = 7.5, 7.5, 2.0 Hz, 2H), 7.01 (ddd, *J* = 7.5, 7.5, 1.5 Hz, 2H), 6.97 (s, 4H), 6.91 (ddd, *J* = 10.0, 8.0, 1.0 Hz, 2H).

^{13}C-NMR (125.8 MHz, $CDCl_3$): δ = 159.55 (d, $^{1}J_{C–F}$ = 246.6 Hz), 141.43, 139.61, 134.51, 132.24 (d, $^{3}J_{C–F}$ = 3.5 Hz), 131.09, 130.16, 129.18 (d, $^{2}J_{C–F}$ = 15.6 Hz), 128.83 (d, $^{3}J_{C–F}$ = 7.8 Hz), 128.83 (2 C), 128.26, 127.24, 123.79 (d, $^{4}J_{C–F}$ = 3.6 Hz), 115.58 (d, $^{2}J_{C–F}$ = 22.5 Hz).

^{19}F-NMR (376.5 MHz, $CDCl_3$): δ = –115.44.

IR (neat, cm^{-1}): 3057*w*, 3027*w*, 1580*w*, 1497*w*, 1471*m*, 1439*m*, 1236*w*, 1208*m*, 1107*w*, 1099*w*, 1008*w*, 841*w*, 824*m*, 751*s*, 588*w*, 514*w*.

MS (EI): *m/z* (%): 418.2 (100), 398.2 (19), 246.1 (20), 207.1 (21), 188.1 (30).

Dibenzo[*f*:*l*]pentahelicene (45)

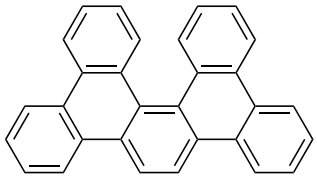

45 was synthesized according to the general procedure A, using **42** (23 mg, 0.055 mmol), [*i*Pr$_3$Si][$CHB_{11}H_5Cl_6$] (6 mg, 0.011 mmol) and DMDMS (44 mg, 0.148 mmol). The mixture was heated at 110 °C for 8 h. Flash column chromatography (SiO_2, hex/DCM 9:1 to 1:1) afforded the product as a white solid (14 mg, 67 %). Crystals could be obtained upon cooling of the reaction mixture.

R_f (silica, Hex/DCM 4:1) = 0.12.

^{1}H-NMR (500 MHz, $CDCl_3$): δ = 8.68 (m, 6H), 8.58 (d, *J* = 8.0 Hz, 2H), 8.27 (d, *J* = 8.0 Hz, 2H), 7.74 (m, 4H), 7.53 (ddd, *J* = 8.0, 7.0, 1.5 Hz, 2H), 7.53 (ddd, *J* = 8.0, 6.5, 1.0 Hz, 2H).

^{13}C-NMR (125.8 MHz, $CDCl_3$): δ = 131.13, 131.04, 130.53, 130.44, 130.05, 129.71, 127.84, 127.64, 127.44, 127.06, 125.37, 123.85, 123.66, 123.37, 121.96.

HR-MS (ESI): *m/z*: Calculated for $C_{30}H_{19}$ $[M+H]^+$: 379.14813, found: 379.14830.

2,2''''-Difluoro-5''-(2'-fluoro[1,1'-biphenyl]-2-yl)-1,1':2',1'':3'',1''':2''',1''''-quinquephenyl (**43**)

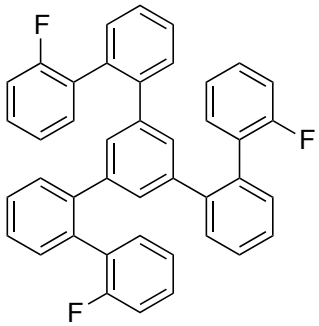

43 was synthesized according to the general procedure E, using 2-fluoro-2'-bromobiphenyl (91 %, 320 mg, 1.17 mmol), *n*-BuLi (0.8 mL, 1.48 M in hexane, 1.20 mmol), $ZnCl_2$ (195 mg, 1.43 mmol), 1,3,5-tribromobenzene (105 mg, 0.33 mmol), and Pd-PEPPSI-*i*Pr (19 mg, 0.03 mmol). The reaction mixture was stirred at 75 °C for 2 h. Flash column chromatography (Hex/DCM 95:5 to 80:20) afforded the desired product as white solid (181 mg, 93 %).

R_f (silica, Hex/DCM 9:1) = 0.14.

M.p.: 156–158 °C.

^{1}H-NMR (500 MHz, $CDCl_3$): δ = 7.35–7.33 (m, 6H), 7.32–7.22 (m, 6H), 7.04–6.98 (m, 6H), 6.86–6.79 (m, 6H), 6.75 (s, 3H).

^{13}C-NMR (125.8 MHz, $CDCl_3$): δ = 159.79 (d, $^1J_{C–F}$ = 247.0 Hz), 141.36 , 140.37 , 134.26 , 132.66 (d, $^3J_{C–F}$ = 3.3 Hz), 130.91 , 130.28 , 129.29 (d, $^2J_{C–F}$ = 15.5 Hz), 128.94 , 128.71 (d, $^3J_{C–F}$ = 7.9 Hz), 127.99 , 127.05 , 123.72 (d, $^4J_{C–F}$ = 3.6 Hz), 115.66 (d, $^2J_{C–F}$ = 22.4 Hz).

^{19}F-NMR (376.5 MHz, $CDCl_3$): δ = –115.48.

IR (neat, cm^{-1}): 3057*w*, 3031*w*, 1591*w*, 1500*w*, 1476*m*, 1444*w*, 1414*w*, 1251*w*, 1207*w*, 1106*w*, 817*w*, 752*s*, 716*w*.

MS (EI): *m/z* (%): 588.2 (100).

HR-MS (EI): *m/z*: Calculated for $C_{42}H_{27}F_3$: 588.20594; measured: 588.20620.

Hexabenzo[*a*,*c*,*g*,*i*,*m*,*o*]triphenylene (46)

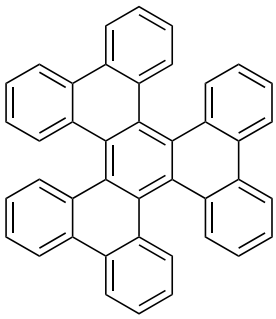

46 was synthesized according to the general procedure A, using **43** (40 mg, 0.068 mmol), [*i*Pr_3Si][$CHB_{11}H_5Cl_6$] (9.5 mg, 0.019 mmol) and DMDMS (73 mg, 0.245 mmol). The mixture was stirred at 110 °C for 8 h. A small amount of hexane was added to the suspension, which was filtered and washed with cool hexane. The yellow residue was found to be the desired product (23 mg, 64 %). ^{1}H NMR spectrum matches the reported one.[102]

^{1}H-NMR (500 MHz, $CDCl_3$): δ = 8.54 (d, *J* = 8.0 Hz, 1H), 8.16 (d, *J* = 8.2 Hz, 1H), 7.55 (ddd, *J* = 8.2, 7.0, 1.2 Hz, 1H), 7.22 (ddd, *J* = 8.3, 7.0, 1.3 Hz, 1H).

^{13}C-NMR (125.8 MHz, $CDCl_3$): δ = 131.78, 130.81, 130.16, 128.41, 126.96, 125.82, 123.48.

MS (EI): *m/z* (%): 528.1 (100), 510.1 (16), 509.1 (19), 261.0 (23), 255.0 (23), 254.0 (17), 249.0 (15).

9-(2-Fluorophenyl)anthracene (47)

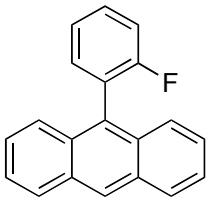

47 was synthesized according to the general procedure A to result in a slightly green solid with a yield of 71 %.

R_f (hexane) = 0.13.

M.p.: 145–147 °C.

^{1}H-NMR (500 MHz, $CDCl_3$): δ = 8.52 (s, 1H), 8.04 (dt, J = 10.5, 1.5 Hz, 2H), 7.60 (dt, J = 11.0, 1.5 Hz, 2H), 7.57–7.50 (m, 1H), 7.45 (ddd, J = 10.5, 8.0, 1.5 Hz, 8H), 7.41–7.27 (m, 5H).

^{13}C-NMR (125.8 MHz, $CDCl_3$): δ = 160.88 (d, $^1J_{C–F}$ = 246.3 Hz), 133.57 (d, $^3J_{C–F}$ = 3.5 Hz), 131.47, 130.53, 130.33, 130.02 (d, $^2J_{C–F}$ = 7.8 Hz), 128.66, 127.58, 126.32, 126.04 (d, $^2J_{C–F}$ = 17.5 Hz), 125.94, 125.32, 124.33 (d, $^4J_{C–F}$ = 3.6 Hz), 116.05 (d, $^2J_{C–F}$ = 22.1 Hz).

^{19}F-NMR (376.5 MHz, $CDCl_3$): δ = –113.47.

MS (EI): *m/z* (%): 272.1 (100), 270 (33), 250.1 (21).

Benzo[*a*,*b*]fluoranthene (49)

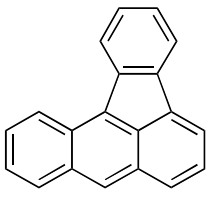

49 was synthesized according to the general procedure A to result in yellow solid with a yield of 45 %.

^{1}H-NMR (500 MHz, $CDCl_3$): δ = 8.76 (d, J = 9.0 Hz, 1H), 8.48 (s, 1H), 8.38 (d, J = 8.0 Hz, 1H), 8.14 (d, J = 7.5, 1H), 8.03–8.00 (m, 3H), 7.68–7.64 (m, 2H), 7.53–7.50 (ddd, J = 8.5, 6.5, 1.0 Hz, 1H), 7.49–7.46 (td, J = 7.5, 7.5, 1.5 Hz, 1H), 7.41–7.38 (td, J = 7.5, 7.5, 1.0 Hz, 1H).

^{13}C-NMR (125.8 MHz, $CDCl_3$): δ = 140.59, 139.15, 137.06, 134.68, 131.53, 130.81, 130.79, 129.20, 128.06, 128.02, 127.66, 127.59, 127.50, 127.36, 126.64, 125.05, 124.44, 123.90, 121.84, 120.43.

syn- and anti-9,10-Bis(2-fluorophenyl)anthracene (48)

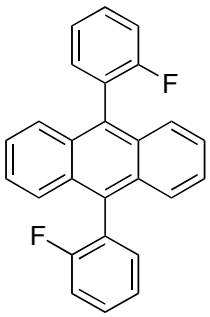

48 was synthesized according to the general procedure A to result in a mixture of slightly yellow solid with a yield of 90 %.

R_f (hexane) = 0.10.

M.p.: 245–255 °C.

^{1}H-NMR (500 MHz, $CDCl_3$): δ = 7.68–7.63 (m, 4H), 7.58–7.51 (m, 2H), 7.47–7.28 (m, 10H).

^{13}C-NMR (125.8 MHz, $CDCl_3$): δ = 160.85 (d, $^{1}J_{C–F}$ = 247 Hz), 160.55 (d, $^{1}J_{C–F}$ = 246 Hz), 133.63 (d, $^{3}J_{C–F}$ = 3.5 Hz), 133.54 (d, $^{3}J_{C–F}$ = 3.5 Hz), 131.31, 131.22, 130.15, 130.11 (2 C), (2 d, $^{3}J_{C–F}$ = 7.9 Hz), 126.61, 126.60, 126.08 (d, $^{2}J_{C–F}$ = 17.4 Hz), 126.07 (d, $^{2}J_{C–F}$ = 17.4 Hz), 125.70, 125.69, 124.44 (d, $^{4}J_{C–F}$ = 3.6 Hz), 124.36 (d, $^{4}J_{C–F}$ = 3.6 Hz), 116.12 (d, $^{2}J_{C–F}$ = 22.0 Hz), 116.03 (d, $^{2}J_{C–F}$ = 22.0 Hz).

IR (neat, cm^{-1}): 3072*w*, 1493*m*, 1456*m*, 1220*m*, 911*m*, 819*w*, 757*s*, 731*m*, 660*w*, 639*w*, 539*m*.

Rubicene (50)

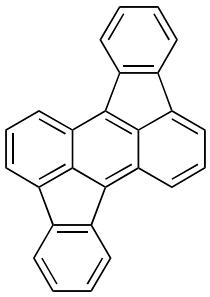

50 was synthesized according to the general procedure A to result in a red powder with a yield of 49 %.

R_f (hex:EtOAc 9:1) = 0.25.

M.p.: 290–300 °C.

^{1}H-NMR (500 MHz, $CDCl_3$): δ = 8.60 (d, J = 8.5 Hz, 2H), 8.33 (d, J = 7.5 Hz, 2H), 8.02 (d, J = 6.5 Hz, 2H), 7.96 (d, J = 7.5 Hz, 2H), 7.78 (dd, J = 8.5, 6.5 Hz, 2H), 7.45 (td, J = 7.5, 7.5, 1.0 Hz, 2H), 7.38 (td, J = 7.5, 7.5, 1.0 Hz, 2H).

^{13}C-NMR (125.8 MHz, $CDCl_3$): δ = 140.04, 139.56, 138.36, 133.67, 133.22, 129.16, 128.27, 127.12, 125.66, 124.71, 123.87, 121.79, 120.47.

1-(2-Fluorophenyl)corannulene (51)

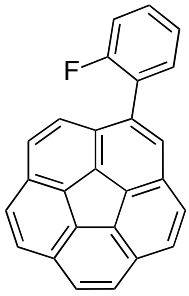

51 was synthesized according to the general A to result in a slightly yellow foam with a yield of 63 %.

R_f (hexane) = 0.10.

M.p.: 65–70 °C.

^{1}H-NMR (400 MHz, $CDCl_3$): δ = 7.86 (d, J = 1.2 Hz, 1H), 7.82 (d, J = 9.2 Hz, 4H), 7.80 (d, J = 3.2 Hz, 2H), 7.75 (d, J = 8.8 Hz, 1H), 7.62 (dd, J = 8.8, 2.0 Hz, 1H), 7.55 (td, J = 7.6, 7.6, 1.6 Hz, 1H), 7.48–7.41 (m, 1H), 7.31–7.25 (m, 2H).

^{13}C-NMR (125.8 MHz, $CDCl_3$): δ = 160.29 (d, $^{1}J_{C-F}$ = 248 Hz), 136.33, 135.92, 135.90, 135.73, 135.70, 135.02, 132.71 (d, $^{3}J_{C-F}$ = 3.1 Hz), 131.10 (2 C), 130.95, 130.63, 130.24, 129.86 (d, $^{3}J_{C-F}$ = 8.1 Hz), 127.78, 127.50, 127.49, 127.36, 127.32, 127.25, 127.19, 127.13, 126.70, 124.52 (d, $^{4}J_{C-F}$ = 3.6 Hz), 116.22 (d, $^{2}J_{C-F}$ = 22.4 Hz). (one signal missing)

^{19}F-NMR (376.5 MHz, $CDCl_3$): δ = –114.53.

MS (EI): *m/z* (%): 344.1 (100), 342.0 (25).

HR-MS (EI): *m/z*: Calculated for $C_{26}H_{13}F$: 344.1001; found: 344.0996.

Indenocorannulene (52)

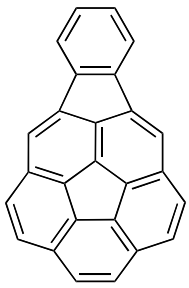

52 was synthesized according to the general procedure A to result in colorless crystals with a yield of 40 %. NMR spectra match the reported ones.[103]

R_f (hexane) = 0.08.

M.p.: 230–238 °C.

^{1}H-NMR (400 MHz, $CDCl_3$): δ = 7.64–7.58 (m, 6H), 7.54 (d, J = 8.8 Hz, 2H), 7.50 (s, 2H), 7.18 (dd, J = 5.6, 3.2 Hz, 2H).

^{13}C-NMR (125.8 MHz, $CDCl_3$): δ = 144.76, 141.42, 139.90, 139.78, 138.63, 137.92, 137.74, 130.19, 128.57, 128.44, 127.27, 127.04, 122.15, 121.90.

4''-Bromo-2-fluoro-1,1':2':1'''-terphenyl (34)

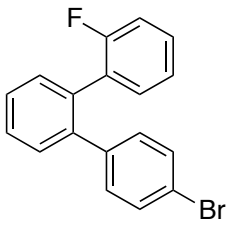

34 was synthesized according to the general procedure E, using 2'-bromo-2-fluorobiphenyl (**75**) (204 mg, 0.81 mmol) in THF (5 mL), *n*-BuLi (2.5 M in hexanes, 0.33 mL, 0.83 mmol), $ZnCl_2$ (118 mg, 0.87 mmol) in THF (4 mL), and $Pd(PPh_3)_4$ (13 mg, 0.01 mmol) and 1-bromo-4-iodobenzene (203 mg, 0.72 mmol) in THF (5 mL). The reaction mixture was stirred at room temperature for 1 h, the product was purified by FC chromatography (Hex/DCM 99:1) to afford product as colorless oil (149 mg, 57 %).

Rf (hexane) = 0.14

^{1}H-NMR (500 MHz, $CDCl_3$): δ = 7.48–7.39 (m, 4H), 7.35–7.31 (m, 2 H), 7.26–7.21 (m, 1H), 7.14 (ddd, *J* = 7.5, 7.5, 1.9 Hz, 1H), 7.06 (ddd, *J* = 7.5, 7.5, 1.2 Hz, 1H), 7.03–6.99 (m, 2H), 6.94 (ddd, *J* = 9.6, 8.2, 1.2 Hz, 1H).

^{13}C NMR (126 MHz, $CDCl_3$): δ = 159.51 (d, $^{1}J_{C-F}$ = 246.6 Hz), 140.56, 140.40, 134.46, 132.11 (d, $^{3}J_{C-F}$ = 3.4 Hz), 131.22, 131.10, 130.96, 130.04, 129.22 (d, $^{3}J_{C-F}$ = 8.0 Hz), 128.92 (d, $^{2}J_{C-F}$ = 15.8 Hz), 128.43, 127.69, 124.03 (d, $^{4}J_{C-F}$ = 3.6 Hz), 121.07, 115.71 (d, $^{2}J_{C-F}$ = 22.3 Hz).

^{19}F-NMR (376.5 MHz, $CDCl_3$): δ = –115.28.

2-Bromotriphenylene (53)

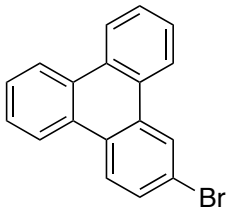

53 was synthesized according to the general procedure A, using **34** (97 mg, 0.296 mmol), [^{i}Pr$_3$Si][CHB$_{11}$H$_5$Cl$_6$] (15 mg, 0.030 mmol), and DMDMS (105 mg, 0.356 mmol). The reaction mixture was heated at 110 °C for 16 h. FC (hex/DCM 99:1) gave the desired product as white solid (86 mg, 94 %).

M.p.: 128–131 °C (lit.: 132.5–133.5 °C)[104]

^{1}H-NMR (500 MHz, $CDCl_3$): δ = 8.77 (d, J = 2.1 Hz, 1H), 8.69–8.62 (m, 2H), 8.62–8.54 (m, 2H), 8.51 (d, J = 8.8 Hz, 1H), 7.75 (dd, J = 8.8, 2.0 Hz, 1H), 7.72–7.64 (m, 4H).

^{13}C-NMR (126 MHz, $CDCl_3$) δ = 131.70, 130.33, 130.25, 129.85, 129.27, 128.71, 128.03, 127.75, 127.60, 127.59, 126.34, 125.24, 123.54, 123.51, 123.32, 121.81 (2 signals missing due to overlaps).

IR (neat, cm^{-1}): 3075*w*, 3058*w*, 3025*w*, 1596*w*, 1578*w*, 1491*w*, 1452*w*, 1432*m*, 1396*w*, 1237*w*, 1015*w*, 1000*w*, 816*w*, 805*m*, 749*s*, 717*m*, 581*w*, 420*w*.

MS (EI): *m/z* (%): 308.0 (76), 306.0 (77), 226.1 (100), 113.1 (75), 100.1 (27).

HR-MS (EI): *m/z*: Calculated for C$_{18}$H$_{11}$^{79}Br: 306.00386; measured: 306.00391.

2'',5''-Difluoro-1,1':2',1'':4'',1''':2''',1''''-quinquephenyl (59)

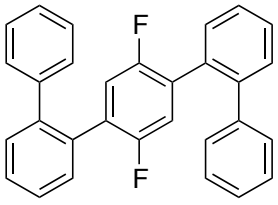

59 was synthesized according to the general procedure E, using 2-bromobiphenyl (265 mg, 1.14 mmol), *n*-BuLi (0.74 mL, 1.6 M in hexanes, 1.19 mmol), $ZnCl_2$ (192 mg, 1.41 mmol), 2,5-dibromo-1,4-difluorobenzene (144 mg, 0.53 mmol), and Pd-PEPPSI-*i*Pr (18 mg, 0.03 mmol). The reaction mixture was stirred at 70 °C for 14 h. Flash column chromatography (Hex/DCM 95:5 to 80:20) afforded the desired product as white solid (178 mg, 83 %). ^{1}H-NMR matches reported compound.[41b]

Rf (hex/DCM 9:1) = 0.21.

^{1}H NMR (400 MHz, $CDCl_3$): δ = 7.49–7.34 (m, 8H), 7.27–7.22 (m, 6H), 7.17–7.11 (m, 4H), 6.72 (dd, *J* = 7.8, 7.8 Hz, 2H).

^{19}F-NMR (376.5 MHz, $CDCl_3$): δ = –121.58

MS (EI): *m/z* (%): 418.1 (100), 398.1 (24), 378.1 (33), 207.0 (16), 165.1 (16), 152 (15), 77.1 (20).

Phenanthreno[9,10-*b*]triphenylene (60)

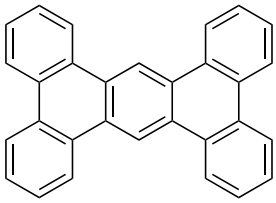

60 was synthesized accroding to the general procedure B, using **59** (41 mg, 0.097 mmol), $[^iPr_3Si][CHB_{11}H_5Cl_6]$ (30 mg, 0.059 mmol), and DMDMS (16 mg, 0.054 mmol). The reaction mixture was subjected to microwave irradiation (250 W) for 2 h. A temperature of 95 °C was reached. After cooling to room temperature, the reaction mixture was filtered and washed with CH_2Cl_2 to give the desired product as colorless crystals (22 mg, 60 %). ^{1}H-NMR matches reported compound.[41b]

^{1}H NMR (400 MHz, CD_2Cl_2): δ = 9.97 (s, 1H), 9.02 (dd, *J* = 8.0, 1.5 Hz, 2H), 8.74 (dd, *J* = 7.9, 1.6 Hz, 1H), 7.84–7.73 (m, 2H).

2-Fluoro-3-(naphthalen-1-yl)pyridine (61)

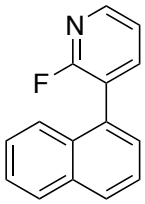

61 was synthesized according to the general procedure D, using 1-bromonaphthalene (0.3 mL, 2.09 mmol), 3-(2-fluoropyridylboronic acid (309 mg, 2.19 mmol), Pd-PEPPSI-iPr (15 mg, 0.02 mmol), and K_2CO_3 (577 mg, 4.18 mmol) in tol/EtOH/H_2O (degassed, 5/2/1, 12 mL). The reaction mixture was stirred at 70 °C for 36 h to afford the desired product as yellow oil (439 mg, 94 %).

^{1}H NMR (400 MHz, $CDCl_3$): δ = 8.34 (ddd, J = 5.1, 2.0, 1.1 Hz, 1H), 7.97–7.91 (m, 2H), 7.86 (ddd, J = 9.3, 7.3, 2.0 Hz, 1H), 7.63–7.42 (m, 5H), 7.35 (ddd, J = 7.0, 4.9, 1.8 Hz, 1H).

^{13}C NMR (101 MHz, $CDCl_3$) δ = 161.11 (d, $^1J_{C–F}$ = 240.0 Hz), 147.21 (d, $^3J_{C–F}$ = 14.3 Hz), 142.84 (d, $^3J_{C–F}$ = 4.6 Hz), 133.73, 131.91 (d, = 3.6 Hz), 131.54, 129.26, 128.62, 127.99, 126.77, 126.29, 125.38, 125.25, 122.98 (d, $^2J_{C–F}$ = 31.6 Hz), 121.56 (d, $^4J_{C–F}$ = 4.4 Hz).

^{19}F-NMR (376.5 MHz, $CDCl_3$): δ = –68.36.

IR (neat, cm^{-1}): 3055*w*, 1605*m*, 1570*m*, 1508*w*, 1468*w*, 1422*s*, 1394*m*, 1244*m*, 1220*w*, 1180*w*, 1098*m*, 962*w*, 857*m*, 798*s*, 776*s*, 766*s*, 689*w*, 621*w*, 565*w*, 481*w*.

HR-MS (APCI): *m/z*: Calculated for $C_{15}H_{11}FN^+$: 224.08700; measured: 224.08663.

Acenaphthyleno[1,2-*b*]pyridine (62)

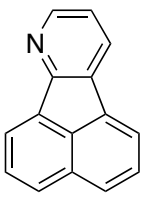

62 was synthesized accroding to the general procedure B, using **61** (11 mg, 0.049 mmol), [^{i}Pr$_3$Si][CHB$_{11}$H$_5$Cl$_6$] (30 mg, 0.059 mmol), and DMDMS (16 mg, 0.054 mmol). The reaction mixture was subjected to microwave irradiation (200 W) for 2 h. A temperature of 95 °C was reached. FC (hex/EtOAc 99:1 to 8:2) gave the desired product as yellow solid (7 mg, 75 %).

^{1}H-NMR (500 MHz, $CDCl_3$): δ = 8.59 (dd, *J* = 5.1, 1.5 Hz, 1H), 8.32 (d, *J* = 6.9 Hz, 1H), 8.17 (dd, *J* = 7.7, 1.5 Hz, 1H), 8.00 (d, *J* = 7.4 Hz, 2H), 7.96 (d, *J* = 8.2 Hz, 1H), 7.76 (dd, *J* = 8.2, 6.9 Hz, 1H), 7.70 (dd, *J* = 8.3, 6.9 Hz, 1H), 7.29 (dd, *J* = 7.7, 4.9 Hz, 1H).

^{13}C-NMR (126 MHz, $CDCl_3$): δ = 159.25, 147.91, 135.47, 133.89, 133.58, 132.20, 129.94, 128.85, 128.72, 128.61, 128.15, 127.92, 122.01, 121.72, 121.36.

IR (neat, cm^{-1}): 3061*w*, 2602*m*, 1637*w*, 1613*w*, 1445*w*, 1425*m*, 1387*w*, 1326*w*, 1282*w*, 1265*w*, 1132*w*, 1033*m*, 1018*s*, 990*s*, 943*m*, 866*s*, 829*w*, 804*m*, 778*s*, 737*m*, 652*w*, 419*w*. (The signal at 2600 cm–1 indicates an impurity containing boron, which might be the carborane anion, or a byproduct similar to the one reported in chapter 2.3)

HR-MS (APCI): *m/z*: Calculated for $C_{15}H_{10}N^{+}$: 204.08078; measured: 204.08043.

((2''-Fluoro[1,1':2',1''-terphenyl]-4-yl)oxy)triisopropylsilane (64)

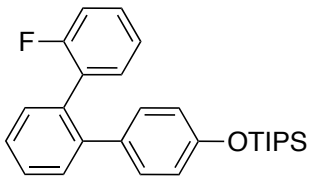

64 was synthesized according to the general procedure E, using **75** (249 mg, 0.99 mmol), *n*-BuLi (1.6 M in hexanes, 0.65 mL, 1.05 mL), $ZnCl_2$ (147 mg, 1.08 mmol), Pd(PPh$_3$)$_4$ (50 mg, 0.05 mmol), and 4-bromophenoxytriisopropylsilane (300 mg, 0.9 mmol). The reaction mixture as stirred at 70 °C for 17 h. And despite the presence of residual starting material, the reaction was quenched. FC (hex/DCM 99:1 to 90:10) gave the desired product as colorless oil (150 mg, 40 %).

R_f (hex/DCM 9:1) = 0.22.

^{1}H-NMR (500 MHz, $CDCl_3$): δ = 7.50–7.37 (m, 4H), 7.21 (dddd, J = 8.3, 7.2, 5.1, 1.9 Hz, 1H), 7.13 (ddd, J = 7.5, 7.5, 1.9 Hz, 1H), 7.06–6.97 (m, 3H), 6.92 (ddd, J = 9.6, 8.2, 1.2 Hz, 1H), 6.78–6.70 (m, 2H), 1.31–1.18 (m, 3H), 1.09 (d, J = 7.3 Hz, 18H).

^{13}C NMR (101 MHz, $CDCl_3$): δ = 159.72 (d, $^{1}J_{C–F}$ = 246.6 Hz), 155.55, 142.91, 141.79, 134.46, 132.25 (d, $^{3}J_{C–F}$ = 3.5 Hz), 131.16, 130.35, 129.32 (d, $^{2}J_{C–F}$ = 15.8 Hz), 128.91, 128.81 (d, $^{3}J_{C–F}$ = 8.1 Hz), 128.18, 127.22, 123.78 (d, $^{4}J_{C–F}$ = 3.6 Hz), 122.38, 121.14, 118.62, 115.57 (d, $^{2}J_{C–F}$ = 22.4 Hz), 18.03, 12.61.

^{19}F-NMR (376.5 MHz, $CDCl_3$): δ = –115.34.

IR (neat, cm^{-1}): 3062*w*, 3031*w*, 2944*w*, 2891*w*, 2866*m*, 1602*w*, 1582*m*, 1487*w*, 1470*m*, 1417*w*, 1307*m*, 1272*w*, 1248*m*, 1208*m*, 1001*w*, 936*m*, 882*m*, 825*w*, 792*m*, 753*s*, 723*w*, 699*m*, 682*m*.

MS (EI): *m/z* (%): 420.2 (44), 377.2 (58), 349.2 (35), 321.1 (26), 285.1 (26), 227.1 (92), 226.1 (100), 160.6 (85), 77.1 (40).

HR-MS (EI): *m/z*: Calculated for $C_{27}H_{33}FOSi$: 420.22792; measured: 420.22843.

Triphenylen-2-ol (65)

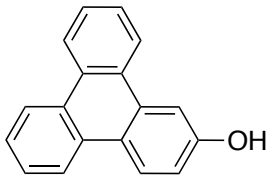

65 was synthesized according to the general procedure B, using **64** (38 mg, 0.090 mmmol), [$^{i}Pr_3Si$][$CHB_{11}H_5Cl_6$] (2.5 mg, 0.005 mmol), and DMDMS (31 mg, 0.104 mmol). The reaction mixture was subjected to microwave irradiation (200 W) for 70 min, in which a temperature of around 95 °C was reached. FC (hex/EtOAc 99:1 to 9:1) gave the product as white solid (15 mg, 68 %).

Rf (hex/EtOAc 4:1) = 0.18

M.p.: 220–222 °C (lit.: 224–225 °C)[105]

^{1}H-NMR (500 MHz, $CDCl_3$): δ = 8.67–8.61 (m, 2H), 8.57–8.51 (m, 3H), 8.03 (dd, *J* = 2.6, 0.6 Hz, 1H), 7.69–7.57 (m, 4H), 7.20 (dd, *J* = 8.9, 2.5 Hz, 1H), 5.09 (s, 1H).

MS (EI): *m/z* (%): 244.0 (100), 215.0 (23), 213.0 (11), 122.0 (10).

HR-MS (EI): *m/z*: Calculated for $C_{18}H_{12}O$: 244.08827; measured: 244.08841.

((2'''-Fluoro[1,1':2',1'':2'',1'''-quaterphenyl]-4-yl)oxy)triisopropylsilane

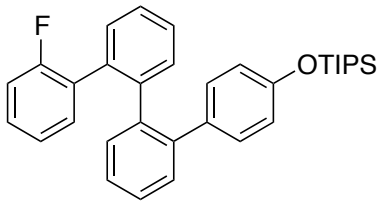

66 was synthesized according to the general procedure C, using 2''-bromo-4'-(triisopropylsiloxy)*o*-terphenyl (60 mg, 0.13 mmol), 2-fluorophenylboronic acid (35 mg, 0.25 mmol), $Pd(PPh_3)_4$ (7 mg, 0.006 mmol), and K_2CO_3 (51 mg, 0.37 mmol) in THF/H_2O (10:1, 5.5 mL, degassed). The reaction mixture was stirred at 70 °C for 15 h. FC chromatography (hex/DCM 95:5 to 80:20) afforded product as colorless oil (27 mg, 44 %).

Rf (hex/DCM 9:1) = 0.21.

^{1}H NMR (500 MHz, $CDCl_3$): δ = 7.36–7.22 (m, 4H), 7.22– 7.18 (m, 1H), 7.16 (dd, *J* = 7.4, 1.6 Hz, 1H), 7.13– 7.06 (m, 1H), 6.82 (ddd, *J* = 7.5, 7.5, 1.2 Hz, 1H), 6.76 (ddd, *J* = 9.7, 8.2, 1.2 Hz, 1H), 6.66–6.58 (m, 4H), 1.28–1.19 (m, 3H), 1.10 (d, *J* = 7.4 Hz, 18H).

MS (EI): *m/z* (%): 496.2 (24), 453.1 (18), 303.1 (29), 281.0 (22), 207.0 (100), 191.0 (28), 77.0 (54).

4-(Triphenylen-1-yl)phenol (67)

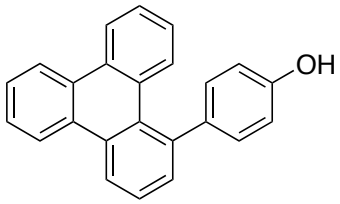

67 was synthesized according to the general procedure B, using **66** (26 mg, 0.052 mmmol), [^{i}Pr$_3$Si][CHB$_{11}$H$_5$Cl$_6$] (1.3 mg, 0.003 mmol), and DMDMS (19 mg, 0.063 mmol). The reaction mixture was subjected to microwave irradiation (200 W) for 50 min, in which a temperature of around 95 °C was reached. FC (hex/DCM 99:1 to pure DCM) afforded **67** as white solid (12 mg, 72 %). NMR spectroscopy showed the presence of an impurity (25 % of deprotected starting material), which implies that a reaction time of 50 min was not enough.

^{1}H NMR (500 MHz, CDCl$_3$): δ = 8.65–8.57 (m, 3H), 8.54 (d, J = 8.3 Hz, 1H), 7.80 (dd, J = 8.5, 1.0 Hz, 1H), 7.66–7.59 (m, 3H), 7.50 (dd, J = 7.2, 1.3 Hz, 1H), 7.46 (ddd, J = 8.2, 6.9, 1.3 Hz, 1H), 7.31–7.27 (m, 2H), 7.09 (ddd, J = 8.4, 6.9, 1.4 Hz, 1H), 6.93–6.87 (m, 2H), 4.74 (s, 1H).

^{13}C NMR (126 MHz, CDCl$_3$): δ = 154.80, 140.39, 138.20, 131.77, 131.51, 131.15, 130.56, 130.41, 130.18, 130.02, 130.01, 129.98, 127.46, 126.70, 126.49, 125.14, 123.80, 123.28, 122.18, 116.10. Only 20 signals visible due to overlap of two pairs of triphenylene CH signals (127.46 and 123.29).

MS (EI): *m/z* (%): 320.0 (100), 303.0 (19), 302.0 (15), 289 (25), 150.0 (16).

HR-MS (EI): *m/z*: Calculated for C$_{24}$H$_{16}$O: 320.11957; measured: 320.11940.

3-Corannulene-1-yl)-2-fluoropyridine (69)

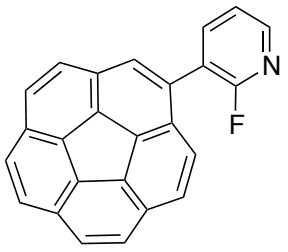

69 was synthesized according to the general procedure C, using 1-Bpin-corannulene (99 mg, 0.26 mmol), 3-bromo-2-fluoropyridine (49 mg, 0.28 mmol), $Pd(PPh_3)_4$ (5 mg, 0.005 mmol), and K_2CO_3 (109 mg, 0.79 mmol) in THF/H_2O (10 mL, 9:1). the reaction mixture was stirred at 70 °C for 15 h. FC chromatography (hex/DCM 7:3 to pure DCM) afforded the product as slightly yellow solid (69 mg, 76 %).

Rf (hex/DCM 1:1) = 0.25

M.p.: 190–193 °C

^{1}H NMR (400 MHz, $CDCl_3$): δ = 8.36 (ddd, J = 4.9, 2.0, 1.2 Hz, 1H), 8.04 (ddd, J = 9.5, 7.4, 2.0 Hz, 1H), 7.90 (d, J = 1.1 Hz, 1H), 7.87–7.78 (m, 7H), 7.60 (dd, J = 8.8, 1.5 Hz, 1H), 7.39 (ddd, J = 7.3, 4.9, 1.8 Hz, 1H).

^{13}C NMR (126 MHz, $CDCl_3$): δ = 161.09 (d, $^1J_{C–F}$ = 240.8 Hz), 147.30 (d, $^3J_{C–F}$ = 14.5 Hz), 142.91 (d, $^3J_{C–F}$ = 4.3 Hz), 136.35, 135.94, 135.91, 135.64, 132.95, 132.92, 131.31, 131.19, 131.04, 130.37, 129.55, 128.25, 128.24, 127.85, 127.72, 127.58, 127.35, 127.18, 127.11, 125.97, 125.96, 122.26 (d, $^2J_{C–F}$ = 29.9 Hz), 121.90 (d, $^4J_{C–F}$ = 4.4 Hz).

^{19}F-NMR (376.5 MHz, $CDCl_3$): δ = –68.73.

IR (neat, cm^{-1}): 3041*w*, 2922*w*, 2854*w*, 1601*m*, 1567*m*, 1429*s*, 1410*m*, 1246*m*, 1203*w*, 887*m*, 831*s*, 809*m*, 765*m*, 737*m*, 693*w*, 663*m*, 547*m*.

MS (EI): *m/z* (%): 345.1 (100), 325.2 (8), 207.1 (18), 172.2 (21), 149.1 (16).

1-Azaindeno[1,2,3-*b*,*c*]corannulene (63)

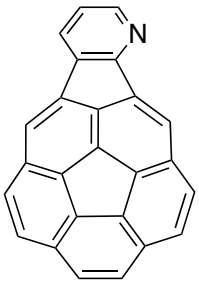

63 was synthesized according to the general procedure B, using **69** (5 mg, 0.014 mmol), [^{i}Pr$_3$Si][$CHB_{11}H_5Cl_6$] (8.5 mg, 0.017 mmol), and DMDMS (4 mg, 0.014 mmol).

The reaction mixture was subjected to microwave irradiation (225 W) for 120 min, in which a temperature of around 110 °C was reached. FC (hex/EtOAc 4:1 to 1:1 and 1 % Et_3N) afforded the product as yellow solid (1.2 mg, 26 %).

Rf (hex/EtOAc 4:1 (1 % Et_3N) = 0.10.

^{1}H NMR (500 MHz, $CDCl_3$): δ = 8.36 (dd, J = 5.1, 1.5 Hz, 1H), 8.03 (s, 1H), 7.89 (dd, J = 7.6, 1.5 Hz, 1H), 7.71 (d, J = 8.8 Hz, 1H), 7.69 (s, 1H), 7.65 (d, J = 8.8 Hz, 1H), 7.61 (d, J = 8.96 Hz, 1H), 7.60 (d, J = 8.96 Hz, 1H), 7.55 (s, 2H), 7.09 (dd, J = 7.7, 5.0 Hz, 1H).

^{13}C NMR (126 MHz, $CDCl_3$): δ = 159.03, 148.36, 144.17, 140.03, 139.69, 139.58, 139.12, 138.06, 137.69, 137.67, 137.60, 137.41, 134.51, 130.60, 130.38, 128.91, 128.65, 128.40, 127.69, 127.59, 127.30, 127.27, 124.01, 123.22, 122.39.

HR-MS (ESI): *m/z*: Calculated for $C_{25}H_{12}N^+$: 326.09643; measured: 326.09652.

_N_-(2'-Fluoro[1,1'-biphenyl]-2-yl)carbazole (70)

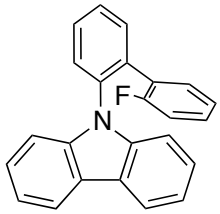

A mixture of N-(2-bromophenyl)carbazole and N-(2-iodophenyl)carbazole was obtained by following a published procedure.[106] **70** was synthesized according to the general procedure C, using the halophenylcarbazole mixture (1.18 g, 3.65 mmol), 2-fluorophenylboronic acid (767 mg, 5.48 mmol), K_2CO_3 (1.52 g, 11.0 mmol), and $Pd(PPh_3)_4$ (40 mg, 0.035 mmol) in THF/H2O (10:1, 22 mL, degassed). The reaction mixture was stirred at 70 °C for 17 h. Reaction control by GC-MS showed that only N-(2-iodophenyl)carbazole had reacted. FC chromatography (hex/DCM 99:1 to 85:5) afforded the desired product as colorless foam (702 mg, 56 %).

Rf (hex/DCM 4:1) = 0.41

M.p.: 93 °C.

^{1}H NMR (400 MHz, $CDCl_3$): δ = 8.01 (ddd, J = 7.7, 1.3, 0.7 Hz, 2H), 7.71–7.64 (m, 1H), 7.63–7.57 (m, 2H), 7.57–7.51 (m, 1H), 7.29 (ddd, J = 8.3, 7.2, 1.3 Hz, 2H), 7.22–7.10 (m, 4H), 7.02–6.92 (m, 1H), 6.87–6.78 (m, 2H), 6.64 (ddd, J = 7.3, 1.2 Hz, 1H).

^{13}C NMR (126 MHz, $CDCl_3$): δ = 159.61 (d, $^{1}J_{C–F}$ = 247.7 Hz), 141.44, 136.09, 135.40, 132.63, 132.62, 130.39 (d, $^{3}J_{C–F}$ = 3.0 Hz), 129.77, 129.59, 129.46 (d, $^{3}J_{C–F}$ = 8.2 Hz), 128.42, 126.26 (d, $^{2}J_{C–F}$ = 14.9 Hz), 125.79, 123.70 (d, $^{4}J_{C–F}$ = 3.6 Hz), 123.27, 120.13, 119.92, 119.69, 115.64 (d, $^{2}J_{C–F}$ = 22.4 Hz), 110.15.

^{19}F-NMR (376.5 MHz, $CDCl_3$): δ = –116.76.

IR (neat, cm^{-1}): 3061*w*, 1597*w*, 1507*w*, 1491*w*, 1476*m*, 1451*s*, 1359*w*, 1336*w*, 1315*m*, 1231*m*, 1209*w*, 1177*w*, 824*w*, 748*s*, 724*m*, 630*w*, 423*w*.

MS (EI): *m/z* (%): 337.1 (100), 315.1 (8), 309.1 (8), 170 (17), 140 (15).

Bis-2,2'-biphenylylene-ammonium hexachlorocarborane (71)

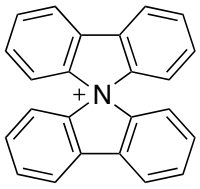

$CHB_{11}H_6Cl_6^-$

71 was synthesized according to the general procedure B, using **70** (39 mg, 0.116 mmol) and [$^{i}Pr_3Si$][$CHB_{11}H_5Cl_6$] (65 mg, 0.127 mmol). The reaction mixture was subjected to microwave irradiation (200 W) during 90 min. Because the set temperature maximum was reached quickly, the power was automatically lowered to 75 W. FC chromatography (hex/DCM 4:1 to DCM/iPrOH 99:1) gave the desired product as slightly brown solid (49 mg, 63 %). Crystals could be obtained from dissolving in aceton and slow evaporation of solvent.

^{1}H NMR (500 MHz, $CDCl_3$): δ = 8.20 (ddd, J = 7.8, 1.3, 0.6 Hz, 4H), 7.80 (ddd, J = 7.7, 7.7, 0.9 Hz, 4H), 7.51 (ddd, J = 8.3, 7.5, 1.2 Hz, 4H), 6.96 (ddd, J = 8.3, 0.7, 0.7 Hz, 4H), 2.05 (s, 1H).

^{13}C NMR (126 MHz, $CDCl_3$): δ = 147.92, 133.35, 131.92, 131.54, 123.78, 118.42.

2-Fluoro-2'-methyl-1,1'-biphenyl (83)

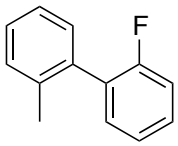

1-Fluoro-2-iodobenzene (680 mg, 3.1 mmol), 2-tolylboronic acid (650 mg, 4.8 mmol), $Pd(PPh_3)_4$ (85 mg, 0.07 mmol) and K_2CO_3 (1.62 g, 9.1 mmol) were dissolved in THF (10 mL, degassed) and water (1.2 mL, degassed), heated to 70 °C and stirred for 35 h. The reaction mixture was cooled to room temperature, diluted with CH_2Cl_2 (30 mL) and washed with a saturated aqueous solution of $NaHCO_3$. The inorganic layer was extracted with CH_2Cl_2 (2x40 mL). The combined organic layers were dried over $MgSO_4$, filtered and concentrated *in vacuo*. The residue was subjected to flash column chromatography (pure Hex to hex/DCM 95:5) to give the product as a colorless oil (510 mg, 89 %). From ^{1}H-NMR, 2.5 % of impurity was determined.

R_f (Hexane)= 0.21. ^{1}H-NMR (400 MHz, $CDCl_3$): δ = 7.38–7.09 (m, 8H), 2.22 (d, J = 4 Hz, 3H).

^{13}C NMR (126 MHz, $CDCl_3$) δ = 159.76 (d, $^1J_{C-F}$ = 245.3 Hz), 136.79, 135.87, 131.69 (d, $^3J_{C-F}$ = 3.8 Hz), 130.19, 130.08, 129.36 (d, $^2J_{C-F}$ = 17.6 Hz) , 129.16 (d, $^3J_{C-F}$ = 8.8 Hz), 128.09, 125.76, 124.10 (d, $^4J_{C-F}$ = 3.8 Hz), 115.64 (d, $^2J_{C-F}$ = 22.6 Hz), 20.08 (d, J_{C-F} = 1.3 Hz).

MS (EI): *m/z* (%): 186.1 (100), 185.1 (64), 184.1 (27), 171.1 (22), 166.1 (23), 165.1 (62).

Fluorene (84)

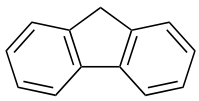

84 was treated according to the general procedure B. Flash column chromatography (pure hex to hex/DCM 99:1) gave the product as white solid (24 mg, 73 %).

R_f (Hexane)= 0.22.

^{1}H-NMR (500 MHz, $CDCl_3$): δ = 7.80 (broad doublet, J = 7.5 Hz, 1H), 7.55 (ddd, J = 7.4, 0.8, 0.8 Hz, 1H), 7.41–7.35 (m, 1H), 7.30 (ddd, J = 7.4, 7.4, 1.2 Hz, 1H), 3.91 (s, 2H).

MS (EI): *m/z* (%): 166.1 (100), 165.1 (93), 139.1 (12), 82.0 (23).

2'-Bromo-2-fluoro-1,1'-biphenyl (75)

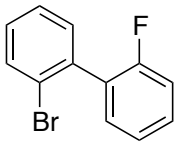

To a solution of 1-bromo-2-fluorobenzene (1.12 g, 6.4 mmol) in THF at –78 °C *n*-BuLi (2.7 mL, 2.5 M in hexanes) was added slowly. The solution turned slightly yellow. After stirring for 30 min, $ZnCl_2$ (950 mg, 7.0 mmol) in THF (8 mL) was added and the reaction mixture turned colorless. In another flask 1-bromo-2-iodobenzene (1.65 g, 5.8 mmol) and $Pd(PPh_3)_4$ (67 mg, 0.06 mmol) were dissolved in THF (10 mL). Thereto the solution containing the zincate was transferred and the mixture was stirred at 50 °C for12 h. Water (50 mL) was added and the aqueous phase was extracted with CH_2Cl_2 (3x50 mL). The combined organic phases were dried over $MgSO_4$, filtered and concentrated *in vacuo*. The residue was subjected to flash column chromatography (hex/DCM 99:1), which afforded the product as a colorless oil (1.32 g, 90 %).

R_f (Hexane)= 0.26.

^{1}H-NMR (500 MHz, $CDCl_3$): δ = 7.69 (dd, J = 8.0, 1.5 Hz, 1H), 7.41–7.35 (m, 2H), 7.33–7.20 (m, 3H), 7.15 (ddd, J = 10, 8.5, 1.5 Hz, 1H).

^{13}C-NMR (125.8 MHz, $CDCl_3$): δ = 159.70 (d, $^1J_{C–F}$ = 247.3 Hz), 137.35, 133.01, 131.76, 131.71 (d, $^3J_{C–F}$ = 3.1 Hz), 129.97 (d, $^3J_{C–F}$ = 8.0 Hz), 129.55, 129.03 (d, $^2J_{C–F}$ = 16.1 Hz), 127.31, 123.99, 123.3 (d, $^4J_{C–F}$ = 3.6 Hz), 115.78 (d, $^2J_{C–F}$ = 22.1 Hz).

^{19}F-NMR (376.5 MHz, $CDCl_3$): δ = –114.68.

MS (EI): *m/z* (%): 251.9 (80), 249.9 (84), 171.0 (42), 170.0 (100), 151.0 (20), 85.0 (24), 75.0 (20).

2-Fluoro-2'-methyl-1,1'-biphenyl-d3

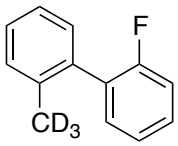

To a solution of 2-bromo-2'-fluorobiphenyl (160 mg, 0.64 mmol) in THF (8 mL) at –78 °C, t-BuLi (0.84 mL, 1.6 M in hexanes) was added dropwise. The reaction mixture turned yellow and after stirring for 20 min, MeI-d3 (141 mg, 0.97 mmol) was added. The solution turned colorless and after stirring for one hour, saturated aq. solution of $NaHCO_3$ (10 mL) was added. The inorganic phase was extracted with CH_2Cl_2 (3x10 mL). The combined organic phases were dried over $MgSO_4$, filtered and concentrated *in vacuo*. The residue was subjected to flash column chromatography (hex), which afforded the product as colorless oil (55 mg, 46 %). Part of the product was lost during evaporation of solvent.

1-(2-Fluorophenyl)-2-methylnaphthalene (96a)

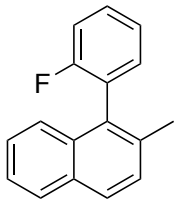

96 was synthesized according to the general procedure C, using 1-bromo-2-methylnaphthalene (319 mg, 1.36 mmol), 2-fluorophenylboronic acid (286 mg, 2.04 mmol), K_2CO_3 (563 mg, 4.07 mmol), and Pd-PEPPSI-iPr (18 mg, 0.027 mmol) in THF/H2O (9:1, 10 mL, degassed). The reaction mixture was stirred at 70 °C for 15 h. FC chromatography (hex/DCM 99:1 to 85:5) afforded the desired product as colorless oil (289 mg, 85 %).

R_f (Hexane)= 0.21.

^{1}H-NMR (500 MHz, $CDCl_3$): δ = 7.86 (d, J = 8.0 Hz, 1H), 7.83 (d, J = 8.5 Hz, 1H), 7.48–7.34 (m, 5H), 7.32–7.21 (m, 3H), 2.28 (s, 3H).

^{13}C NMR (100 MHz, $CDCl_3$) δ = 160.38 (d, $^1J_{C–F}$ = 243.9 Hz), 134.45, 132.89, 132.58 (d, $^3J_{C–F}$ = 3.7 Hz), 132.12, 131.70, 129.54 (d, $^3J_{C–F}$ = 7.8 Hz), 128.62, 128.12,

128.06, 126.96 (d, $^{2}J_{C-F}$ = 17.6 Hz), 126.26, 125.62, 125.03, 124.28 (d, $^{4}J_{C-F}$ = 3.6 Hz), 115.98 (d, $^{2}J_{C-F}$ = 22.2 Hz), 20.65.

^{19}F-NMR (376.5 MHz, $CDCl_3$): δ = –114.76.

IR (neat, cm^{-1}): 3054*w*, 2922*w*, 2859*w*, 1508*w*, 1492*m*, 1447*m*, 1382*w*, 1242*w*, 1220*m*, 1099*w*, 1031*w*, 842*w*, 828*w*, 811*s*, 784*m*, 757*s*, 744*s*, 666*w*, 619*w*, 537*w*, 521*w*, 467*w*, 419*w*.

HR-MS (EI): *m/z*: Calculated for $C_{17}H_{13}F$: 236.09958; measured: 236.09948.

Mixture of 1-methylfluoranthene (97a) and 7*H*-benzo[c]fluorene (98a)

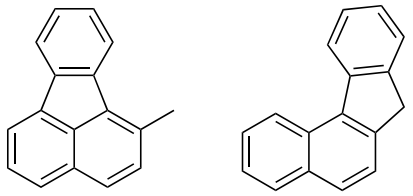

96a was treated according to the general procedure B. Flash column chromatography (pure hex to hex/DCM 4:1) gave a mixture of products as slightly yellow oil. The ratio of the products was determined by comparing integrals in the ^{1}H-NMR spectrum. Therefore the integrated signal of the methyl group of **97a** was compared to the integral of the CH_2-signal of **98a**. This analysis gave a ratio of 1.8 to 1.0 in favor of the product of the intramolecular arylation (**97a**). The signals were compared to the corresponding compounds, which are already reported in literature.[107]

MS (EI): *m/z* (%): **97**: 216.1 (100), 215.1 (90), 214.1 (26), 189.1 (15), 107.7 (20), 106.7 (20), 95.6 (30). **101**: 216.1 (100), 215.1 (72), 214.1 (24), 189.1 (12), 107.7 (22), 106.7 (21), 95.6 (25).

1-(2-Fluorophenyl)-2-isopropylnaphthalene (96b)

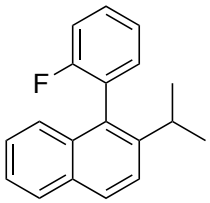

The starting material (1-bromo-2-isopropylnaphthalene) was synthesized from methyl-2-naphtylketone according to literature procedures[108] and contained a substantial amount of regioisomers. For the synthesis of **96b**, 1-bromo-2-isopropylnaphthalene (540 mg, 2.17 mmol), 2-fluorophenylboronic acid (379 mg, 2.71 mmol), K_2CO_3 (899 mg, 6.50 mmol) and $Pd(PPh_3)_4$ (50 mg, 2 mol-%) were dissolved in a mixture of THF (degassed, 10 mL) and water (degassed, 1 mL). After stirring at 70 °C for 17 h, the reaction was worked up (DCM/$NaHCO_3$) despite low conversion. FC chromatography afforded the product as colorless oil (97 mg, 17 %) and recovered starting material (405 mg, 75 %). Due to the various isomers in the starting material, also different coupling products were formed, which could not be separated. The purity of the product was determined to be around 75 % according to ^{1}H NMR.

R_f (Hexane)= 0.22.

^{1}H-NMR (500 MHz, $CDCl_3$): δ = 7.91 (d, J = 8.6 Hz, 1H), 7.85 (d, J = 7.9 Hz, 1H), 7.56 (d, J = 8.7 Hz, 1H), 7.49–7.40 (m, 3H), 7.37–7.32 (m, 1H), 7.31–7.20 (m, 3H), 2.88 (hept, J = 6.9 Hz, 1H), 1.23 (d, J = 6.9 Hz, 3H), 1.19 (d, J = 6.9 Hz, 3H).

^{13}C-NMR (126 MHz, $CDCl_3$) δ = 160.61 (d, $^1J_{C–F}$ = 244.7 Hz), 144.73 , 132.92 , 132.74 (d, $^3J_{C–F}$ = 3.6 Hz), 132.07 , 130.15 , 129.49 (d, $^3J_{C–F}$ = 7.8 Hz), 128.75 , 127.98 , 126.86 (d, $^2J_{C–F}$ = 17.8 Hz), 126.21 , 126.11 , 125.18 , 124.17 (d, $^4J_{C–F}$ = 3.6 Hz), 123.77 , 115.85 (d, $^2J_{C–F}$ = 22.3 Hz), 31.09, 24.13, 23.60.

MS (EI): *m/z* (%): 264.1 (76), 249.1 (100), 234.1 (60), 233.1 (71), 220.1 (15), 202.1 (11), 152.1 (10), 116.7 (16), 96.0 (15).

1-(2-Fluorophenyl)-2-isopropylnaphthalene (97b) and 5,5-dimethylbenzo[*c*]fluorene(98b)

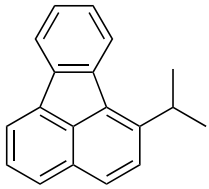
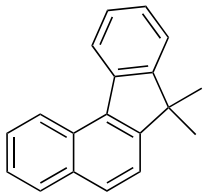

96b was treated according to the general procedure B. Flash column chromatography (pure hex to hex/DCM 4:1) gave a mixture of products as slightly yellow oil. The ratio of the products was determined by comparing integrals in the ^{1}H-NMR spectrum. Therefore the integrated signal of the isopropyl group of **97b** (at 1.51 ppm) was compared to the integral of the CH_3-signal of **98b** (at 1.56 ppm). This analysis gave a ratio of 1.0 to 1.5 in favor of the product of the C–H insertion (**98b**).

1-(2-Fluorophenyl)2,7-diisopropylnaphthalene (96c)

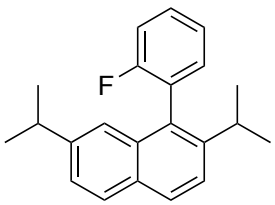

1-Bromo-2,7-diisopropylnaphthalene (487 mg, 1.67 mmol), 2-fluorophenylboronic acid (416 mg, 2.99 mmol), K_2CO_3 (0.69 g, 2.0 mmol) and $Pd(PPh_3)_4$ (39 mg, 0.02 mmol) were suspended in a mixture of THF/water (15:1, 16 mL, degassed). The reaction mixture was heated to 70 °C and the clear solution was stirred for 77 h. Although the conversion was only about 50 %, a saturated aq. solution of $NaHCO_3$ (20 mL) was added. The inorganic phase was extracted with DCM (3x20 mL). The combined organic layers were dried over $MgSO_4$, filtered and concentrated *in vacuo*. The residue was subjected to flash column chromatography (hex/DCM 99:1 to 95:5) to afford the product as colorless crystals (130 mg, 25 %).

M.p.: 58–60 °C.

^{1}H-NMR (500 MHz, $CDCl_3$): δ = 7.85 (d, J = 8.6 Hz, 1H), 7.78 (d, J = 8.4 Hz, 1H), 7.49 (d, J = 8.6 Hz, 1H), 7.49–7.39 (m, 1H), 7.34 (dd, J = 8.4, 1.7 Hz, 1H), 7.31–7.19

(m, 3H), 7.06 (broad singlet, 1H), 2.89 (h, J = 6.9 Hz, 2H), 2.85 (h, J = 6.9 Hz, 2H), 1.27–1.11 (m, 12H).

^{13}C NMR (126 MHz, $CDCl_3$) δ = 160.61 (d, $^1J_{C-F}$ = 244.9 Hz), 146.72, 144.71, 132.99, 132.78 (d, $^3J_{C-F}$ = 3.7 Hz), 130.69, 129.80, 129.38 (d, $^3J_{C-F}$ = 7.7 Hz), 128.43, 128.00, 126.99 (d, $^2J_{C-F}$ = 18.0 Hz), 124.55, 124.12 (d, $^4J_{C-F}$ = 3.7 Hz), 122.92, 122.70, 115.78 (d, $^2J_{C-F}$ = 22.4 Hz), 34.56, 31.07, 24.14, 24.06, 24.03, 23.61.

^{19}F-NMR (376.5 MHz, $CDCl_3$): δ = –114.04.

IR (neat, cm^{-1}): 3052*w*, 2960*m*, 2928*w*, 2868*w*, 1625*w*, 1508*w*, 1489*m*, 1446*m*, 1386*w*, 1363*w*, 1243*w*, 1227*w*, 1205*w*, 1096*w*, 1042*w*, 841*s*, 807*m*, 758*s*, 620*w*, 530*w*, 470*w*.

MS (EI): *m/z* (%): 306.1 (94), 291.1 (63), 249.1 (100), 234.1 (48), 233.1 (66).

HR-MS (EI): *m/z*: Calculated for $C_{22}H_{23}F$: 306.17783; measured: 306.17783.

1,6-Diisopropylfluoranthene (97c) and 2-isopropyl-7,7-dimethylbenzo[*c*]fluorene (98c)

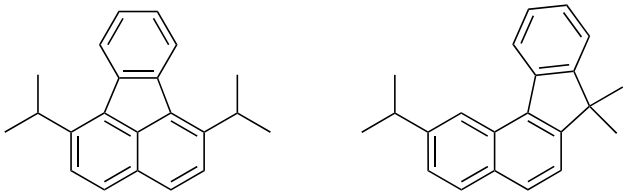

96c was treated according to the general procedure B. Flash column chromatography (pure hex to hex/DCM 4:1) gave a mixture of products as slightly yellow oil. The ratio of the products was determined by comparing integrals in the ^{1}H-NMR spectrum. Therefore the integrated signal of the isopropyl groups of **97c** (at 1.51 ppm) was compared to the integral of the CH_3-signal of **98c** (at 1.55 ppm). This analysis gave a ratio of 1.0 to 2.0 in favor of the product of the C–H insertion (**98c**).

2-*tert*-Butyl-2'-fluoro-1,1'-biphenyl (99)

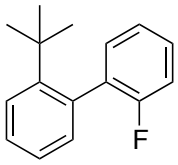

2-*tert*-Butyl-1-bromobenzene (170 mg, 0.80 mmol), 2-fluorophenylboronic acid (180 mg, 1.29 mmol), K_2CO_3 (333 mg, 2.41 mmol) and Pd-PEPPSI-iPr (11 mg, 0.016 mmol) were dissolved in a mixture of THF/water (9:1, 10 mL, degassed). The reaction mixture was heated to 70 °C and the clear solution was stirred for 17 h. After cooling down, a saturated aq. solution of $NaHCO_3$ (10 mL) was added. The inorganic phase was extracted with DCM (3x15 mL). The combined organic layers were dried over $MgSO_4$, filtered and concentrated *in vacuo*. The residue was subjected to flash column chromatography (SiO_2, pure hexane) to afford the product as colorless oil (125 mg, 25 %).

R_f (Hexane)= 0.32.

^{1}H-NMR (400 MHz, $CDCl_3$): δ = 7.56 (dd, J = 8.1, 1.3 Hz, 1H), 7.38–7.29 (m, 2H), 7.26 (ddd, J = 7.6, 7.3, 1.8 Hz, 1H), 7.20 (ddd, J = 7.4, 7.4, 1.3 Hz, 1H), 7.13 (ddd, J = 7.5, 7.5, 1.2 Hz, 1H), 7.08 (ddd, J = 8.3, 8.2, 1.1 Hz, 1H), 7.01 (dd, J = 7.6, 1.7 Hz, 1H).

^{13}C NMR (100 MHz, $CDCl_3$) δ = 159.89 (d, $^1J_{C–F}$ = 242.3 Hz), 148.64, 134.83, 132.77 (d, $^2J_{C–F}$ = 17.3 Hz), 132.57, 132.50 (d, $^3J_{C–F}$ = 3.2 Hz), 129.01 (d, $^3J_{C–F}$ = 7.9 Hz), 128.06, 127.08, 125.33, 123.12 (d, $^4J_{C–F}$ = 3.6 Hz), 115.39 (d, $^2J_{C–F}$ = 22.4 Hz), 36.50, 32.08.

^{19}F-NMR (376.5 MHz, $CDCl_3$): δ = –111.94.

HR-MS (EI): *m/z*: Calculated for $C_{16}H_{17}F$: 228.13088; measured: 228.13098.

10,10-Dihydro-9,9-dimethylphenanthrene (100)

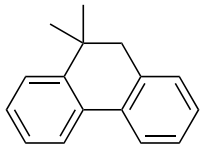

100 was synthesized according to the general procedure B, using **99** (15 mg, 0.066 mmol), $[^{i}Pr_3Si][CHB_{11}H_5Cl_6]$ (1.5 mg, 0.003 mmol), and DMDMS (20 mg, 0.070 mmol). Flash column chromatography (pure hex to hex/DCM 98:2) gave the product as colorless crystals (29 mg, 79 %).

R_f (Hexane)= 0.30

^{1}H-NMR (500 MHz, $CDCl_3$): δ = 7.81–7.73 (m, 2H), 7.44–7.39 (m, 1H), 7.34–7.28 (m, 3H), 7.23 (ddd, *J* = 7.3, 7.3, 1.2 Hz, 1H), 7.19 (d, *J* = 7.3 Hz, 1H), 2.79 (s, 2H), 1.27 (s, 6H).

^{13}C NMR (125 MHz, $CDCl_3$) δ = 145.57, 136.17, 134.34, 133.40, 128.77, 128.08, 127.56, 126.98, 126.68, 124.39, 124.22, 123.64, 44.22, 34.30, 28.07.

MS (EI): *m/z* (%): 208.1 (31), 193.1 (100), 178.1 (68), 165.2 (17), 89.1 (13),0.30

HR-MS (EI): *m/z*: Calculated for $C_{22}H_{23}F$: 208.12465; measured: 208.12470.

1,6-Bis(2-fluorophenyl)-2,5-dimethylcorannulene (102)

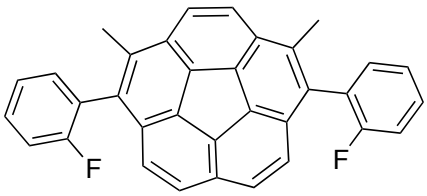

1,6-Dibromo-2,5-dimethylcorannulene (143 mg, 0.33 mmol), 2-fluorophenylboronic acid (164 mg, 1.17 mmol), K_2CO_3 (278 mg, 2.01 mmol) and $Pd(PPh_3)_4$ (23 mg, 0.02 mmol) were suspended in a mixture of THF/water (9:1, 10 mL, degassed). The reaction mixture was heated to 70 °C and the clear solution was stirred for 15 h. A saturated aq. solution of $NaHCO_3$ (15 mL) was added. The inorganic phase was

extracted with DCM (3x20 mL). The combined organic layers were dried over $MgSO_4$, filtered and concentrated *in vacuo*. The residue was subjected to flash column chromatography (hex/DCM 95:5 to 80:20) to afford the product as a slightly yellow solid (128 mg, 84 %).

R_f (hex/DCM 9:1)= 0.19

^{1}H NMR (400 MHz, $CDCl_3$): δ = 8.03 (d, J = 0.4 Hz, 2H), 7.65 (d, J = 8.8 Hz, 2H), 7.54–7.23 (m, 10H), 2.66 (d, J = 0.6 Hz, 6H).

^{19}F NMR (376 MHz, $CDCl_3$): δ = –113.65, –113.83.

Diindeno[3,2-*a*:2,3-*g*]corannulene (103)

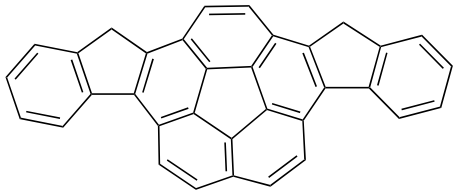

103 was synthesized according to the general procedure B, using **105** (17.5 mg, 0.038 mmol), [^{i}Pr$_3$Si][$CHB_{11}H_5Cl_6$] (1.9 mg, 0.004 mmol), and DMDMS (23 mg, 0.079 mmol). The reaction mixture was subjected to microwave irradiation (200 W) for 1 h. Reaction control performed by TLC revealed the presence of starting material, intermediate, and product. Only addition of more silyl cation and DMDMS, and additional heating for 2 h led to full consumption of starting material. FC chromatography (hex/DCM 9:1 to 7:3) afforded product as yellow solid (3.7 mg, 23 %).

R_f (hex/DCM 7:3) = 0.24.

^{1}H NMR (400 MHz, $CDCl_3$): δ = 8.47 (d, J = 8.8 Hz, 2H), 8.41 (d, J = 7.5 Hz, 2H), 8.01 (s, 2H), 7.95 (d, J = 8.8 Hz, 2H), 7.69 (d, J = 7.6 Hz, 2H), 7.53 (dd, J = 7.6, 7.6 Hz, 2H), 7.37 (ddd, J = 7.5, 7.5, 1.1 Hz, 2H), 4.31 (s, 4H).

MS (EI): *m/z* (%): 426.2 (100), 411.2 (38), 212.2 (16).

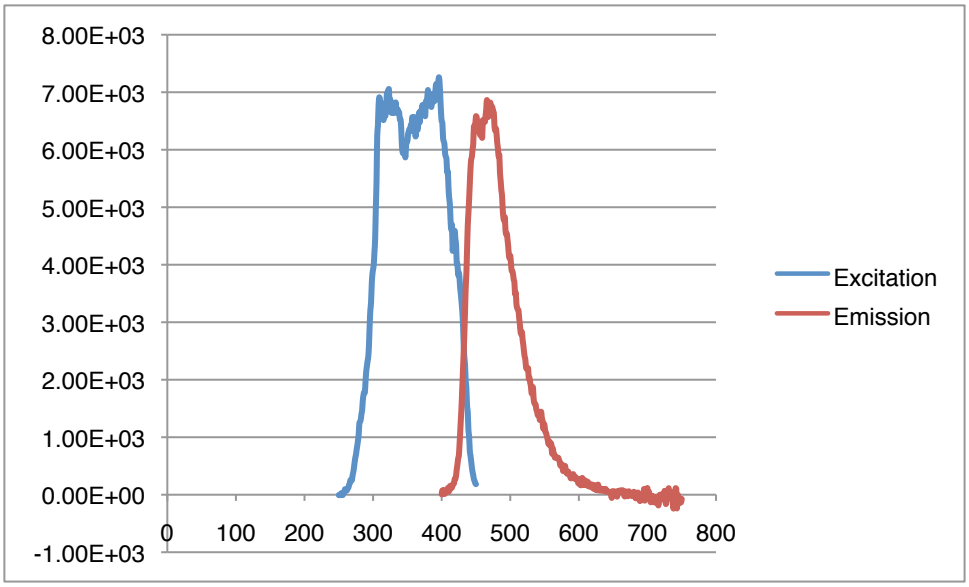

Figure 4.1. Excitation/Emission spectrum of compound 106 in DCM at an optical density of 0.1.

Quantum yield: 0.29.

Crystal Structures

Figure Captions

1. *ORTEP*[109] representation of the molecule (50% probability ellipsoids; H atoms given arbitrary displacement parameters for clarity)

Definition of Terms

Function minimized: $\Sigma w(F_o^2 - F_c^2)^2$

where $w = [\sigma^2(F_o^2) + (aP)^2 + bP]^{-1}$ and $P = (F_o^2 + 2F_c^2)/3$

$F_o^2 = S(C - RB)/Lp$

and $\sigma^2(F_o^2) = S^2(C + R^2B)/Lp^2$

S = Scan rate

C = Total integrated peak count

R = Ratio of scan time to background counting time

B = Total background count

Lp = Lorentz-polarization factor

R-factors:

$R_{int} = \Sigma|<F_o^2> - F_o^2|/\Sigma F_o^2$ summed only over reflections for which more than one symmetry equivalent was measured.

$R(F) = \Sigma||F_o| - |F_c||/\Sigma|F_o|$ summed over all observed reflections.

$wR(F^2) = [\Sigma w(F_o^2 - F_c^2)^2/\Sigma w(F_o^2)^2]^{1/2}$ summed over all reflections.

Standard deviation of an observation of unit weight (goodness of fit):

$[\Sigma w(F_o^2 - F_c^2)^2/(N_o - N_v)]^{1/2}$

where N_o = number of observations; N_v = number of variables

Byproduct of aza-indenocorannulene synthesis

Conformation A:

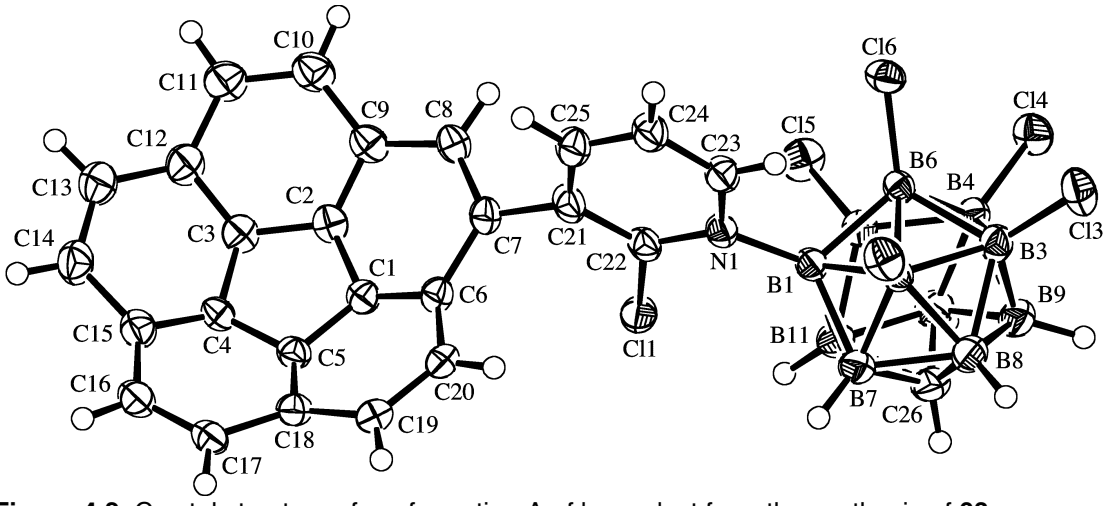

Figure 4.2. Crystal structure of conformation A of byproduct from the synthesis of **63**.

Conformation B:

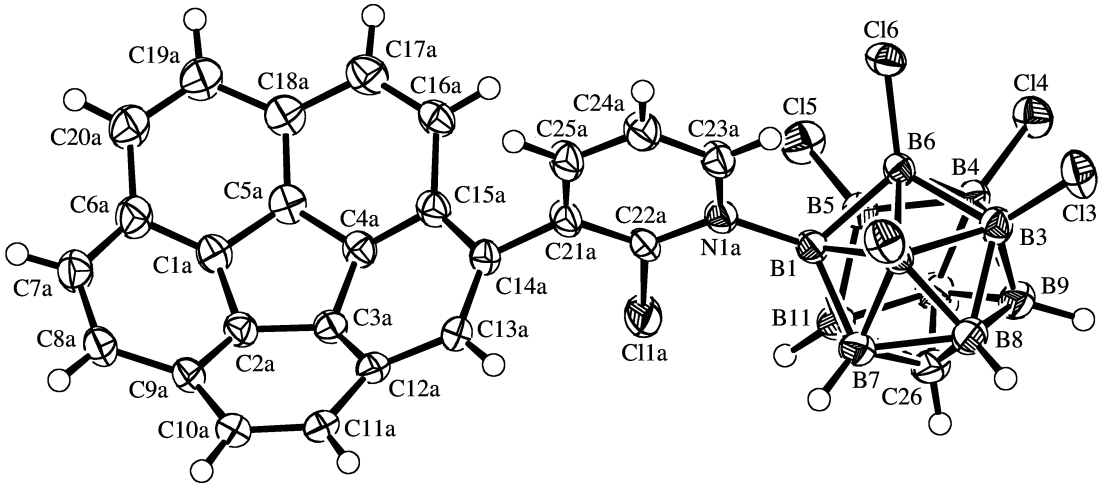

Figure 4.3. Crystal structure of conformation B of byproduct from the synthesis of **63**.

Table 4.2. Crystallographic data of byproduct

Crystallised from		dichloromethane / hexane
Empirical formula		$C_{27}H_{19}B_{11}Cl_9N$
Formula weight [g mol^{-1}]		795.44
Crystal colour, habit		yellow, prism
Crystal dimensions [mm]		0.05 ´ 0.09 ´ 0.12
Temperature [K]		160(1)
Crystal system		monoclinic
Space group		$P2_1/n$ (#14)
Z		4
Reflections for cell determination		16741
2θ range for cell determination [°]		6 – 148
Unit cell parameters	a [Å]	15.36818(15)
	b [Å]	12.13018(10)
	c [Å]	18.30918(18)
	α [°]	90
	β [°]	100.9903(10)
	γ [°]	90
	V [Å^3]	3350.58(6)
F(000)		1584
D_X [g cm^{-3}]		1.577
μ(Cu $K\alpha$) [mm^{-1}]		7.071
Scan type		ω
$2\theta_{(max)}$ [°]		148.8
Transmission factors (min; max)		0.686; 1.000
Total reflections measured		32463
Symmetry independent reflections		6741
R_{int}		0.052
Reflections with $I > 2\sigma(I)$		5773
Reflections used in refinement		6741
Parameters refined; restraints		677; 944
Final		$R(F)$ [$I > 2\sigma(I)$ reflections] 0.0446
		$wR(F^2)$ (all data) 0.1274
Weights:		$w = [\sigma^2(F_o^2) + (0.0791P)^2 + 1.7201P]^{-1}$ where $P = (F_o^2 + 2F_c^2)/3$
Goodness of fit		1.028
Final Δ_{max}/σ		0.001
$\Delta\rho$ (max; min) [e Å^{-3}]		0.55; -0.49
$\sigma(d_{(C-C)})$ [Å]		0.004 – 0.007

First polymorph of tetraarylammonium hexachlorocarborane (71)

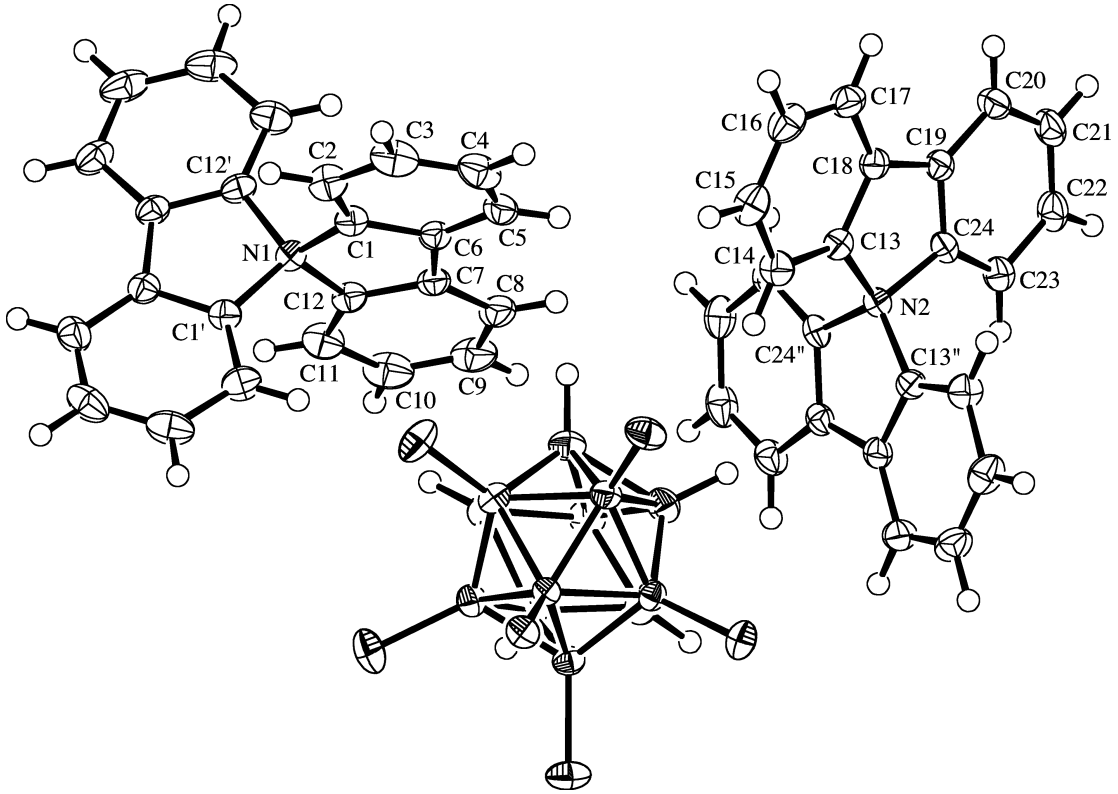

Figure 4.4. Crystal structure of first polymorph of **71**.

Table 4.3. Crystallographic data of **71**.

Crystallised from	deuterochloroform / hexane
Empirical formula	$C_{25}H_{22}B_{11}Cl_6N$
Formula weight [g mol^{-1}]	668.08
Crystal colour, habit	colourless, prism
Crystal dimensions [mm]	0.21 × 0.22 × 0.23
Temperature [K]	160(1)
Crystal system	orthorhombic
Space group	*Pbcn* (#60)
Z	8
Reflections for cell determination	21201
2θ range for cell determination [°]	4−61
Unit cell parameters	*a* [Å] 18.70332(19)
	b [Å] 18.4574(3)
	c [Å] 18.40020(17)
	α [°] 90
	β [°] 90
	γ [°] 90
	V [Å^3] 6352.02(13)

$F(000)$	2688	
D_X [g cm^{-3}]	1.397	
μ(Mo $K\alpha$) [mm^{-1}]	0.561	
Scan type	ω	
2θ(max) [°]	60.9	
Transmission factors (min; max)	0.866; 1.000	
Total reflections measured	39043	
Symmetry independent reflections	8322	
R_{int}	0.021	
Reflections with $I > 2\sigma(I)$	7016	
Reflections used in refinement	8322	
Parameters refined	389	
Final	$R(F)$ [$I > 2\sigma(I)$ reflections]	0.0307
	$wR(F^2)$ (all data)	0.0833
Weights:	$w = [\sigma^2(F_o^2) + (0.0403P)^2 + 2.4227P]^{-1}$	
where $P = (F_o^2 + 2F_c^2)/3$		
Goodness of fit	1.025	
Final Δ_{max}/σ	0.002	
$\Delta\rho$ (max; min) [e Å^{-3}]	0.34; -0.44	
$\sigma(d_{(C-C)})$ [Å]	0.0018 – 0.003	

Second polymorph of tetraarylammonium hexachlorocarborane (71)

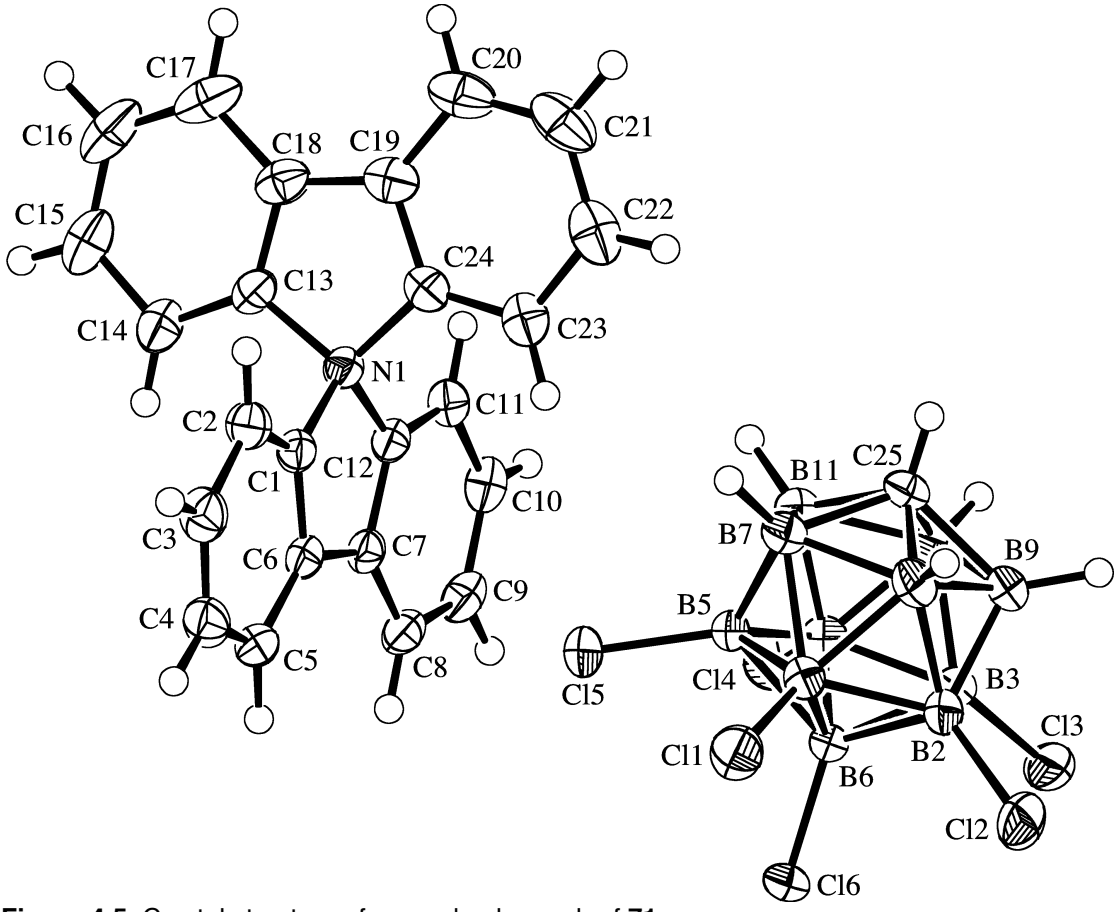

Figure 4.5. Crystal structure of second polymorph of **71**.

Table 4.4. Crystallographic data of **71**.

Crystallised from	acetone / hexane	
Empirical formula	$C_{25}H_{22}B_{11}Cl_6N$	
Formula weight [g mol^{-1}]	668.08	
Crystal colour, habit	colourless, prism	
Crystal dimensions [mm]	0.22 × 0.25 × 0.25	
Temperature [K]	160(1)	
Crystal system	orthorhombic	
Space group	*Pbcn* (#60)	
Z	8	
Reflections for cell determination	75479	
2θ range for cell determination [°]	4 – 55	
Unit cell parameters	*a* [Å]	18.0150(2)
	b [Å]	14.8013(1)
	c [Å]	23.3476(2)
	α [°]	90

	β [°]	90
	γ [°]	90
	V [Å^3]	6225.5(2)
F(000)	2688	
D_x [g cm^{-3}]	1.425	
μ(Mo $K\alpha$) [mm^{-1}]	0.573	
Scan type	ϕ and ω	
$2\theta_{(max)}$ [°]	55	
Transmission factors (min; max)	0.813; 0.887	
Total reflections measured	78563	
Symmetry independent reflections	7125	
R_{int}	0.046	
Reflections with $I > 2\sigma(I)$	5755	
Reflections used in refinement	7120	
Parameters refined	388	
Final	$R(F)$ [$I > 2\sigma(I)$ reflections]	0.0396
	$wR(F^2)$ (all data)	0.1059
Weights:	$w = [\sigma^2(F_o^2) + (0.0458P)^2 + 5.1407P]^{-1}$	
where $P = (F_o^2 + 2F_c^2)/3$		
Goodness of fit	1.024	
Final Δ_{max}/σ	0.001	
$\Delta\rho$ (max; min) [e Å^{-3}]	0.73; -0.48	
$\sigma(d_{(C-C)})$ [Å]	0.003 – 0.004	

Dibenzo[5]helicene (45)

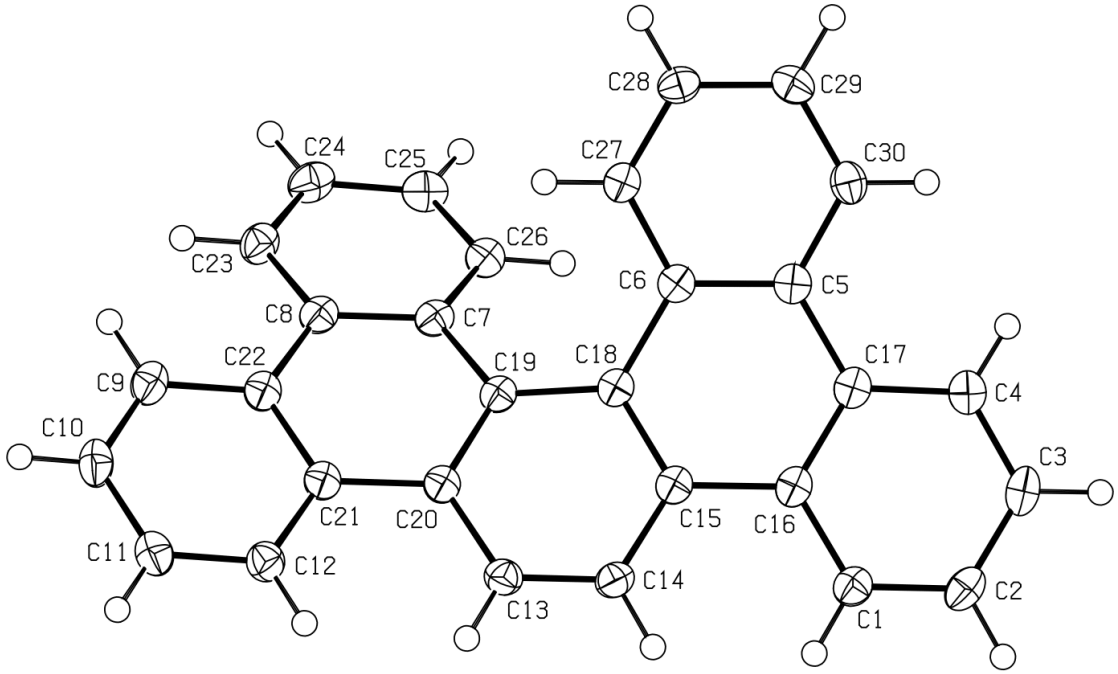

Figure 4.6. Crystal structure of **45**.

Table 4.5. Crystallographic data of **45**.

Crystallised from	hot PhCl	
Empirical formula	$C_{30}H_{18}$	
Formula weight [g mol^{-1}]	378.47	
Crystal colour, habit	colourless, plate	
Crystal dimensions [mm]	0.04 × 0.28 × 0.44	
Temperature [K]	100(1)	
Crystal system	monoclinic	
Space group	$P2_1/n$ (#14)	
Z	4	
Reflections for cell determination	10218	
2θ range for cell determination [°]	4−148	
Unit cell parameters	a [Å]	19.3549(3)
	b [Å]	5.12886(5)
	c [Å]	19.9604(3)
	α [°]	90
	β [°]	115.0553(19)
	γ [°]	90
	V [Å^3]	1794.99(4)
F(000)	792	
D_X [g cm^{-3}]	1.400	
μ(Cu $K\alpha$) [mm^{-1}]	0.604	

Scan type	ω	
2θ(max) [°]	148.0	
Transmission factors (min; max)	0.208; 1.000	
Total reflections measured	18317	
Symmetry independent reflections	774977329	
R_{int}	0.018	
Reflections with $I > 2\sigma(I)$	3308	
Reflections used in refinement	3588	
Parameters refined	272	
Final	$R(F)$ [$I > 2\sigma(I)$ reflections]	0.0326
	$wR(F^2)$ (all data)	0.0894
Weights:	$w = [\sigma^2(F_o^2) + (0.0456P)^2 + 0.6114P]^{-1}$	
where $P = (F_o^2 + 2F_c^2)/3$		
Goodness of fit	1.040	
Secondary extinction coefficient	0.0007(2)	
Final Δ_{max}/σ	0.004	
$\Delta\rho$ (max; min) [e Å^{-3}]	0.24; -0.17	
$\sigma(d_{(C-C)})$ [Å]	0.001 – 0.002	

5 References

[1] a)J. B. Lambert, S. Zhang, C. L. Stern, J. C. Huffman, *Science* **1993**, *260*, 1917; b)C. A. Reed, Z. Xie, R. Bau, A. Benesi, *Science* **1993**, *262*, 402.

[2] J. B. Lambert, W. J. Schulz, J. A. McConnell, W. Schilf, *Journal of the American Chemical Society* **1988**, *110*, 2201.

[3] I. Krossing, I. Raabe, *Angewandte Chemie International Edition* **2004**, *43*, 2066.

[4] C. A. Reed, *Chemical Communications* **2005**, 1669.

[5] a)Z. W. Xie, C. W. Tsang, E. T. P. Sze, Q. C. Yang, D. T. W. Chan, T. C. W. Mak, *Inorganic Chemistry* **1998**, *37*, 6444; b)C. A. Reed, *Accounts of Chemical Research* **1998**, *31*, 133.

[6] C. A. Reed, N. L. P. Fackler, K. C. Kim, D. Stasko, D. R. Evans, P. D. W. Boyd, C. E. F. Rickard, *Journal of the American Chemical Society* **1999**, *121*, 6314.

[7] Z. Xie, T. Jelinek, R. Bau, C. A. Reed, *Journal of the American Chemical Society* **1994**, *116*, 1907.

[8] K. Shelly, C. A. Reed, Y. J. Lee, W. R. Scheidt, *Journal of the American Chemical Society* **1986**, *108*, 3117.

[9] Z. W. Xie, J. Manning, R. W. Reed, R. Mathur, P. D. W. Boyd, A. Benesi, C. A. Reed, *Journal of the American Chemical Society* **1996**, *118*, 2922.

[10] Z. Xie, R. Bau, A. Benesi, C. A. Reed, *Organometallics* **1995**, *14*, 3933.

[11] S. Duttwyler, Q. Q. Do, A. Linden, K. Baldridge, J. Siegel, *Angewandte Chemie International Edition* **2008**, *47*, 1719.

[12] a)P. Romanato, S. Duttwyler, A. Linden, K. K. Baldridge, J. S. Siegel, *Journal of the American Chemical Society* **2010**, *132*, 7828; b)P. Romanato, S. Duttwyler, A. Linden, K. K. Baldridge, J. S. Siegel, *Journal of the American Chemical Society* **2011**, *133*, 11844.

[13] H. F. T. Klare, K. Bergander, M. Oestreich, *Angewandte Chemie-International Edition* **2009**, *48*, 9077.

[14] K. C. Kim, C. A. Reed, D. W. Elliott, L. J. Mueller, F. Tham, L. J. Lin, J. B. Lambert, *Science* **2002**, *297*, 825.

[15] K. Hara, R. Akiyama, M. Sawamura, *Organic Letters* **2005**, *7*, 5621.

[16] R. K. Schmidt, K. Müther, C. Mück-Lichtenfeld, S. Grimme, M. Oestreich, *Journal of the American Chemical Society* **2012**, *134*, 4421.

[17] M. Kira, T. Hino, H. Sakurai, *Chemistry Letters* **1992**, 555.

[18] K. Muther, M. Oestreich, *Chemical Communications* **2011**, *47*, 334.

[19] K. Müller, C. Faeh, F. Diederich, *Science* **2007**, *317*, 1881.

[20] T. Umemoto, S. Fukami, G. Tomizawa, K. Harasawa, K. Kawada, K. Tomita, *Journal of the American Chemical Society* **1990**, *112*, 8563.

[21] T. Umemoto, G. Tomizawa, *The Journal of Organic Chemistry* **1995**, *60*, 6563.

[22] Y. Kiso, K. Tamao, M. Kumada, *Journal of Organometallic Chemistry* **1973**, *50*, C12.

[23] a)D. R. Fahey, J. E. Mahan, *Journal of the American Chemical Society* **1977**, *99*, 2501; b)M. Reinhold, J. E. McGrady, R. N. Perutz, *Journal of the American Chemical Society* **2004**, *126*, 5268.

[24] L. Cronin, C. L. Higgitt, R. Karch, R. N. Perutz, *Organometallics* **1997**, *16*, 4920.

[25] N. A. Jasim, R. N. Perutz, A. C. Whitwood, T. Braun, J. Izundu, B. Neumann, S. Rothfeld, H.-G. Stammler, *Organometallics* **2004**, *23*, 6140.
[26] P. Ke Chan, W. Kee Leong, *Organometallics* **2008**, *27*, 1247.
[27] T. G. Richmond, C. E. Osterberg, A. M. Arif, *Journal of the American Chemical Society* **1987**, *109*, 8091.
[28] I. M. Piglosiewicz, S. Kraft, R. Beckhaus, D. Haase, W. Saak, *European Journal of Inorganic Chemistry* **2005**, *2005*, 938.
[29] U. Jäger-Fiedler, P. Arndt, W. Baumann, A. Spannenberg, V. V. Burlakov, U. Rosenthal, *European Journal of Inorganic Chemistry* **2005**, *2005*, 2842.
[30] M. Aizenberg, D. Milstein, *Science* **1994**, *265*, 359.
[31] V. P. W. Böhm, C. W. K. Gstöttmayr, T. Weskamp, W. A. Herrmann, *Angewandte Chemie International Edition* **2001**, *40*, 3387.
[32] K. Inamoto, J. Kuroda, T. Sakamoto, K. Hiroya, *Synthesis-Stuttgart* **2007**, 2853.
[33] F. Mongin, L. Mojovic, B. Guillamet, F. Trécourt, G. Quéguiner, *The Journal of Organic Chemistry* **2002**, *67*, 8991.
[34] a)B. M. Kraft, R. J. Lachicotte, W. D. Jones, *Journal of the American Chemical Society* **2000**, *122*, 8559; b)B. M. Kraft, R. J. Lachicotte, W. D. Jones, *Journal of the American Chemical Society* **2001**, *123*, 10973.
[35] G. A. Olah, W. S. Tolgyesi, R. E. A. Dear, *Journal of Organic Chemistry* **1962**, *27*, 3441.
[36] J. Terao, S. A. Begum, Y. Shinohara, M. Tomita, Y. Naitoh, N. Kambe, *Chemical Communications* **2007**, 855.
[37] G. A. Olah, S. J. Kuhn, *The Journal of Organic Chemistry* **1964**, *29*, 2317.
[38] M. A. Keegstra, T. H. A. Peters, L. Brandsma, *Tetrahedron* **1992**, *48*, 3633.
[39] V. E. Platonov, A. Haas, M. Schelvis, M. Lieb, K. V. Dvornikova, O. I. Osina, Y. V. Gatilov, *Journal of Fluorine Chemistry* **2001**, *109*, 131.
[40] Y.-J. Cherng, *Tetrahedron* **2002**, *58*, 4931.
[41] a)K. Y. Amsharov, M. A. Kabdulov, M. Jansen, *Angewandte Chemie International Edition* **2012**, *51*, 4594; b)K. Y. Amsharov, P. Merz, *The Journal of Organic Chemistry* **2012**, *77*, 5445.
[42] H. Amii, K. Uneyama, *Chemical Reviews* **2009**, *109*, 2119.
[43] J. Ichikawa, M. Yokota, T. Kudo, S. Umezaki, *Angewandte Chemie International Edition* **2008**, *47*, 4870.
[44] V. J. Scott, R. Celenligil-Cetin, O. V. Ozerov, *Journal of the American Chemical Society* **2005**, *127*, 2852.
[45] C. Douvris, O. V. Ozerov, *Science* **2008**, *321*, 1188.
[46] C. Douvris, C. M. Nagaraja, C. H. Chen, B. M. Foxman, O. V. Ozerov, *Journal of the American Chemical Society* **2010**, *132*, 4946.
[47] R. Panisch, M. Bolte, T. Müller, *Journal of the American Chemical Society* **2006**, *128*, 9676.
[48] N. Luhmann, R. Panisch, T. Muller, *Applied Organometallic Chemistry* **2010**, *24*, 533.
[49] S. Duttwyler, C. Douvris, N. L. P. Fackler, F. S. Tham, C. A. Reed, K. K. Baldridge, J. S. Siegel, *Angewandte Chemie International Edition* **2010**, *49*, 7519.
[50] E. A. Rohlfing, D. M. Cox, A. Kaldor, *The Journal of Chemical Physics* **1984**, *81*, 3322.
[51] H. W. Kroto, J. R. Heath, S. C. O'Brien, R. F. Curl, R. E. Smalley, *Nature* **1985**, *318*, 162.
[52] W. Kratschmer, L. D. Lamb, K. Fostiropoulos, D. R. Huffman, *Nature* **1990**, *347*, 354.

[53] S. Iijima, *Nature* **1991**, *354*, 56.
[54] C. Journet, W. K. Maser, P. Bernier, A. Loiseau, M. L. de la Chapelle, S. Lefrant, P. Deniard, R. Lee, J. E. Fischer, *Nature* **1997**, *388*, 756.
[55] A. Thess, R. Lee, P. Nikolaev, H. Dai, P. Petit, J. Robert, C. Xu, Y. H. Lee, S. G. Kim, A. G. Rinzler, D. T. Colbert, G. E. Scuseria, D. Tom√°nek, J. E. Fischer, R. E. Smalley, *Science* **1996**, *273*, 483.
[56] P. Nikolaev, M. J. Bronikowski, R. K. Bradley, F. Rohmund, D. T. Colbert, K. A. Smith, R. E. Smalley, *Chemical Physics Letters* **1999**, *313*, 91.
[57] K. S. Novoselov, A. K. Geim, S. V. Morozov, D. Jiang, Y. Zhang, S. V. Dubonos, I. V. Grigorieva, A. A. Firsov, *Science* **2004**, *306*, 666.
[58] M. D. Watson, A. Fechtenkötter, K. Müllen, *Chemical Reviews* **2001**, *101*, 1267.
[59] a)L. Dössel, L. Gherghel, X. Feng, K. Müllen, *Angewandte Chemie International Edition* **2011**, *50*, 2540; b)A. Pradhan, P. Dechambenoit, H. Bock, F. Durola, *Angewandte Chemie International Edition* **2011**, *50*, 12582.
[60] V. S. Iyer, M. Wehmeier, J. D. Brand, M. A. Keegstra, K. Müllen, *Angewandte Chemie International Edition in English* **1997**, *36*, 1604.
[61] a)V. M. Tsefrikas, L. T. Scott, *Chemical Reviews* **2006**, *106*, 4868; b)G. Mehta, H. S. P. Rao, *Tetrahedron* **1998**, *54*, 13325.
[62] A. Necula, L. T. Scott, *Journal of Analytical and Applied Pyrolysis* **2000**, *54*, 65.
[63] a)K. Y. Amsharov, M. A. Kabdulov, M. Jansen, *European Journal of Organic Chemistry* **2009**, *2009*, 6328; b)L. T. Scott, *Angewandte Chemie International Edition* **2004**, *43*, 4994.
[64] a)J. E. Rice, Z.-W. Cai, *Tetrahedron Letters* **1992**, *33*, 1675; b)J. E. Rice, Z. W. Cai, *The Journal of Organic Chemistry* **1993**, *58*, 1415; c)H. A. Reisch, M. S. Bratcher, L. T. Scott, *Organic Letters* **2000**, *2*, 1427; d)A. M. Echavarren, B. Gomez-Lor, J. J. Gonzalez, O. de Frutos, *Synlett* **2003**, 585.
[65] A. Sygula, P. W. Rabideau, *Journal of the American Chemical Society* **2000**, *122*, 6323.
[66] T. J. Seiders, K. K. Baldridge, J. S. Siegel, *Journal of the American Chemical Society* **1996**, *118*, 2754.
[67] M. C. Bonifacio, C. R. Robertson, J.-Y. Jung, B. T. King, *The Journal of Organic Chemistry* **2005**, *70*, 8522.
[68] C.-H. Kuo, M.-H. Tsau, D. T. C. Weng, G. H. Lee, S.-M. Peng, T.-Y. Luh, P. U. Biedermann, I. Agranat, *The Journal of Organic Chemistry* **1995**, *60*, 7380.
[69] K. Fent, *Ökotoxikologie*, Thieme, Stuttgart, **2007**.
[70] D. Mackay, *Environmental Science & Technology* **1982**, *16*, 274.
[71] A. W. Wood, W. Levin, A. Y. H. Lu, D. Ryan, S. B. West, R. E. Lehr, M. Schaefer-Ridder, D. M. Jerina, A. H. Conney, *Biochemical and Biophysical Research Communications* **1976**, *72*, 680.
[72] T. H. Chan, I. Fleming, *Synthesis* **1979**, 761.
[73] F. H. Allen, O. Kennard, D. G. Watson, L. Brammer, A. G. Orpen, R. Taylor, *Journal of the Chemical Society, Perkin Transactions 2* **1987**, S1.
[74] C. J. Wilkins, L. E. Sutton, *Transactions of the Faraday Society* **1954**, *50*, 783.
[75] a)M. Juhasz, S. Hoffmann, E. Stoyanov, K. C. Kim, C. A. Reed, *Angewandte Chemie-International Edition* **2004**, *43*, 5352; b)E. S. Stoyanov, S. P. Hoffmann, M. Juhasz, C. A. Reed, *Journal of the American Chemical Society* **2006**, *128*, 3160.
[76] P. Romanato, *unpublished results* **2010**.

[77] A. Schäfer, M. Reißmann, A. Schäfer, W. Saak, D. Haase, T. Müller, *Angewandte Chemie International Edition* **2011**, *50*, 12636.
[78] S. Da Ros, Universität Zürich (Zürich), **2013**.
[79] T. J. Seiders, K. K. Baldridge, G. H. Grube, J. S. Siegel, *Journal of the American Chemical Society* **2001**, *123*, 517.
[80] D. Hellwinkel, H. Seifert, *Chemische Berichte-Recueil* **1972**, *105*, 880.
[81] M. F. Ibad, P. Langer, A. Schulz, A. Villinger, *Journal of the American Chemical Society* **2011**, *133*, 21016.
[82] J. Seibel, O. Allemann, J. S. Siegel, K.-H. Ernst, *Journal of the American Chemical Society* **2013**, *135*, 7434.
[83] a)L. Mascarelli, *Gazzetta Chimica Italiana* **1936**, *66*, 843; b)L. Mascarelli, B. Longo, *Gazzetta Chimica Italiana* **1941**, *71*, 289.
[84] R. W. Stumpe, *Tetrahedron Letters* **1980**, *21*, 4891.
[85] D. Ferraris, C. Cox, R. Anand, T. Lectka, *Journal of the American Chemical Society* **1997**, *119*, 4319.
[86] T. Cohen, J. Lipowitz, *Journal of the American Chemical Society* **1964**, *86*, 2514.
[87] T. Cohen, J. Lipowitz, *Journal of the American Chemical Society* **1964**, *86*, 2515.
[88] A. S. Daudpota, H. Heaney, *Tetrahedron Letters* **1978**, *19*, 3471.
[89] I. Puskas, E. K. Fields, *The Journal of Organic Chemistry* **1968**, *33*, 4237.
[90] S. J. Blanksby, G. B. Ellison, *Accounts of Chemical Research* **2003**, *36*, 255.
[91] W. M. Haynes, *CRC Handbook of Chemistry and Physics*, CRC Press, Boca Raton, FL, **2012**.
[92] M. W. Schmidt, K. K. Baldridge, J. A. Boatz, S. T. Elbert, M. S. Gordon, J. H. Jensen, S. Koseki, N. Matsunaga, K. A. Nguyen, S. Su, T. L. Windus, S. T. Elbert, *Journal of Computational Chemistry* **14**, 1347 (1999).
[93] Truhlar/Zhang local module revision of D.01 *Gaussian 03*, Gaussian Inc., Pittsburgh PA, 2003.
[94] A. D. Becke, *Journal of Chemical Physics* **108**, 9624-9631 (1998).
C. Moller, M. S. Plesset, Physical Review **46**, 618-622 (1934).
[95] T. H. Dunning, *Journal of Chemical Physics* **90**, 1007 (1998).
[96] K. K. Baldridge, A. Klamt, *Journal of Chemical Physics* **106**, 6622 (1997).
[97] T. A. Keith, R.F.W. Bader, *Chemical Physics Letters* **210***,* 223 (1993).
[98] *WEBMO*: T. Cundari, J. R. Schmidt, *www.webmo.net*.
[99] K. K. Baldridge, J.P. Greenberg, *Journal of Molecular Graphics* **13**, 63 (1995).
[100] C. A. Reed, *Accounts of Chemical Research* **1998**, *31*, 325.
[101] a)C. A. Reed, K.-C. Kim, E. S. Stoyanov, D. Stasko, F. S. Tham, L. J. Mueller, P. D. W. Boyd, *Journal of the American Chemical Society* **2003**, *125*, 1796; b)S. Duttwyler, Y. Zhang, A. Linden, C. Reed, K. Baldridge, J. Siegel, *Angewandte Chemie International Edition* **2009**, *48*, 3787.
[102] D. Pena, A. Cobas, D. Pérez, E. Guitian, L. Castedo, *Organic Letters* **2000**, *2*, 1629.
[103] B. D. Steinberg, E. A. Jackson, A. S. Filatov, A. Wakamiya, M. A. Petrukhina, L. T. Scott, *Journal of the American Chemical Society* **2009**, *131*, 10537.
[104] A. Streitwieser, A. Lewis, I. Schwager, R. W. Fish, S. Labana, *Journal of the American Chemical Society* **1970**, *92*, 6525.
[105] H. Plieninger, G. Ege, M. I. Ullah, *Chemische Berichte* **1963**, *96*, 1610.
[106] S. Chun To, F. Yee Kwong, *Chemical Communications* **2011**, *47*, 5079.
[107] a)D. A. Peake, A. R. Oyler, K. E. Heikkila, R. J. Liukkonen, E. C. Engroff, R. M. Carlson, *Synthetic Communications* **1983**, *13*, 21; b)K. K. Laali, T.

Okazaki, F. Sultana, S. D. Bunge, B. K. Banik, C. Swartz, *European Journal of Organic Chemistry* **2008**, *2008*, 1740.
[108] a)A. Baroudi, J. Mauldin, I. V. Alabugin, *Journal of the American Chemical Society* **2009**, *132*, 967; b)L. Vieille-Petit, X. Luan, R. Mariz, S. Blumentritt, A. Linden, R. Dorta, *European Journal of Inorganic Chemistry* **2009**, *2009*, 1861.
[109] C.K. Johnson, *ORTEPII*, Report ORNL-5138, Oak Ridge National Laboratory, Oak Ridge, Tennessee, 1976.

6 Appendix

Lebenslauf

PERSÖNLICHE DATEN

Name:	**Allemann**
Vorname:	**Oliver**
Geburtstag:	24. February 1985
Bürgerort:	Welschenrohr (SO)
Adresse:	Tägernaustrasse 14, 8645 Jona, Schweiz.
Telefon:	0041-76-4713105
Email:	allemann.oliver@gmail.com

AUSBILDUNG

04/2010 – 12/2013	Doktorat bei Prof. Jay S. Siegel über Silizium Kationen an der Universität Zürich
10/2007 – 01/2009	Master Studium in Chemie and der ETH Zürich Abschluss: Master of Science, Januar 2009 Titel der Abschlussarbeit: "*Investigation of a Novel Hydrophobic Pocket of the Enzyme Catechol-O-Methyltransferase (COMT)*" Betreuer: M. Ellermann und Prof. Dr. F. Diederich
10/2004 – 10/2007	Bachelor Studium in Chemie an der ETH Zürich Abschluss: Bachelor, Februar 2008
03/2004 – 08/2004	Rekrutenschule in Dübendorf bei der Luftwaffe

08/1999 – 09/2003	Kantonsschule Wattwil Abschluss: Matura, September 2003

BERUFSERFAHRUNG

05/2009 – 01/2010	Praktikum bei Syngenta Crop Protection AG in Stein AG unter Dr. Andrew J. F. Edmunds.

PUBLIKATIONEN

Proton-Catalyzed, Silane-Fueled Friedel–Crafts Coupling of Fluoroarenes. O. Allemann, S. Duttwyler, P. Romanato, K. K. Baldridge, J. S. Siegel, *Science* **2011**,*332*, 274–277.

M. Ellermann, C. Lerner, G. Burgy, A. Ehler, C. Bissantz, R. Jakob-Roetne, R. Paulini, O. Allemann, H. Tissot, D. Grunstein, M. Stihle, F. Diederich, M. G. Rudolph, *Acta Crystallographica Section D-Biological Crystallography* **2012**, *68*, 253.

J. Seibel, O. Allemann, J. S. Siegel, K.-H. Ernst, *Journal of the American Chemical Society* **2013**, *135*, 7434.

KONFERENZTEILNAHMEN

Mündliche Präsentation:

06/2013	Doktorandentag OCI 2013

Poster:

09/2010	3rd EuCheMS Chemistry Congress, Nürnberg.
08/2011	17th European Symposium on Organic Chemistry (ESOC), Crete.
09/2011	SCS Fall Meeting 2011
08/2012	4th EuCheMS Chemistry Congress, Prag.
10/2012	7th Dorothy Crowfoot Hodgkin Symposium
07/2013	15th International Symposium on Novel Aromatic Compounds, Taipei.
10/2013	8th Dorothy Crowfoot Hodgkin Symposium